

AD-A054 791 HUGHES AIRCRAFT CO FULLERTON CALIF
PORTABLE EARTH STATION ANTENNA STUDY SYSTEM. (U)
MAR 78

F/G 17/2.1

UNCLASSIFIED

FR-78-14-287

NL

OF 2
AD
A054791



AD A 054791

FOR FURTHER INFORMATION

100

FINAL REPORT

FOR

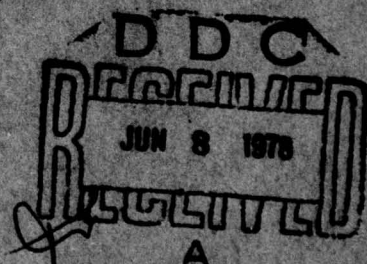
PORTABLE EARTH STATION
ANTENNA STUDY SYSTEM

1 MARCH 1978

FR-78-14-287

FOR

NAVAL RESEARCH LABORATORY
WASHINGTON, D. C.

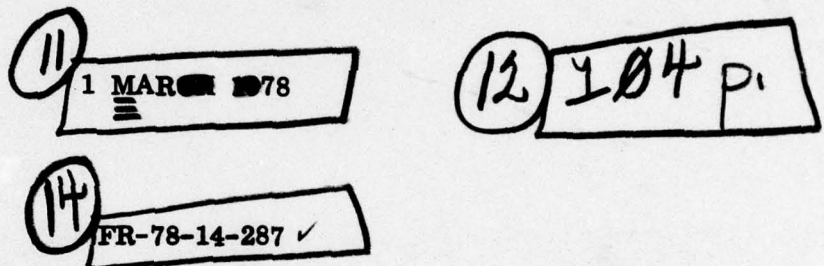
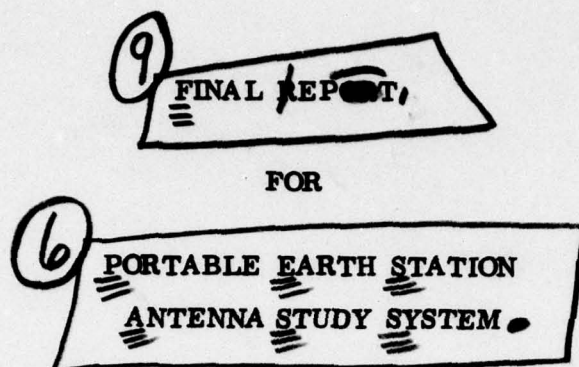


HUGHES AIRCRAFT COMPANY

FULLERTON, CALIFORNIA 92634

DISTRIBUTION STATEMENT A

Approved for public release
Distribution Unlimited



FOR

NAVAL RESEARCH LABORATORY

WASHINGTON, D. C.

HUGHES AIRCRAFT COMPANY ✓

FULLERTON, CALIFORNIA 92634

172350

alt

TABLE OF CONTENTS

	<u>Page Number</u>
1.0 Introduction	1
2.0 Summary	2
3.0 Design Requirements/Considerations	3
4.0 System Tradeoffs, Electrical	4
4.1 Antenna Configuration	4
4.2 Feed Configuration and Beamwidth Control	4
Four-Element Feed	5
Seven-Element Feed	5
Low G/T Operation	9
High G/T Operation	9
Single Element Feed	9
Feed Selection Considerations	17
4.3 Reflector Size and F/D	17
4.4 Blockage	21
Strut Blockage	21
Seven-Element Feed Blockage	28
Center Supported Feed	28
4.5 A/J Considerations	28
Phase Error Control of Sidelobe Level	28
Sidelobe Suppression	36
Shroud	36
Low Angle Multipath	39
4.6 Tradeoff Summary	39
5.0 System Tradeoffs, Mechanical	45

	<u>Page Number</u>
5.1 Van Mounted Antenna	45
5.2 Tower Mounted Antenna	45
5.3 Flat Bed Mounted Antenna	52
6.0 Baseline System	55
6.1 System Description	55
6.2 Antenna Controls	59
6.3 System Performance	62
7.0 Conclusions	68

Appendices

I Antenna Efficiency Analysis - Candidate Antenna Configurations	69
II Computed Secondary Patterns - Candidate Antenna Systems	74
III Measured Primary Patterns-Amplitude and Phase	84

ACCESSION NO.			
NTIS	White Section <input checked="" type="checkbox"/>		
DDC	Buff Section <input type="checkbox"/>		
UNANNOUNCED <input type="checkbox"/>			
JUSTIFICATION <i>Notes on file</i>			
BY			
DISTRIBUTION/AVAILABILITY CODES			
BEL	AVAIL AND/OR SPECIAL		
<table border="1" style="width: 100%; border-collapse: collapse;"> <tr> <td style="width: 50%; text-align: center; vertical-align: middle; padding: 5px;">A</td> <td style="width: 50%; text-align: center; vertical-align: middle; padding: 5px;"> </td> </tr> </table>		A	
A			

1.0 Introduction

1.0 Introduction

A detailed study has been performed to define the optimum system configuration to meet the desired specifications. Tradeoffs were performed for various antenna configurations and transportation methods and changes in the desired performance and packaging were incorporated. A system has been defined which meets the desired performance over most of the coverage region, and is simple, reliable, and cost effective. This report details the tradeoff studies performed and the recommendations for a baseline system.

2.0 Summary

Summary

The Mobile Antenna System requirements should be satisfied by solutions which offer the best antenna system approach and provide the latest in the state-of-the-art technology with little or no risk. The antenna system should be very reliable yet cost effective. For the purpose of this study, only a single main reflector with a single beam system is considered. The recommended approach used to meet the requirements is the result of parametric tradeoffs of mechanical, electrical, logistic, reliability, and cost considerations.

The recommended antenna system is a ten-foot diameter parabolic reflector mounted on an az-el pedestal that is tied to an erectable tower. The tower and the antenna assembly is mounted on a 26-foot flat bed that can be easily transported by C130 cargo plane.

The erection mechanism is hydraulic and requires no special tools. Outriggers are provided for stabilizing the flat bed which becomes the pedestal for the tower. The system is designed for an antenna height of 25 feet.

The feed is a center-fed cup dipole feed, the cup measuring approximately 9 inches in diameter and about 4 inches deep. The center support is a two-inch diameter lightweight pipe with a support cone at the attachment point of the reflector. The transmit and receive transmission lines plus a polarizing 90-degree hybrid are placed inside this support strut.

The solid state transmitter, filters and preamplifier are all located directly behind the vertex of the reflector.

3.0 Design Requirements/Considerations

3.0 Design Requirements/Considerations

The antenna system must be able to communicate with several targets that are clustered in a predetermined volume at known elevation angles. The antenna should be deployable in a short time and operate throughout temperature and equatorial zones. A minimum grazing angle of 5 degrees or less is desired. During the course of the study, system requirements and emphasis were changed as a result of the interim design review. The pertinent design requirements and changes are tabulated below:

G/T	+8.5 dB low angle -1.5 dB high angle	no change
Stowed Volume	1-1/2' x 7' x 20'	7-1/2' x 7' x 38'
Transportable	Van mounted/shipborne	Flat bed mounted C130/not shipborne
Erection Time	Several tens of minutes	Several hours or more
A/J	Very important	Moderately important
Pedestal	2 and 3 axis	2 axis, az-el
Beam		
5° elevation	> 2.5° horizontal > 1.6° vertical	No change
90° elevation	> 8.5° horizontal > 5.4° vertical	No change
Polarization	RCP transmit LCP receive	No change No change

4.0 System Tradeoffs, Electrical

4.0 System Tradeoffs, Electrical

A number of tradeoffs were made in choosing the recommended antenna system. Items considered include the antenna configuration, reflector size and F/D, feed configuration, performance impact of feed and strut blockage, and anti-jam considerations of sidelobe control techniques.

4.1 Antenna Configuration

Several antenna configurations were initially considered to accomplish the desired antenna performance. Principal consideration was given to Cassegrain, offset reflectors, shaped reflectors, and front-fed paraboloids.

The Cassegrain antenna has several advantages including short transmission lines from the feed to the receiver, lower wide angle sidelobes, and more versatility in feed design. However, for main reflector sizes less than $D/\lambda=100$ the subreflector blockage and diffraction losses become significant. For the present antenna size ($D/\lambda \approx 14$), blockage and these losses would severely degrade performance in both gain loss and increased sidelobes. This configuration was thus eliminated.

Offset reflectors eliminate the blockage problems of Cassegrain systems, however, a fairly directive feed is required. Also, the depth of the reflector increases to maintain the same aperture size. This is undesirable from a mechanical packaging viewpoint as well as increased weight for a given aperture size. Also, the deeper asymmetrical dish required tends to generate more cross polarization.

Initially, an elliptically shaped aperture paraboloid was considered to provide the elliptical beam shape desired in the vertical and horizontal planes. However, the aperture size required to meet the beamwidth desired is much larger than necessary to meet the gain and G/T required. As it was desirable to minimize the size to use a circular aperture.

The above considerations led to the choice of a front fed paraboloid as the best choice for this application. Tradeoffs to optimize this configuration were then made to determine the feed type, reflector size and F/D and feed support structure.

4.2 Feed Configuration and Beamwidth Control

Three basic feed types were studied to evaluate the antenna performance. Since both G/T and far-out sidelobe reduction for increased rejection of interfering signals (anti-jam) were initially important considerations, a tradeoff of gain versus sidelobe level was made.

The three feeds considered included a single cup dipole feed, a four-element feed, and a seven-element feed. The four and seven-element feeds were primarily for beamwidth control and sidelobe suppression.

Initial performance analysis was made by computation of the secondary radiation patterns of a 10-foot diameter paraboloid fed with one, four and seven-element feeds. Measured primary pattern data on a cup dipole feed was used for the single element feed. This pattern was also used as an element factor for determining the primary patterns for the four and seven-element feeds.

Four Element Feed

The four element feed provides a convenient means of electronically changing the far field pattern characteristics to meet the G/T requirements. However, very little is gained in performance by this technique as illustrated in Figure 4-1. High gain patterns are achieved by feeding the four elements in phase. By phasing the elements at 0° , 90° and 180° as shown, it is possible to broaden the beam somewhat, but at an expense of increased sidelobes. In addition, this phasing results in scanning of the primary feed pattern off the reflector, Figure 4-2, which will result in increased spillover and thus much higher wide angle sidelobes. This would be very undesirable for the anti-jam environment, and therefore the technique is not considered as a viable approach.

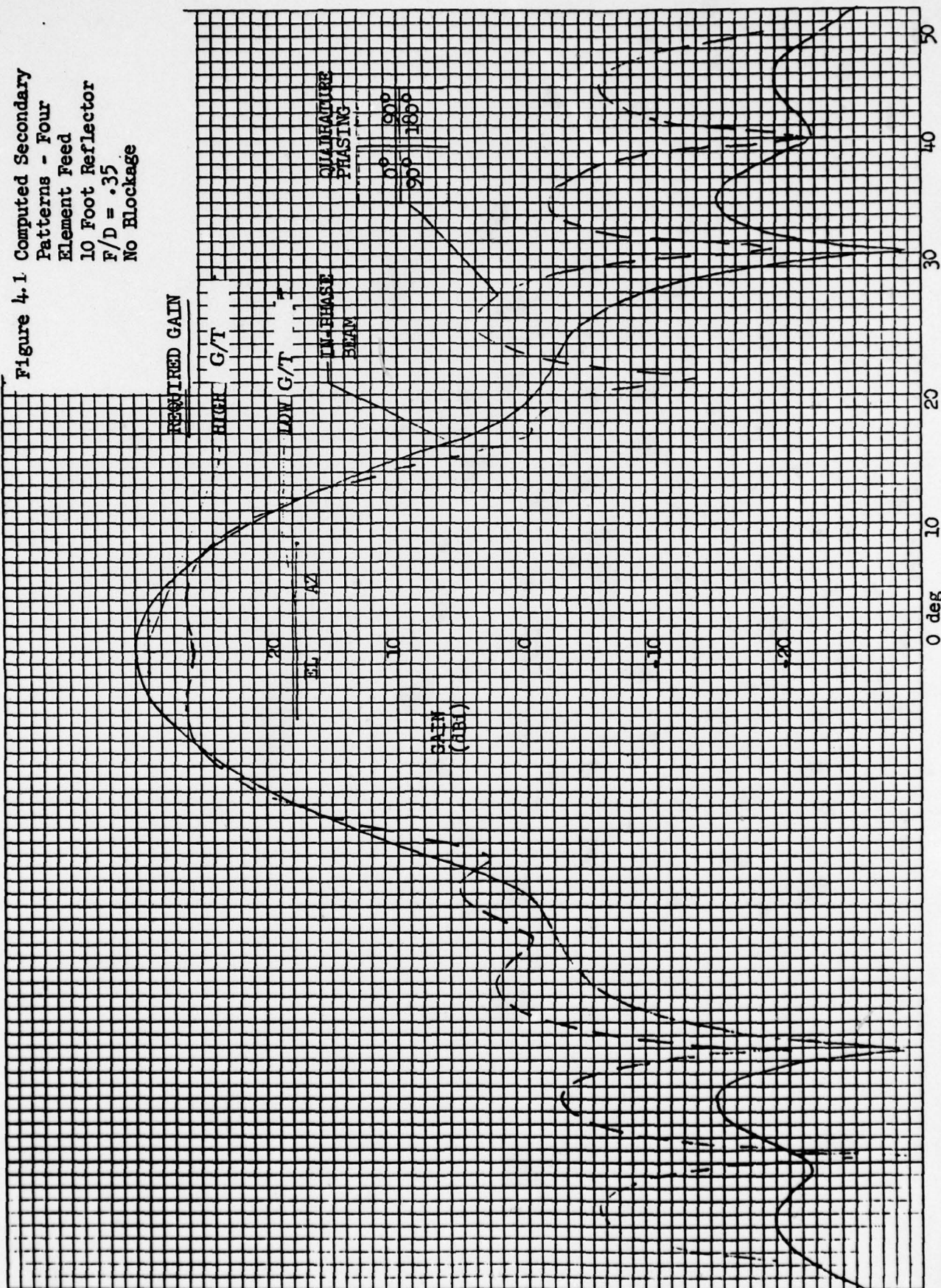
Seven Element Feed

The seven-element feed approach consists of a central element with six contiguous elements spaced equally around the circumference. The seven-element feed pattern beamwidth is varied by amplitude tapering. The high gain horizon beam requires efficient dish illumination to achieve the required gain, thus resulting in higher spillover. For the lower gain required near zenith, it is possible to form a narrower beam primary pattern which under-illuminates the reflector, Figure 4-3. This results in very low spillover for the lower gain beam, thus providing low far-out sidelobe levels.

A schematic of the seven-element beam selectable feed is shown in Figure 4-4. The switching circuit as shown allows this feed to operate in either of two modes for left circular polarization (receive) and one mode for right circular polarization (transmit). On transmit only the center element is illuminated. This provides the broad primary pattern for high efficiency illumination of the parabolic reflector.

The system requires simultaneous transmit and receive in two orthogonal circular polarizations and at a four percent frequency separation. This requirement necessitates the use of RF filters in both the transmit and the receive lines. In the transmit line, filtering will attenuate any transmitter noise generated in the receive frequency band. The signal entering the receive channel consists of the desired receive signal and a component of the transmit signal at the transmit frequency. An RF filter in the receive line attenuates the undesirable transmit component. As the filtering requirements are not fully defined at this time, only a low loss bandstop filter has been assumed to be utilized in the following analysis. However, this factor should be more fully considered in the final system definition. If the system environment requires the use of a bandpass filter, the circuit losses would increase thus reducing the G/T performance.

Figure 4.1 Computed Secondary
Patterns - Four
Element Feed
10 Foot Reflector
 $F/D = .35$
No Blockage



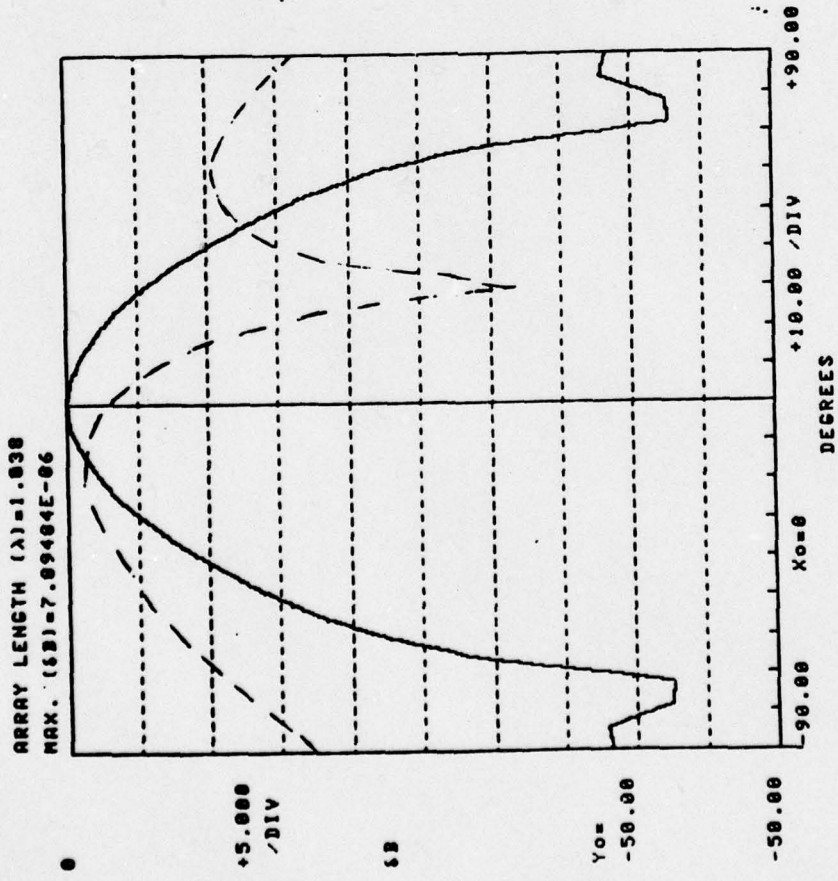


Figure 4.2 Four Element Feed
Computed Primary Patterns

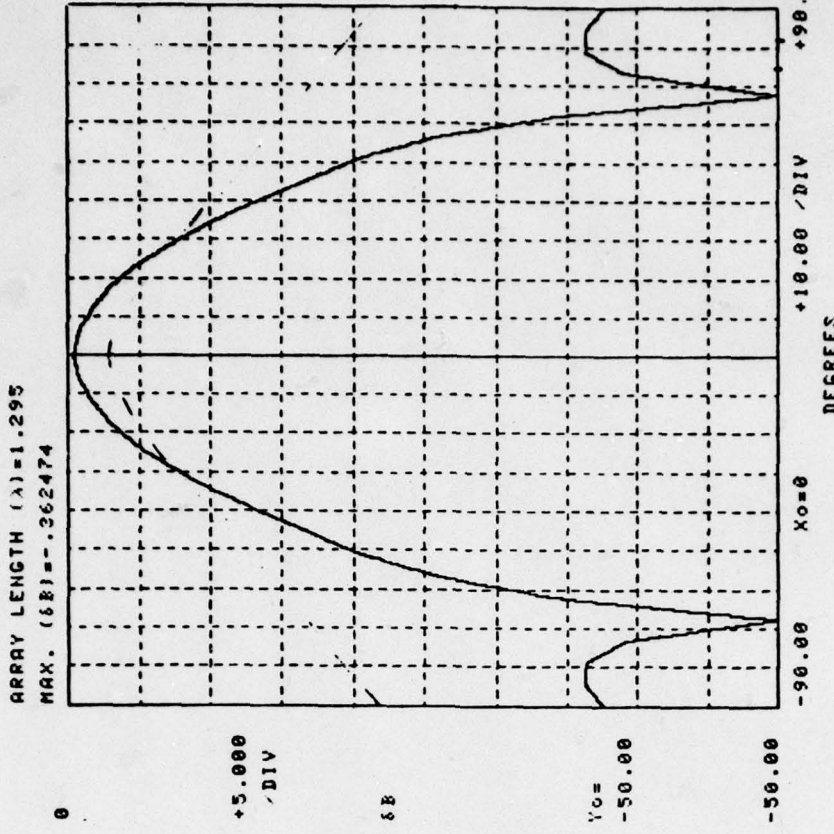


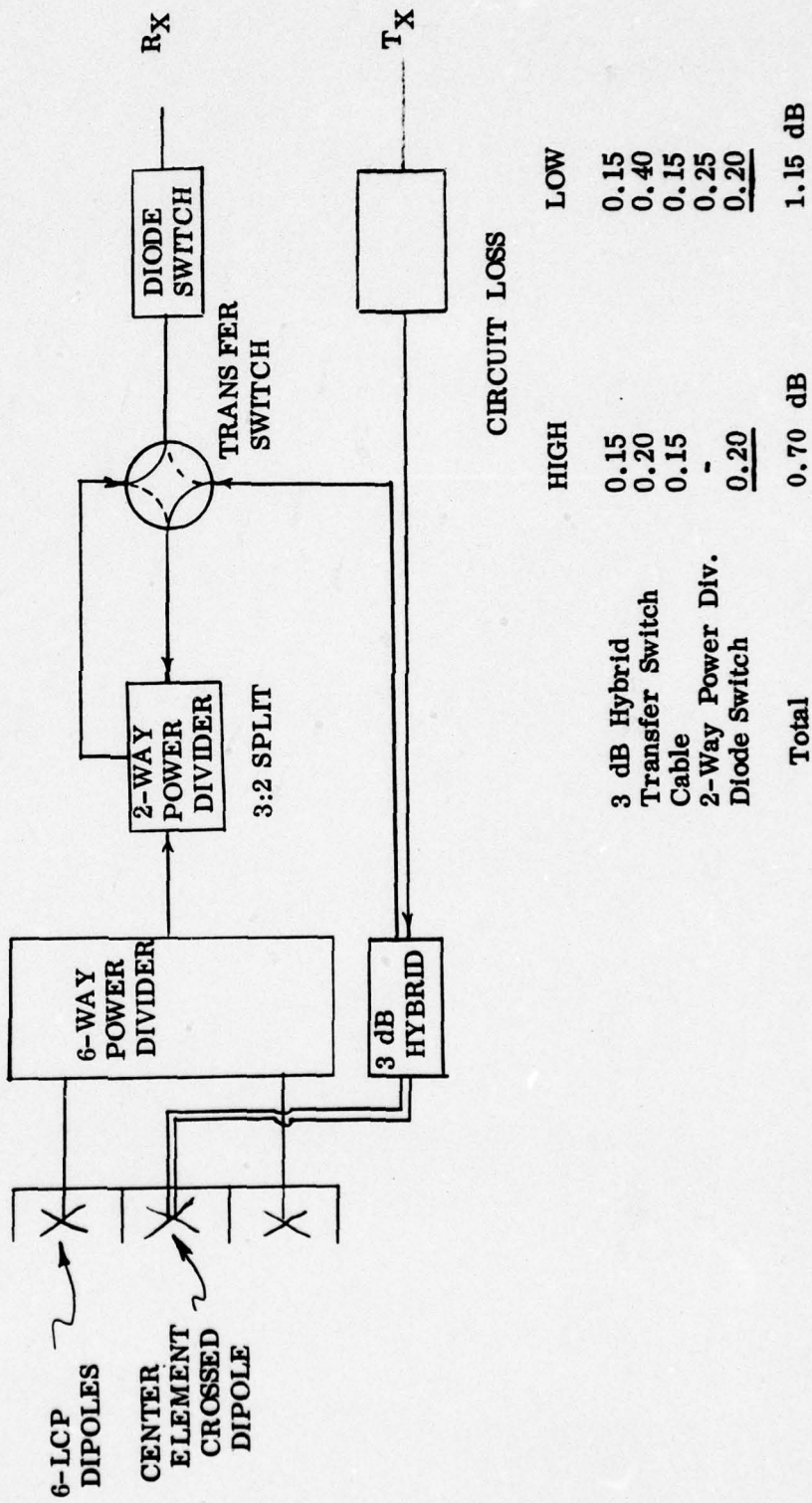
Figure 4.3 Seven-Element Feed
Computed Primary Patterns

Low Gain Beam
High Gain Beam

In Phase
Quadrature Phasing

Figure 4.4
SCHEMATIC OF SEVEN ELEMENT FEED

HUGHES



Low G/T Receive Operation - Seven-Element Feed

In the receive mode all seven elements are illuminated when the transfer switch is in the position shown. This circuit, as shown in Figure 4.4, equally combines the receive power of the six outer LCP dipoles in the six-way power combiner. The combined signal is then input to the two-way power combiner. The receive signal from the center crossed dipole is sent to the 3 dB hybrid, which determines the sense of polarization, and the LCP signal then goes to one port of the transfer switch. From the transfer switch the signal goes to the two-way power combiner and is summed with the power incident from the six outer elements. The combined signal goes back through the transfer switch to the receiver.

The primary feed beamwidth in this mode is determined by the ratio of power in the center element to that in the outer six elements as set by the two-way power divider. The primary pattern of the seven-element array, Figure 4-5, is narrow and thus tends to underilluminate the paraboloid reflector. This results in low energy spillover and backlobes and a broad secondary beam which is the optimum beam configuration for low G/T requirements.

High G/T Receive Operation - Seven-Element Feed

For the high G/T secondary beam, the transfer switch is put in the opposite position to that shown, and the signal from the center crossed dipole element goes through the 3 dB hybrid and through the transfer switch to the receiver. The outer elements are not illuminated for this beam. This element provides a broad primary pattern, Figure 4-6, and results in a very efficient feed illumination. The resulting high gain secondary beam is ideal for high G/T requirements near the horizon. The broad primary pattern, however, results in a high spillover level and thus high far-out sidelobes.

Plots of the aperture efficiency versus feed half angle are shown in Figures 4-7 and 4-8. For the low gain secondary beam the integrated efficiency maximizes at a subtended angle of 40° and decays rapidly for larger angles. For the high gain secondary beam the efficiency is maximum at approximately 70° ($F/D = 0.35$). These efficiency curves are very useful in choosing the optimum F/D where

$$\tan(\theta/2) = 0.25/(F/D)$$

θ = paraboloid half angle

Single Element Feed

A schematic of the single non-switchable feed is shown in Figure 4.9. The circuit consists of a cupped crossed dipole radiating element, a 3 dB hybrid, and transmit and receive ports. As in the previous case, a receive noise stopband filter in the transmit line, and a transmit stopband filter in the receive line are required. A measured feed pattern, Figure 4-10, is chosen as a compromise between the high and low gain beams provided by the seven-element switchable feed. The peak feed efficiency, Figure 4-11, occurs at approximately 50° . At 71° ($f/D =$

CHART NO. 17

SCIENTIFIC-ATLANTA, INC., ATLANTA, GEORGIA, U.S.A.

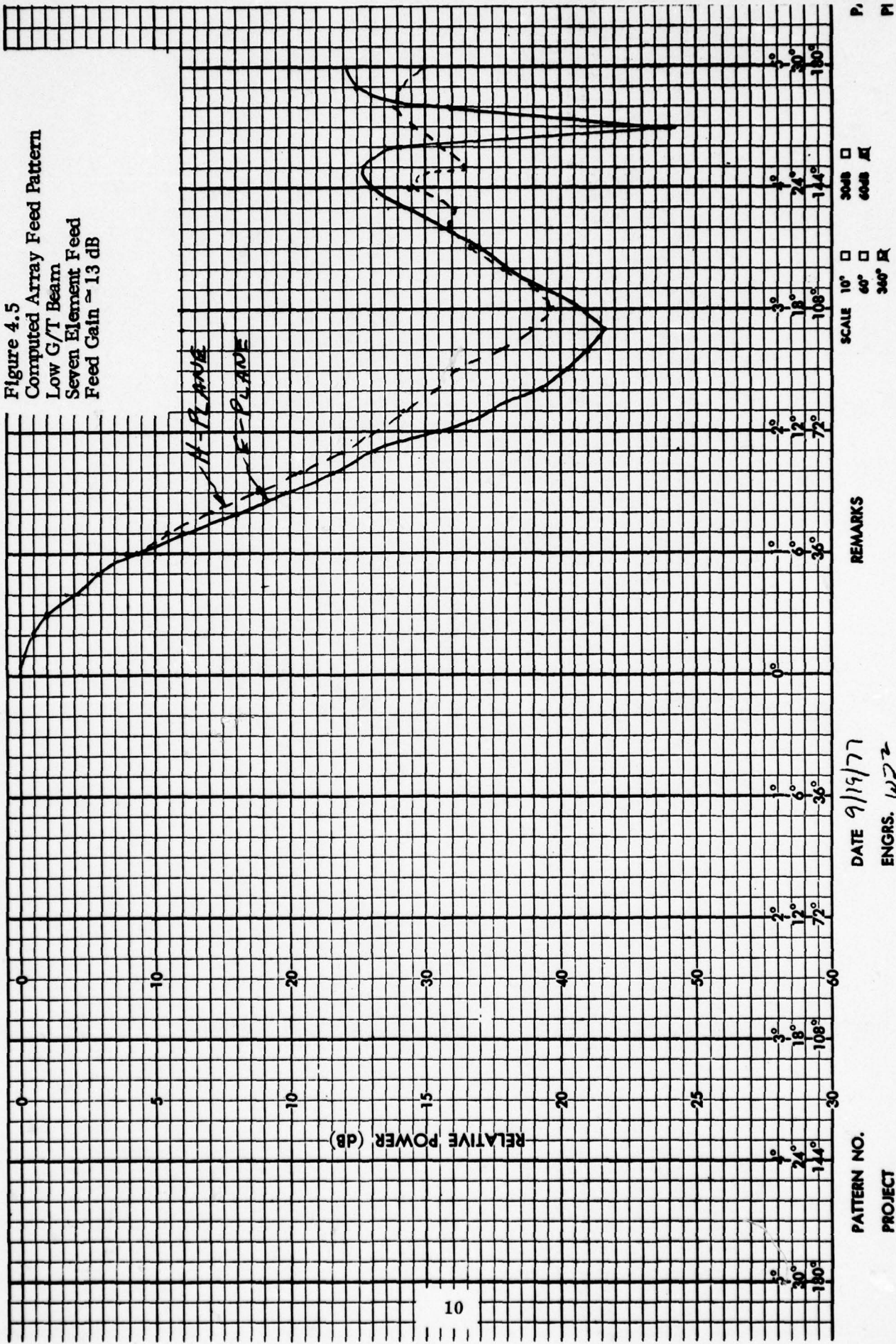


CHART NO. 179

SCIENTIFIC ATLANTA, INC., ATLANTA, GEORGIA, U.S.A.

G_{PEAK} = 7.2 dBi

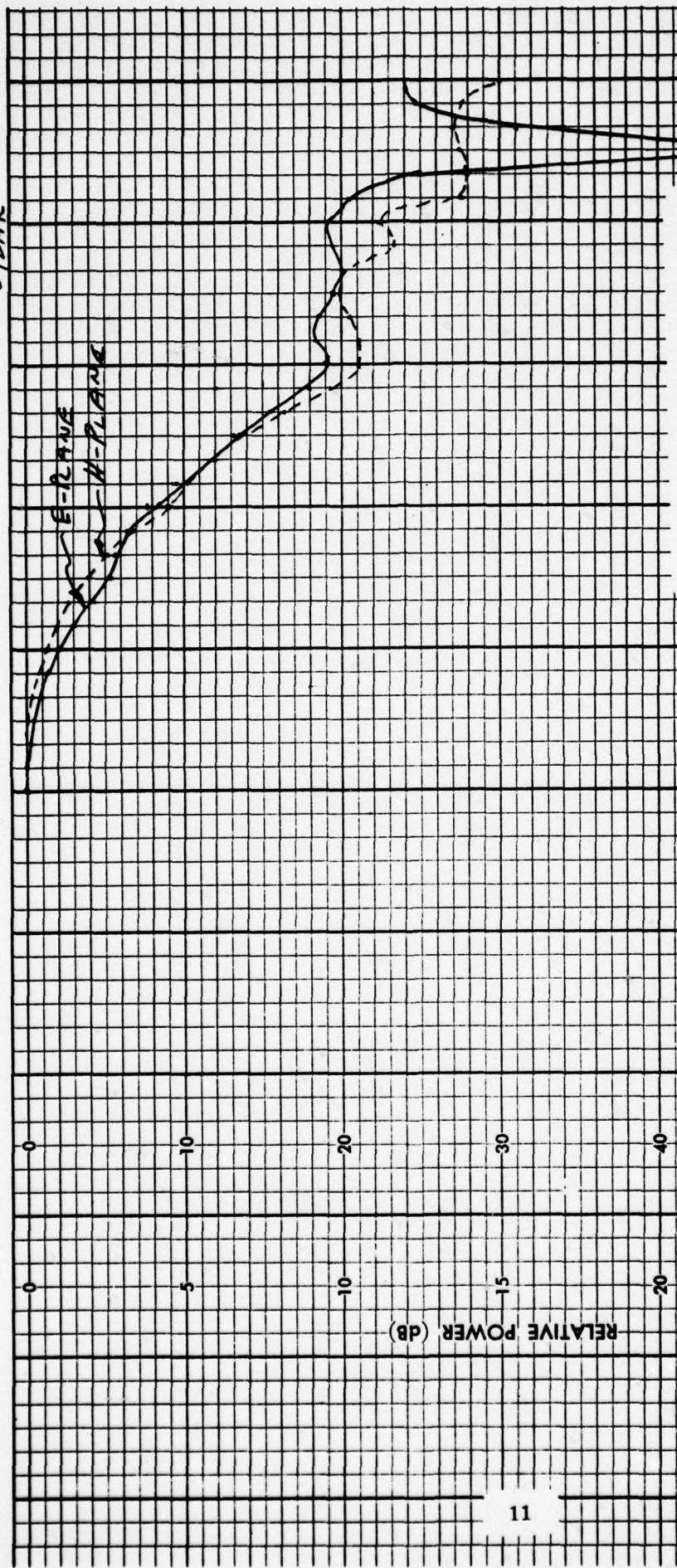
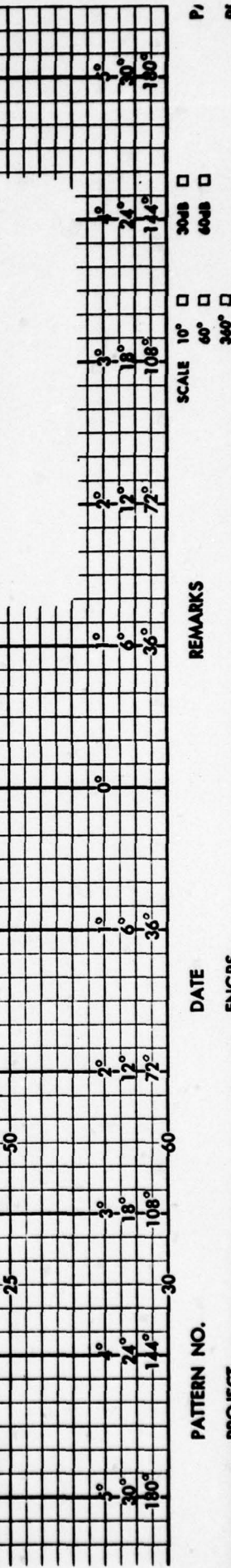
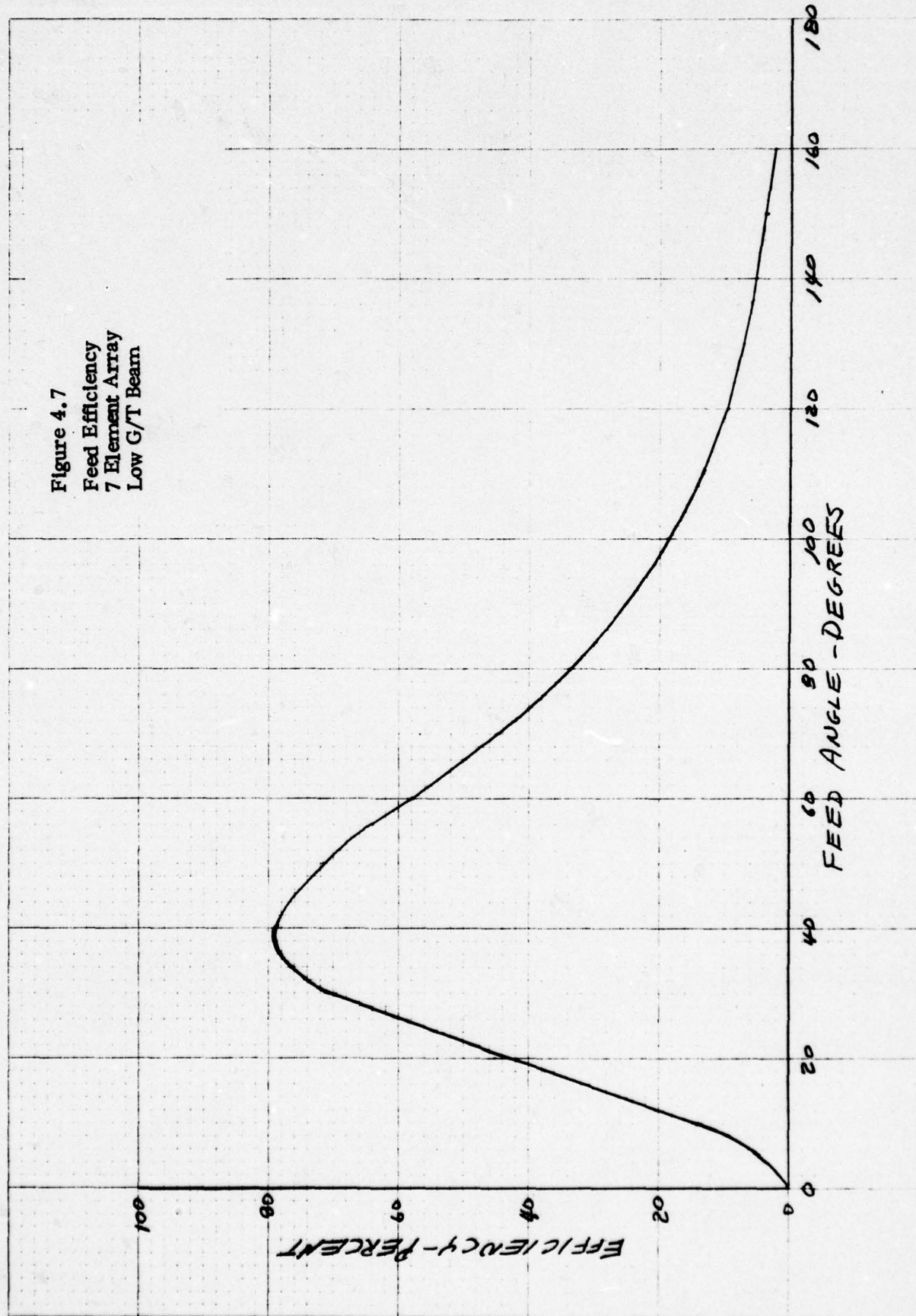


Figure 4.6
Computed Array Feed Pattern
High G/T Beams
Seven Element Feed
Feed Gain = 7.2 dB





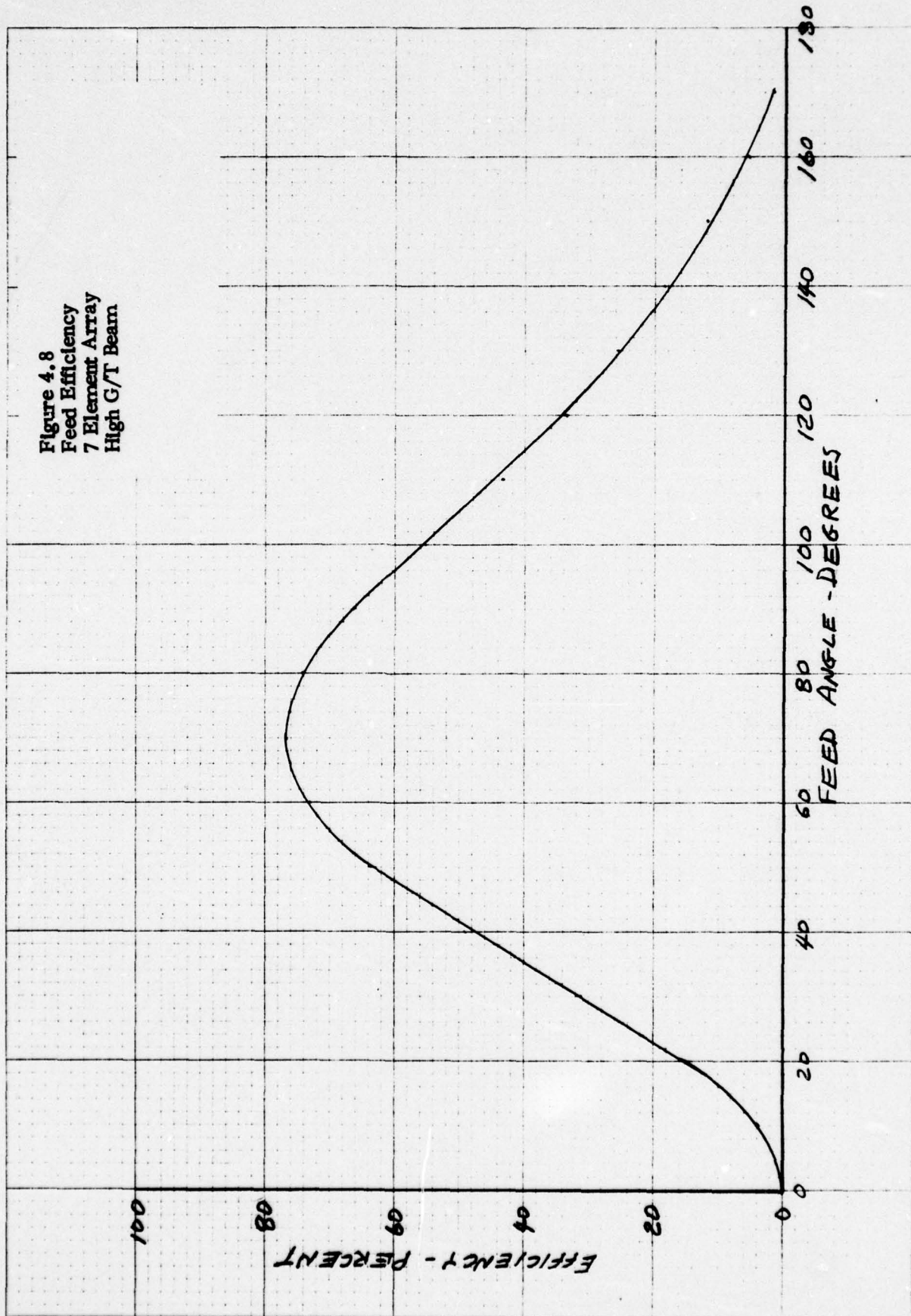
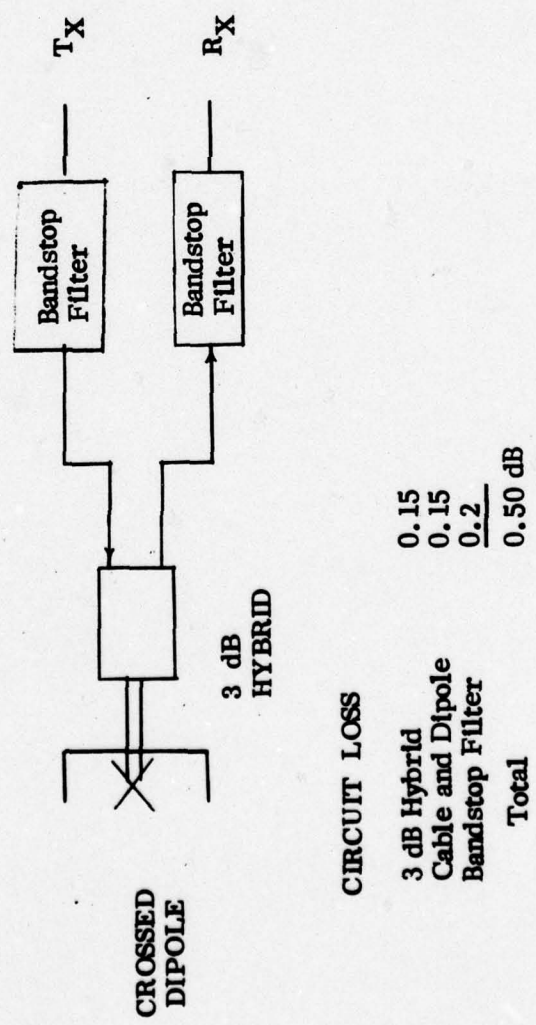


Figure 4.9
SCHEMATIC OF SINGLE ELEMENT FEED

HUGHES



CIRCUIT LOSS

3 dB Hybrid	0.15
Cable and Dipole	0.15
Bandstop Filter	0.2
Total	0.50 dB

CHART NO. 173

SCIENTIFIC ATLANTA, INC., ATLANTA, GEORGIA, U.S.A.

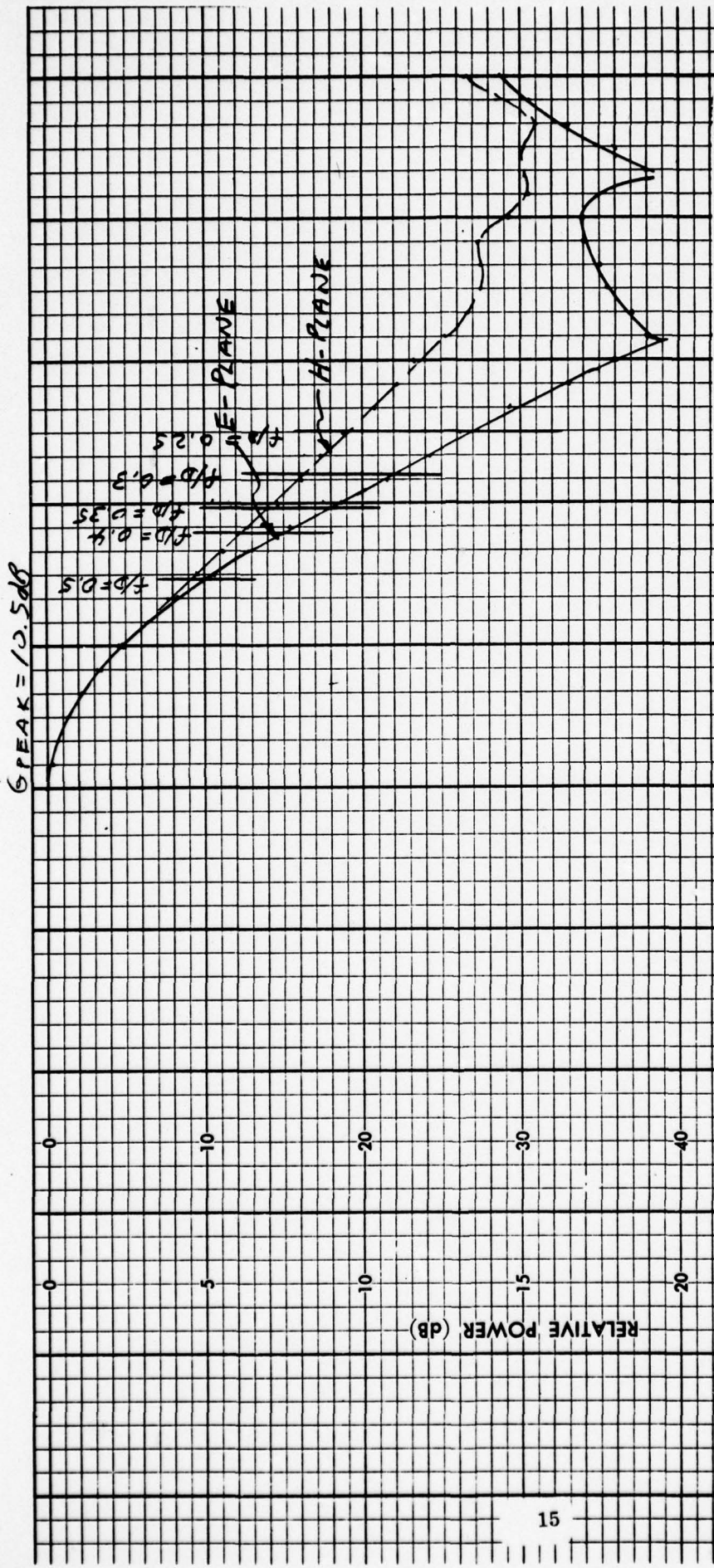
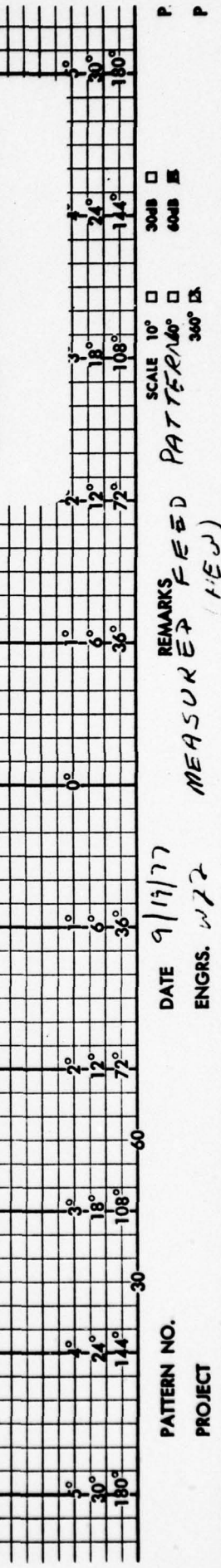
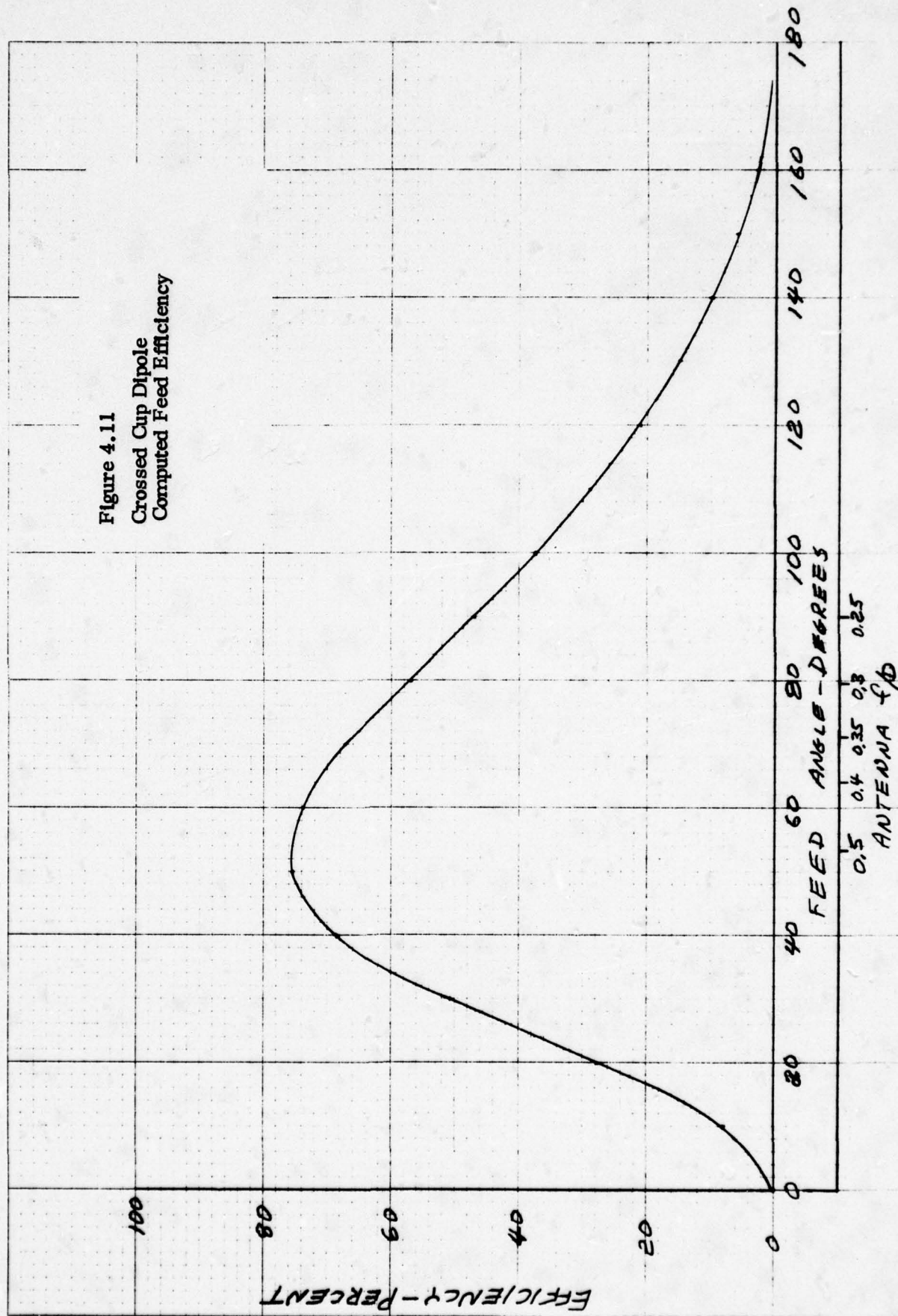


Figure 4.10
Crossed Cup Dipole
Measured Feed Patterns
Cup Dia. = 1.07λ
Feed Gain ≈ 10.5 dB (calculated)



KELLEFF & ESSER CO. MADE IN U.S.A.
10 X 10 TO THE INCH - 7 X 10 INCHES

460700



0.35) the efficiency has dropped about 15 percent, but this is still high enough to meet the G/T specification. The feed spillover level has also dropped about 6 dB from the switchable high gain beam case resulting in lower far-out sidelobes.

Feed Selection Considerations

The four-element feed is unacceptable because of its poor performance in the wide beam mode. Both the single element crossed dipole feed and the seven-element switchable feed have advantages and disadvantages. The single element feed has minimum complexity and no active components are used. It is significantly smaller than the seven-element feed and the smaller feed size minimizes aperture blockage and pattern degradation of the secondary beam. However, the single element feed does not have the flexibility of the seven-element feed of varying the gain, beamwidth, and feed spillover as a function of the elevation look angle. The disadvantages of the seven-element feed are the additional feed and switch complexity, higher RF circuit loss, and the larger aperture blockage due to the larger feed size. For an on axis feed the larger aperture blockage of the seven-element feed significantly degrades the sidelobe level and gain, and thus lesses the advantage of this feed.

From the above considerations, it appears that a single element feed would be the best choice for this application.

4.3 Reflector Size and F/D

Performance tradeoffs were performed on candidate reflectors of 10 and 12-foot diameter and F/D ratios varying from 0.292 to 0.35. A single element feed was utilized for the initial design and a seven-element feed was evaluated in a 10-foot, 0.35 F/D reflector after this was determined to be a reasonable reflector choice.

Reflectors with higher F/D's are perhaps more commonly available, but they are not included because the deeper dishes chosen tend to shadow or block interfering signals over a larger angular region. The deeper the dish, (lower F/D's), the less susceptible to interference from the rear, however, this also requires a broader feed pattern and generates more cross polarization, along with becoming physically heavier and deeper to stow.

A summary of the computed antenna parameters is given in Table 4.1. The only candidate that does not meet the G/T requirements is the 10-foot reflector with F/D of 0.30. The high feed taper resulting from the large subtended primary feed angle has reduced the peak efficiency by 0.7 dB from the F/D = 0.35 case. The 12-foot dish with .292 F/D does meet the gain even with the reduced efficiency feed due to the extra antenna area. The lower F/D cases were included in the tradeoff because these antennas have reduced spillover and backlobes. As expected the lowest far-out sidelobes are computed for the low gain beam of the switchable feed. However, relatively good sidelobe performance is predicted for all the feed configurations.

Table 4.1
ANTENNA PARAMETERS

HUGHES

Dia.	F/D	Feed		Edge Taper		Gain @ 1.25		Gain @ 4.25		Wide Angle SLL dB			Backlobe	
		E	H	Peak	Req.	Calc.	Req.	Calc.	Req.	E	H	Avg	dB	
10'	0.35	Cup	Dipole	17	13	30.1	29.0	29.5	17.7	20.7	-44	-37	-39	-4
10'	0.30	Cup	Dipole	22	16	29.4	29.0	28.9	17.7	21.4	-46	-39	-41	-7
12'	0.292	Cup	Dipole	22	16	30.9	29.0	29.8	17.7	19.2	-48	-40	-42	-4
10'	0.35	7-Element	Hi-Gain	8	9	30.6	29.0	29.8	NA	NA	-35	-35	-35	-3
10'	0.35	7-Element	Lo-Gain	30	26	27.4	NA	NA	17.7	18.0	-52	-43	-45	-2

Tables in Appendix I illustrate the efficiency analysis utilized to predict the gain of the candidate antennas. Computed secondary patterns for the five cases summarized in Table 4-1 are included in Appendix II for reference. Efficiency factors considered in the analysis include the primary feed aperture illumination and spillover efficiencies, feed insertion loss, and VSWR. Reflector efficiency factors include blockage, surface tolerance, and astigmatism. Feed and strut blockage are assumed to lie in the plane of the aperture. This assumption provides a good estimate of the blockage losses and close-in sidelobe level. The feed blockage is assumed to be centered in the aperture. For the single element feed, nine-inch square blockage is used, and for the seven-element option a 16-inch feed blockage is used. Feed support strut blockage is assumed due to four 1.5 inch diameter supports radially spaced at 90°. The struts extend from the feed to the edge of the reflector. Secondary radiation patterns are computed and shown both in the plane of the struts and the 45-degree diagonal planes. As expected the diagonal plane patterns have lower sidelobe levels.

To compute the system noise temperature, it is necessary to consider antenna loss, secondary pattern characteristics, and the noise temperature of the preamplifier. The computed antenna noise temperature for the ten-foot reflector is shown in Figure 4-12. The system noise temperature is given by:

$$N_T = (1-a) T_{ant} + a T_o + T_{amp}$$

where

N_T = system noise temperature

a = antenna feed RF loss factor

= .11 for single element feed (0.5 dB loss)

T_{ant} = antenna noise temperature (shown in Figure 4.12)

T_o = temperature of feed resistive losses = 250 degrees

A_{amp} = noise temperature of preamplifier = 36 degrees

The required antenna gain to meet the specified G/T is given by:

$$(G/T)_{dB} = G_{ant} - 10 \log_{10} (N_T)$$

or,

$$G_{ant} = (G/T)_{dB} + 10 \log_{10} (N_T)$$

where,

G_{ant} = antenna gain.

Figure 4.12

ANTENNA NOISE TEMPERATURE
VS ELEVATION ANGLE

$$N_T = 10 \log_{10} [(1-\alpha) T_{ant} + \alpha T_0 + T_{amp}]$$

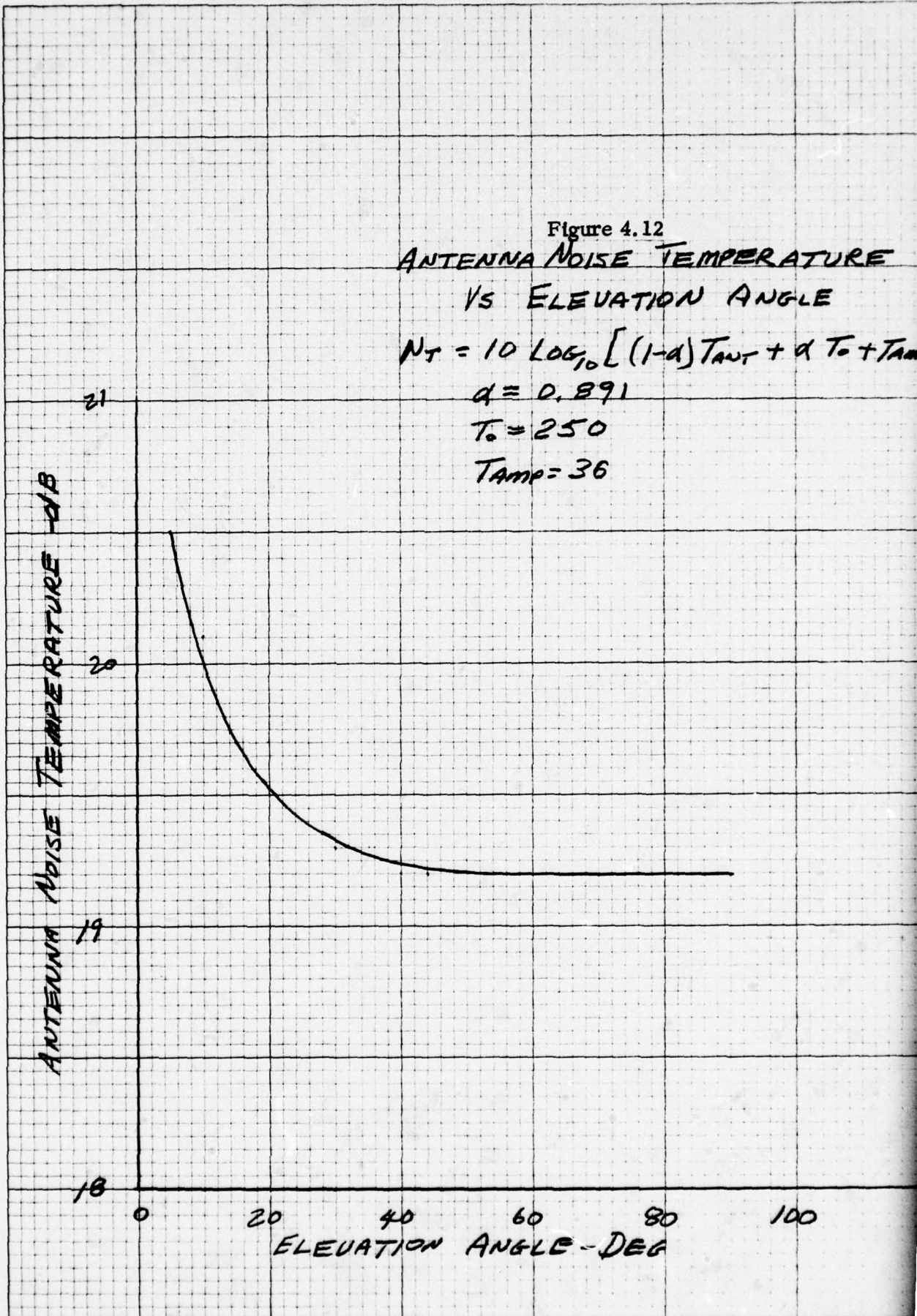
$$\alpha = 0.891$$

$$T_0 = 250$$

$$T_{amp} = 36$$

46 0700

K-E 10 X 10 TO THE INCH • 7 X 10 INCHES
KEUFFEL & ESSER CO. MADE IN U.S.A.



The required gain to meet the G/T requirements at $\pm 1.25^\circ$ and $\pm 4.25^\circ$ is shown in Table 4.1.

4.4 Blockage

An attempt was made to verify the pattern computations of the previous sections by experimental measurements on a scaled antenna. A two-foot reflector with $F/D = .346$ was fed with a cup dipole feed for these measurements. Measured primary amplitude and phase patterns for this feed are shown in Appendix III. For the test reflector used, the subtended half angle at the focal point is 71.7° , which yields an average pattern edge taper of about 12 dB.

Figures 4-13 and 4-14 are reference patterns on the reflector with minimal strut blockage. For this case the feed was supported by a single 0.125 thick support orthogonal to the E-plane to minimize the blockage effects, Figure 4-15. The first sidelobe level is -24 dB for this case, and the spillover lobe at 90° from boresight is -34 dB or about -4.3 dB below isotropic.

Strut Blockage

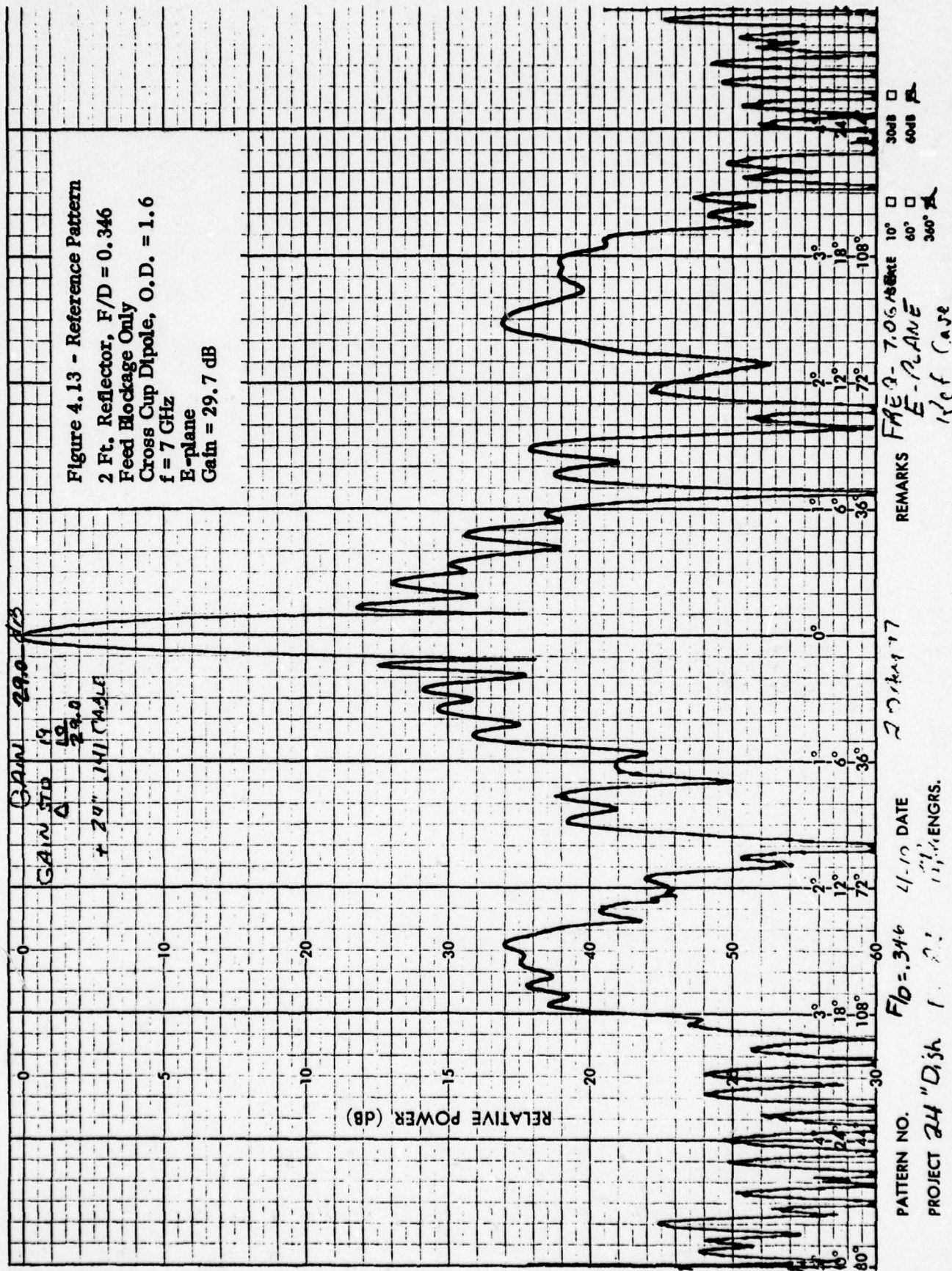
Figures 4-16 and 4-17 illustrate the effect of adding a quadripod of four 0.18λ wide struts, scaling a 1.5 inch diameter strut on the actual 10-foot reflector. The first sidelobe level increases to -20 dB, and the near-in sidelobes all increase as expected. The wide angle spillover near 90° changes shape somewhat, however, the actual level changes very little. These patterns are in the plane of struts, which is the worst case.

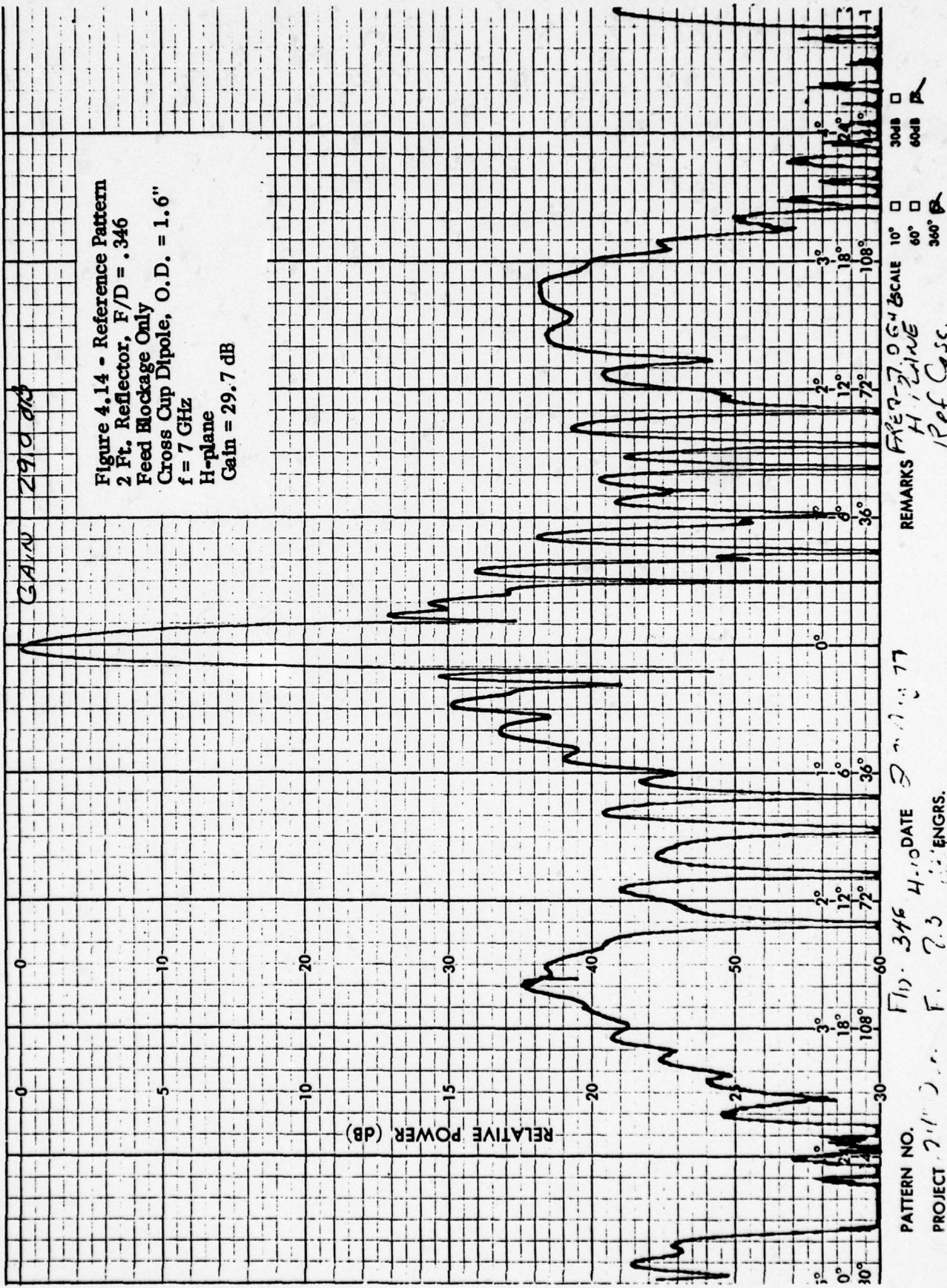
It is somewhat interesting to compare Figure 4-17 with the calculated H-plane pattern for the 10-foot reflector, Figure 4-18. The primary illumination used for the calculated pattern was 14 dB in the H-plane and 18 dB in the E-plane compared to essentially a 12 dB rotationally symmetric pattern for the measured case. Thus one would expect the calculated pattern to have slightly lower sidelobes. This is found to be the case, and the overall correlation is quite good as illustrated below:

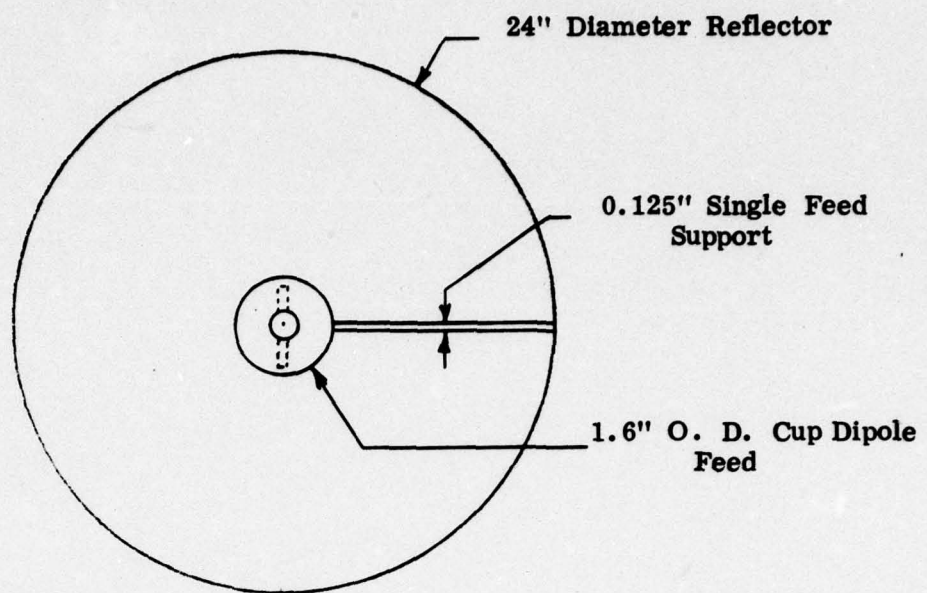
Measured and Calculated Pattern Comparison

	Near-In Sidelobe dB	Spillover Sidelobe dBi	Gain dBi	Rearlobe dBi
Measured (12 dB taper) 2-foot reflector, 7 GHz	-21	-2.3	29.7	-9
Calculated (14 dB taper plane) 10-foot reflector, 1.4 GHz	-26	-6.5	30.1	-4

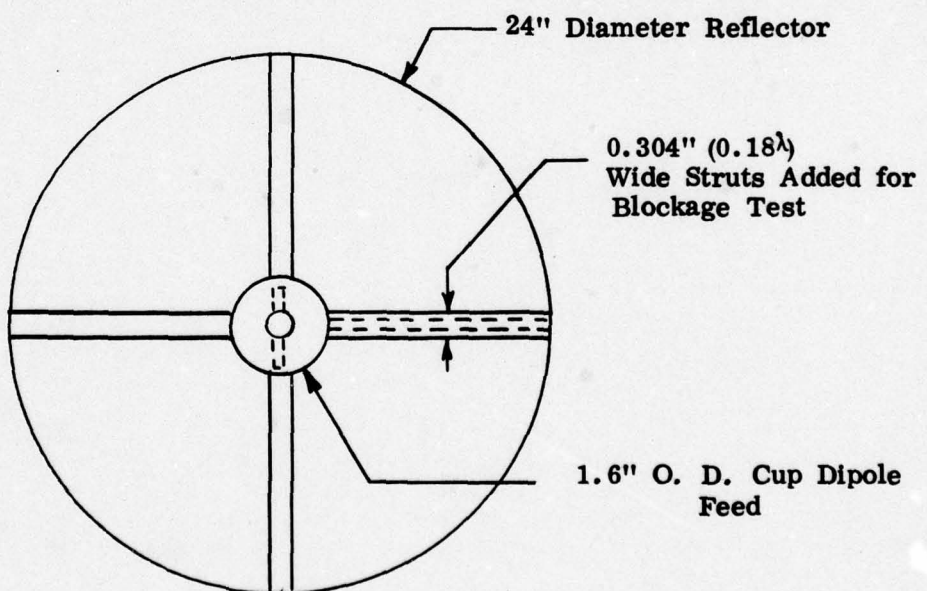
Although the two cases are not identical there is enough similarity to provide a reasonable comparison. The result illustrated gives a fairly high confidence level to the accuracy of the calculated result.







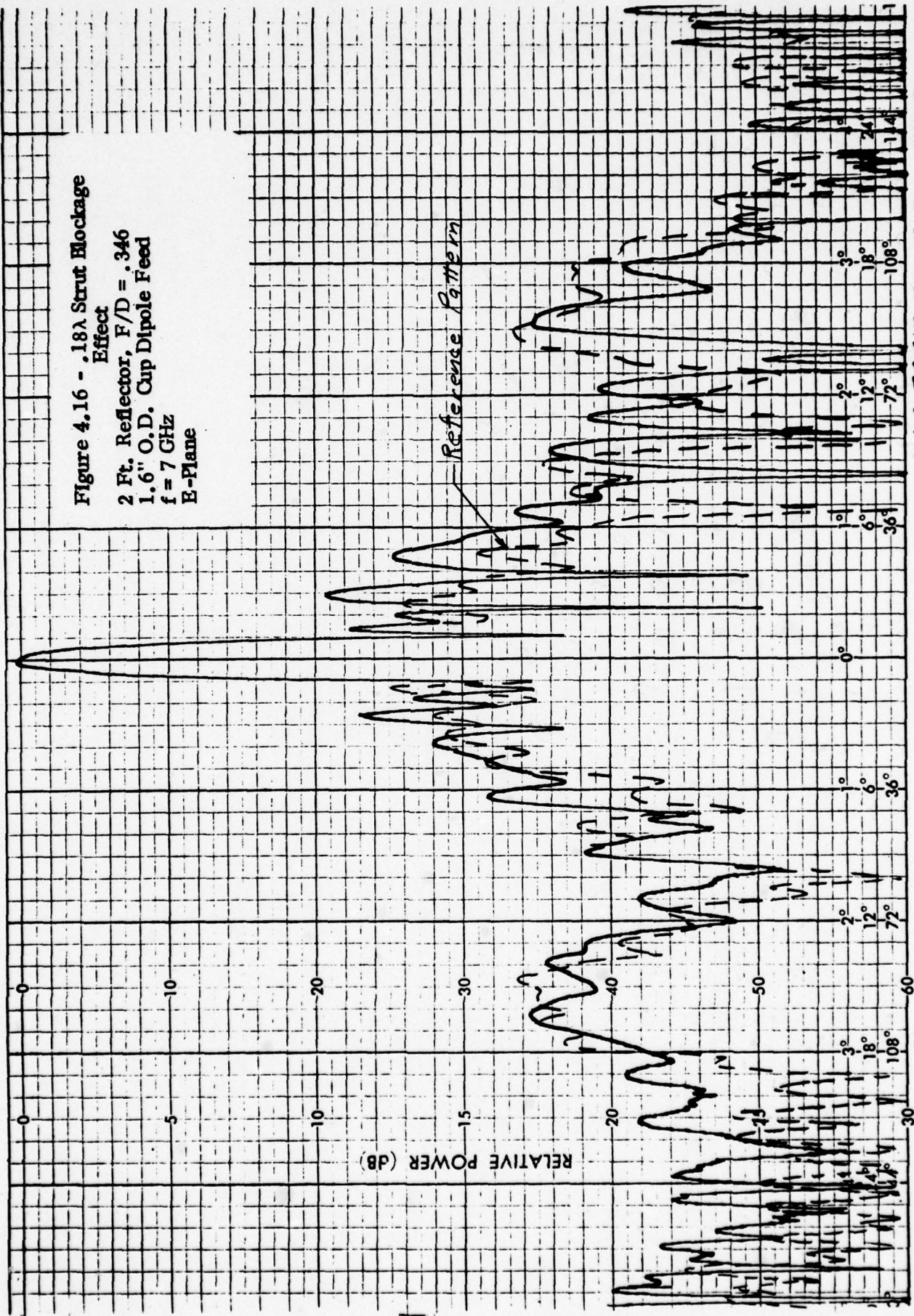
a. Reference Configuration



b. Strut Blockage Configuration

Figure 4.15 - Test Reflector Configuration Utilized for Secondary Pattern Tests

Figure 4.16 - $.18\lambda$ Strut Blockage Effect
 2 Ft. Reflector, F/D = .346
 1.6" O.D. Cup Dipole Feed
 f = 7 GHz
 E-Plane



REMARKS
 1. 7.06 GHz SCALE 10° □
 2. PLANE 60° □
 3. 041 ORTHO STRUTS 30° □
 4. EDGE OF DISH

3041
 60°
 30°

THIS PAGE IS BEST QUALITY PRACTICABLE
FROM COPY FURNISHED TO DDC

SCIENTIFIC-ATLANTA, INC., ATLANTA, GEORGIA, U.S.A.

CHART NO. 179

916

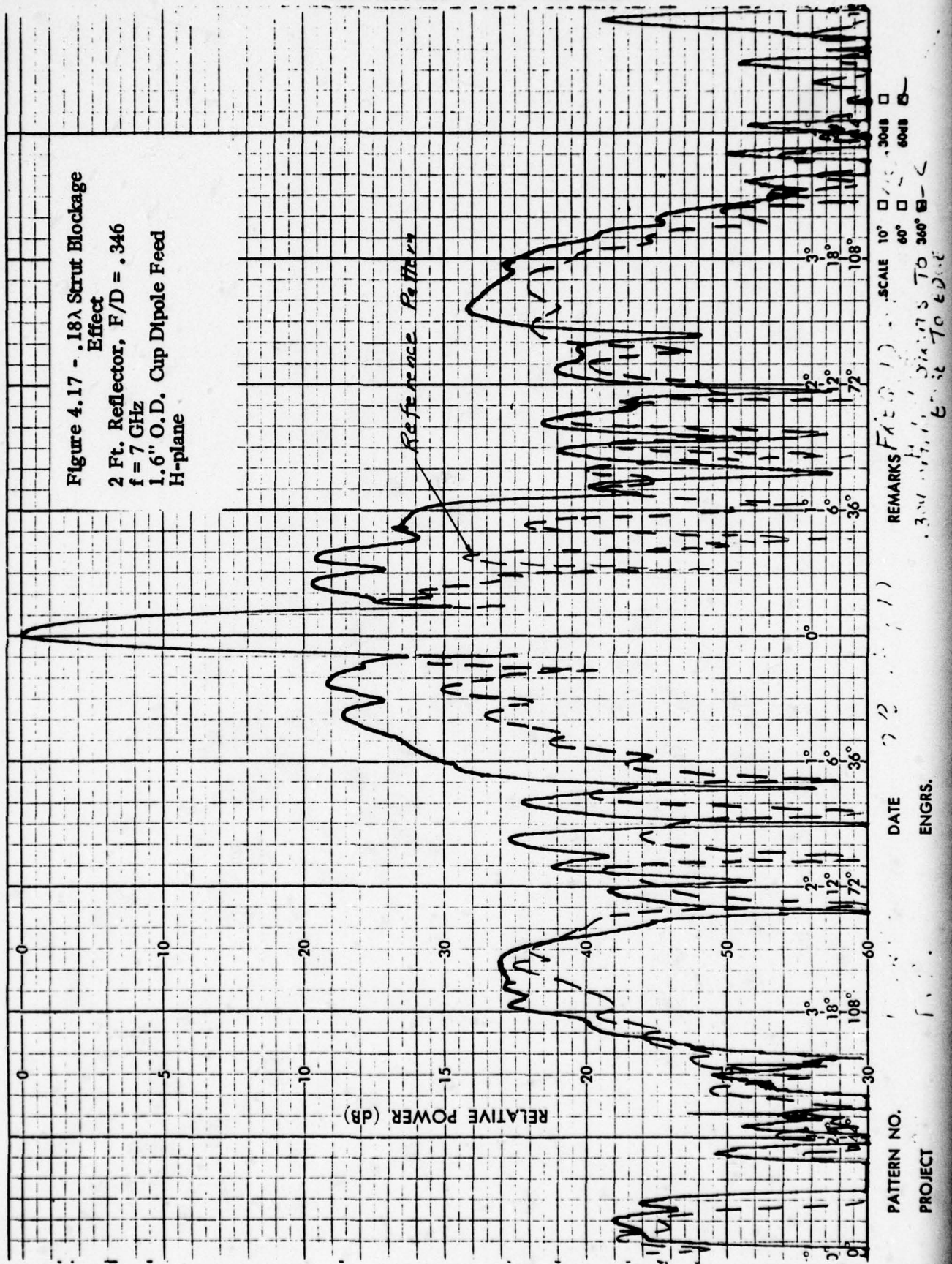
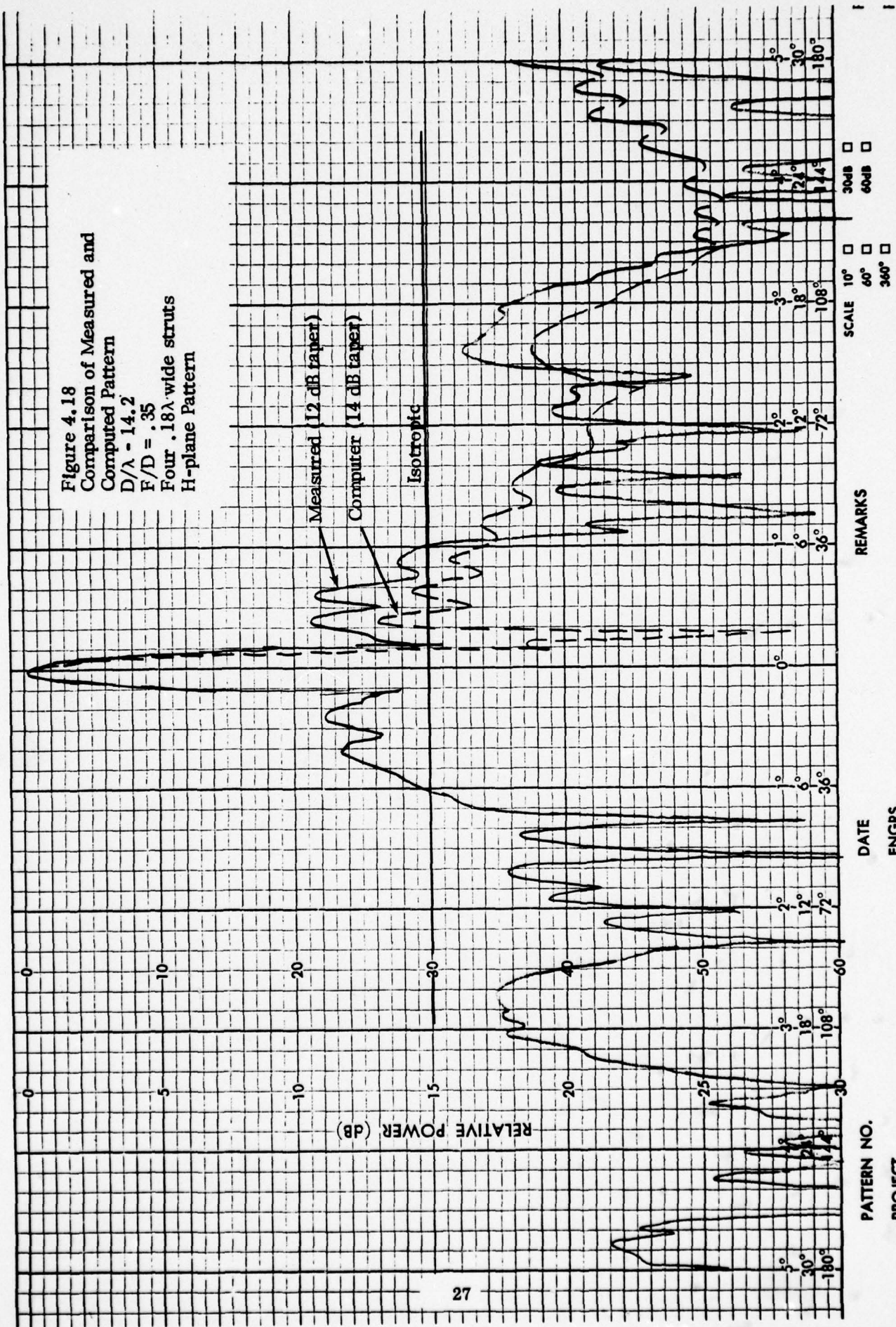


Figure 4.18
Comparison of Measured and
Computed Pattern
 $D/\lambda = 14.2$
 $F/D = .35$
Four $.18\lambda$ -wide struts
H-plane Pattern



Seven-Element Feed Blockage Test

Another set of measurements was also taken with this model. To simulate the blockage which would result from using a seven-element feed, a 3" diameter disc was attached to the feed to measure the blockage effect. Figures 4-19 and 4-20 illustrate this case. The four $.18\lambda$ wide struts were in place. The first sidelobe level increased to -18 dB, and the gain dropped to 28.6 dB or a 1.1 dB loss. However, the wide angle radiation for this case did not change staying at -34 dB or -4.3 dBi.

Center Supported Feed

In an attempt to evaluate the advantage of using a center supported feed to eliminate strut blockage and the associated sidelobe increase, a new cup dipole feed was fabricated supported by a .25" diameter center shaft. This feed was scaled from a previous design and unfortunately had significantly broader primary patterns, Figure 4-21, than the strut supported feed used for the preceding measurements on the two-foot reflector resulting in about an 8 dB edge taper. The spillover from this feed therefore results in significantly higher far-out sidelobes.

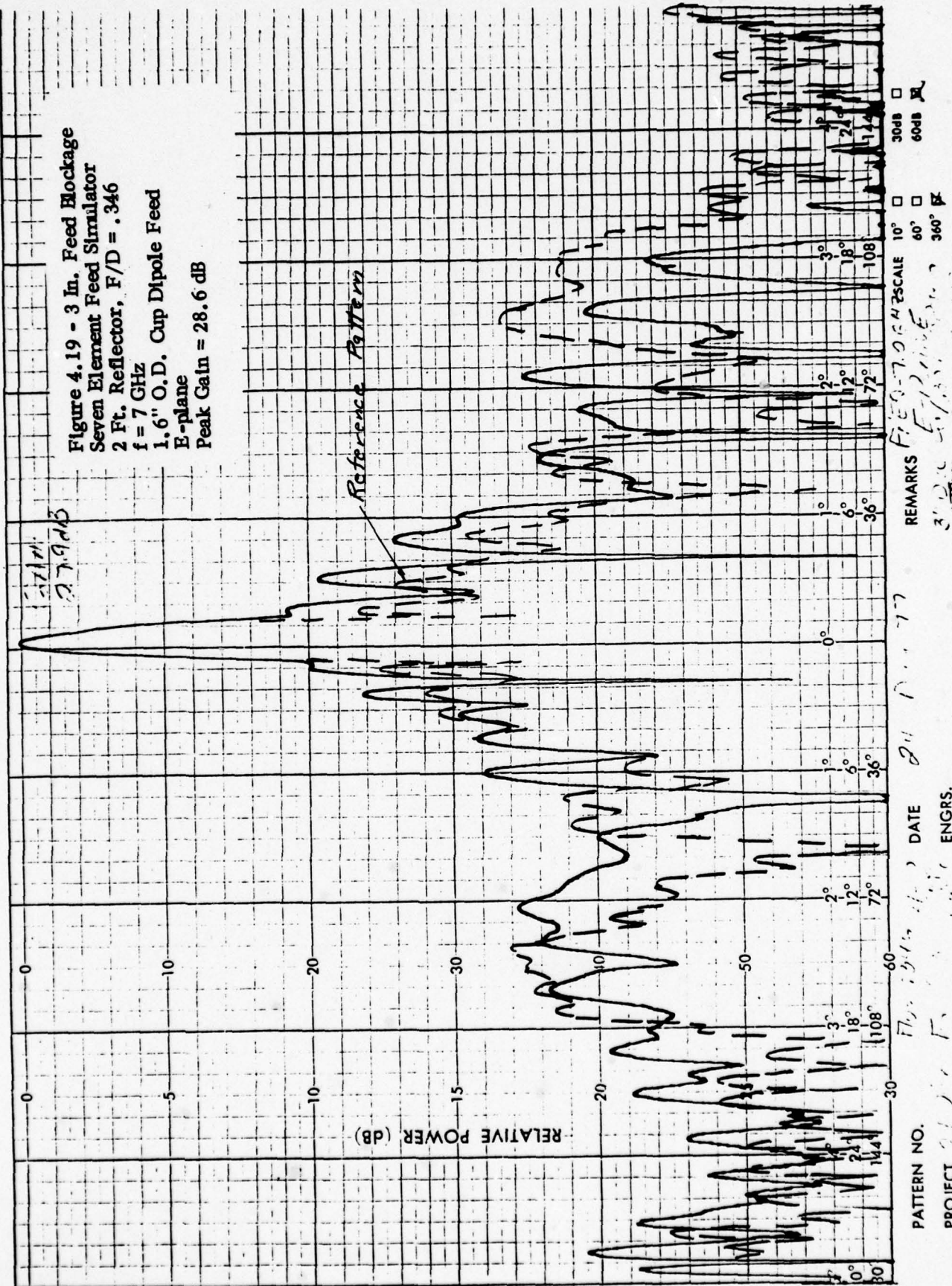
Figures 4-22 and 4-23 illustrate the secondary patterns of the two-foot reflector with this feed. Figures 4-24 and 4-25 illustrate the effect of adding the four .304" wide (.18 λ) struts. As can be seen the center supported feed does provide better sidelobe performance than a strut supported feed. By optimizing the design of this feed it would be possible to achieve similar primary patterns to those illustrated in Figure 4-10 for the conventional cup dipole feed. This would in turn reduce the far-out (near 90°) sidelobes which result principally from feed spillover. Also, the lower edge illumination would further reduce the near-in sidelobe level. Gain measurements were not made for this test configuration.

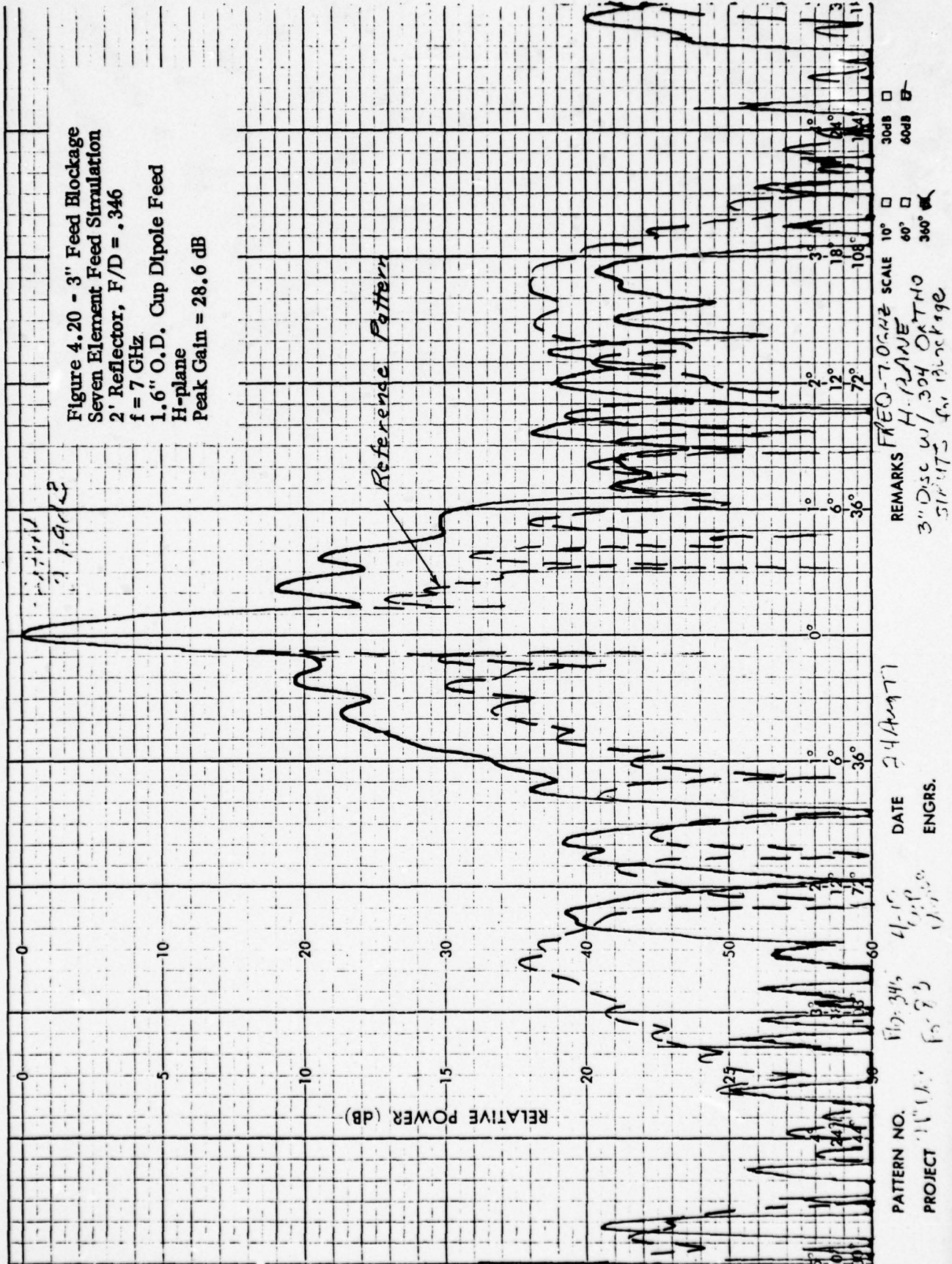
4.5 A/J Considerations

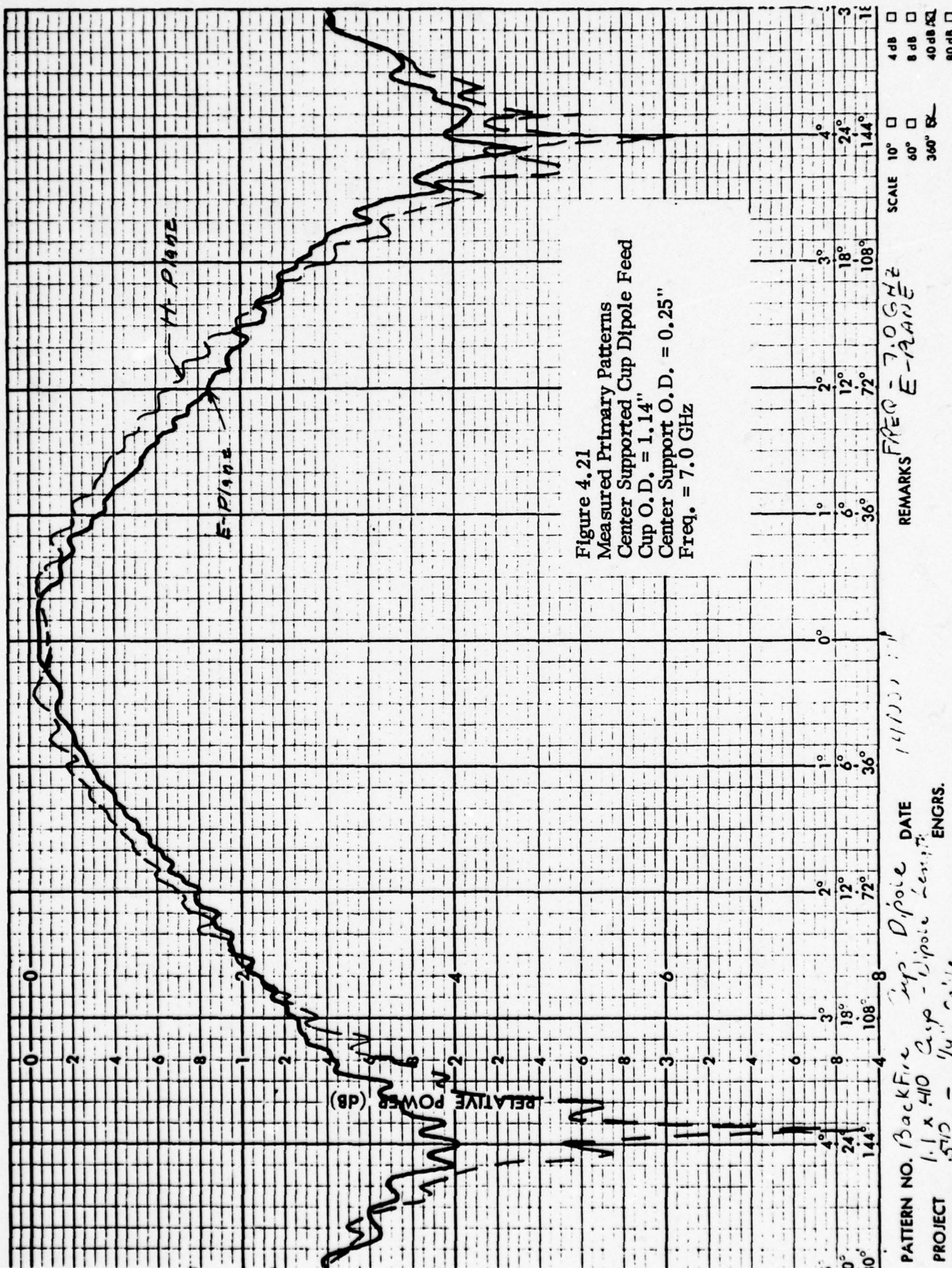
Several factors were considered with respect to the anti-jam requirements, all in an attempt to reduce the sidelobe levels both near and far from the main beam. Some of these were discussed above such as the effects of primary feed illumination control to reduce the near-in sidelobes as well as the wide angle spillover radiation. Also discussed were the effects of strut and feed blockage on the radiation patterns. Other techniques which have been considered were the use of phase errors to control sidelobe levels, sidelobe suppression techniques by use of additional radiating elements, and the use of a shroud around the antenna to reduce the wide angle spillover radiation.

Phase Error Control of Sidelobe Level

It is well known that by offsetting a feed in a paraboloid (which generates a cubic phase error) a coma lobe is formed in the secondary pattern on the axis side of the main beam. At the same time, the sidelobe levels on the opposite side of the beam are suppressed. Thus it would be







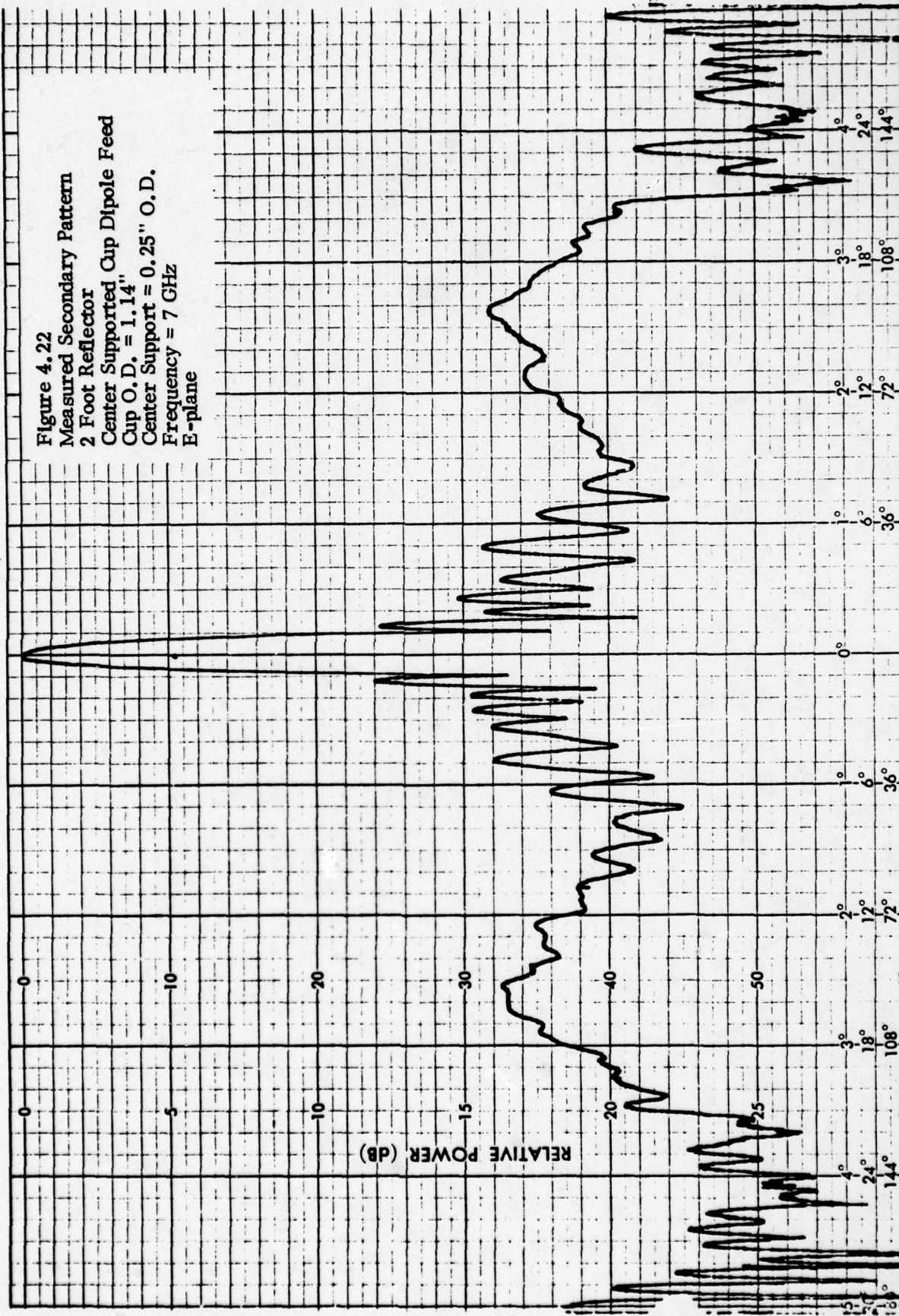
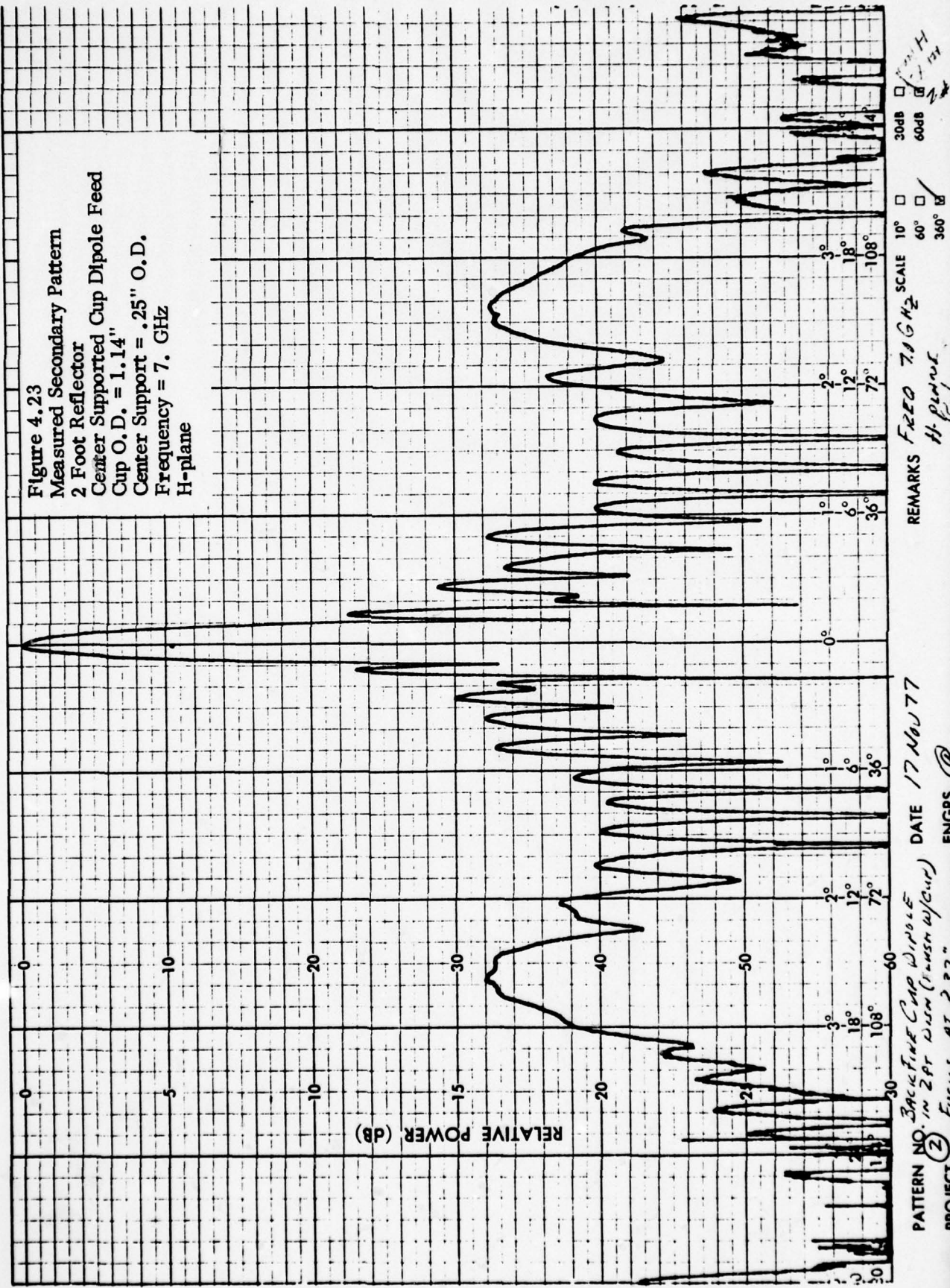
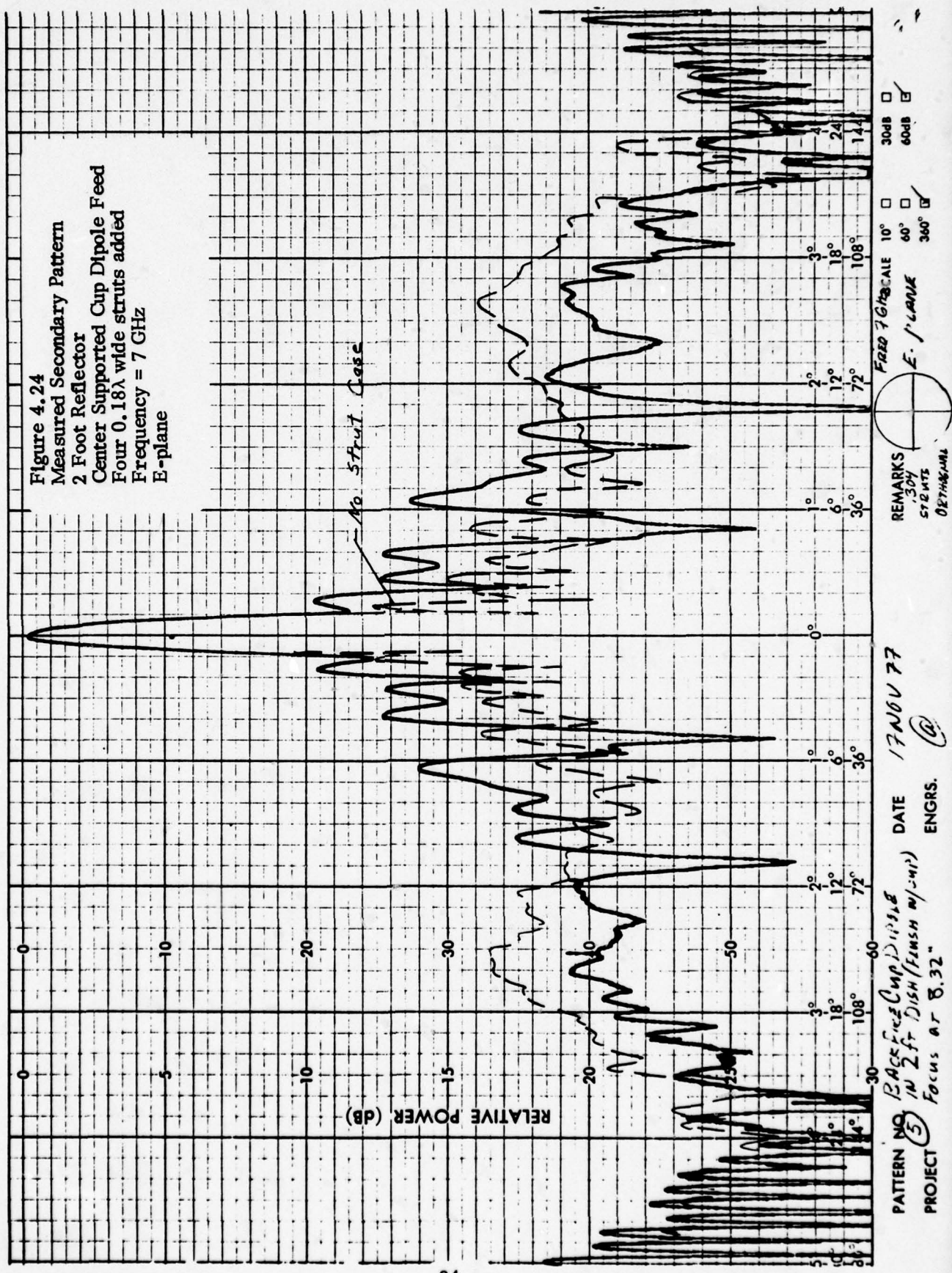


Figure 4.23
Measured Secondary Pattern
2 Foot Reflector
Center Supported Cup Dipole Feed
Cup O. D. = 1.14"
Center Support = .25" O. D.
Frequency = 7. GHz
H-plane



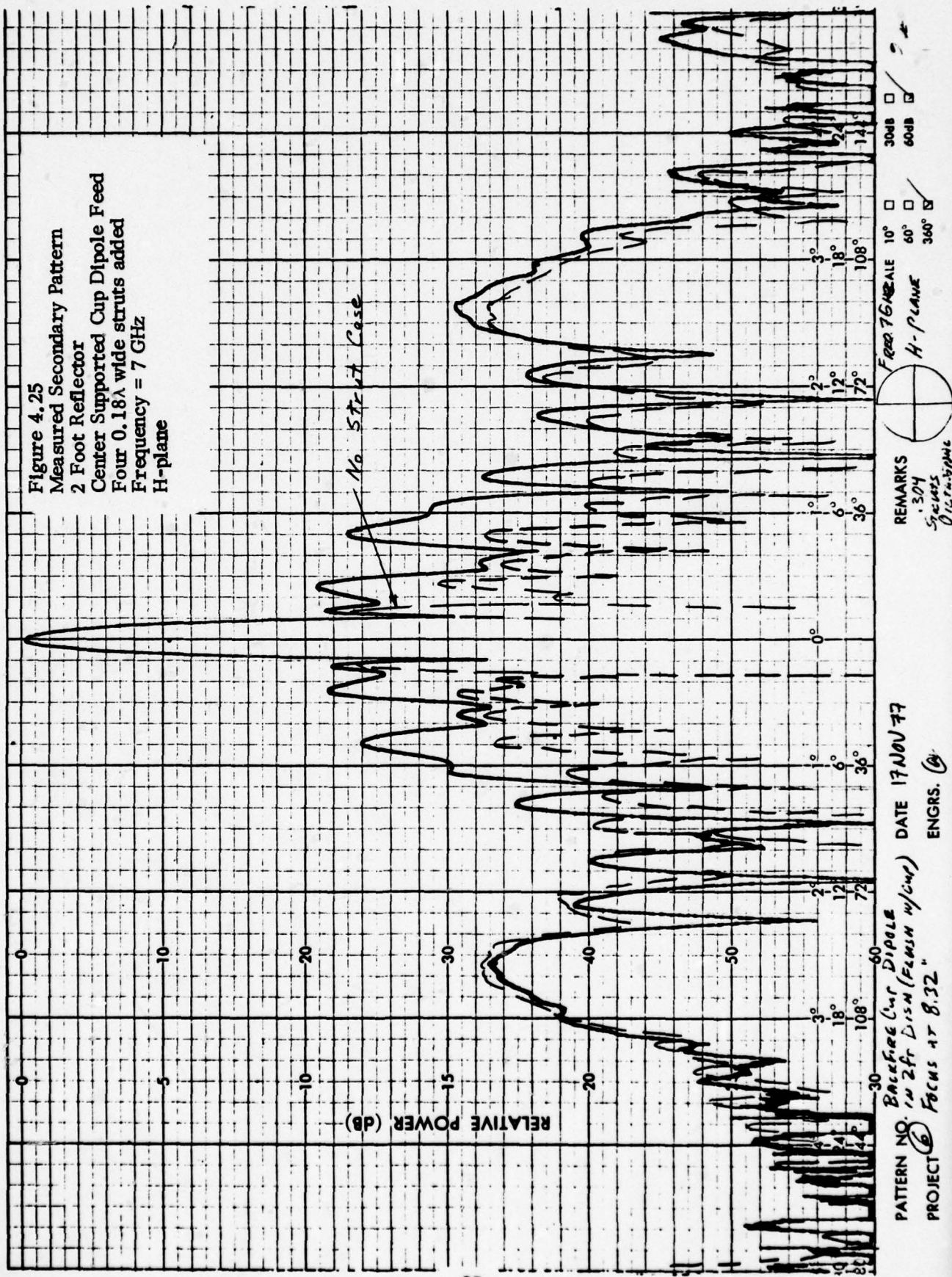
THIS PAGE IS BEST QUALITY PRACTICABLE
FROM COPY FURNISHED TO DDC



THIS PAGE IS BEST QUALITY PRACTICABLE
FROM COPY FURNISHED TO DDC

SCIENTIFIC ATLANTA, INC., ATLANTA, GEORGIA, U.S.A.

CHART NO. 173



possible to selectively reduce the sidelobe level in a given region by physically offsetting the feed. This would provide a simple technique of selectively controlling sidelobes, however, the extent of improvement using this technique was not analyzed.

Sidelobe Suppression

Most sidelobe suppression schemes utilize a separate antenna or horn mounted on the main antenna with a radiation pattern which is higher in gain than all the sidelobes to be suppressed, but lower in gain than the antenna main beam. A comparison is then made to determine if a receive signal is stronger in the main antenna or in the sidelobe suppression (SLS) antenna. If the SLS signal is larger, the signal is then ignored. The technique for cancellation depends on the sophistication required which impacts the signal processing required. To permit reception of a signal on the main beam while rejecting a signal on a sidelobe requires a coherent cancellation scheme which effectively cancels the offending sidelobe, or places a null in the direction of the interfering signal.

Shroud

It is relatively a common practice to put a shroud over a paraboloidal reflector to reduce the wide angle interference, especially for small communication antennas. This shroud generally is more effective if the shroud is lined with absorbing material. In the present application it is not practical to add effective absorbing material inside the shroud due to the reflector size and because of the thickness of the material that must be added at such a low frequency. The use of a shroud for the present application was restricted to a metallic one where its effect cannot easily be computed.

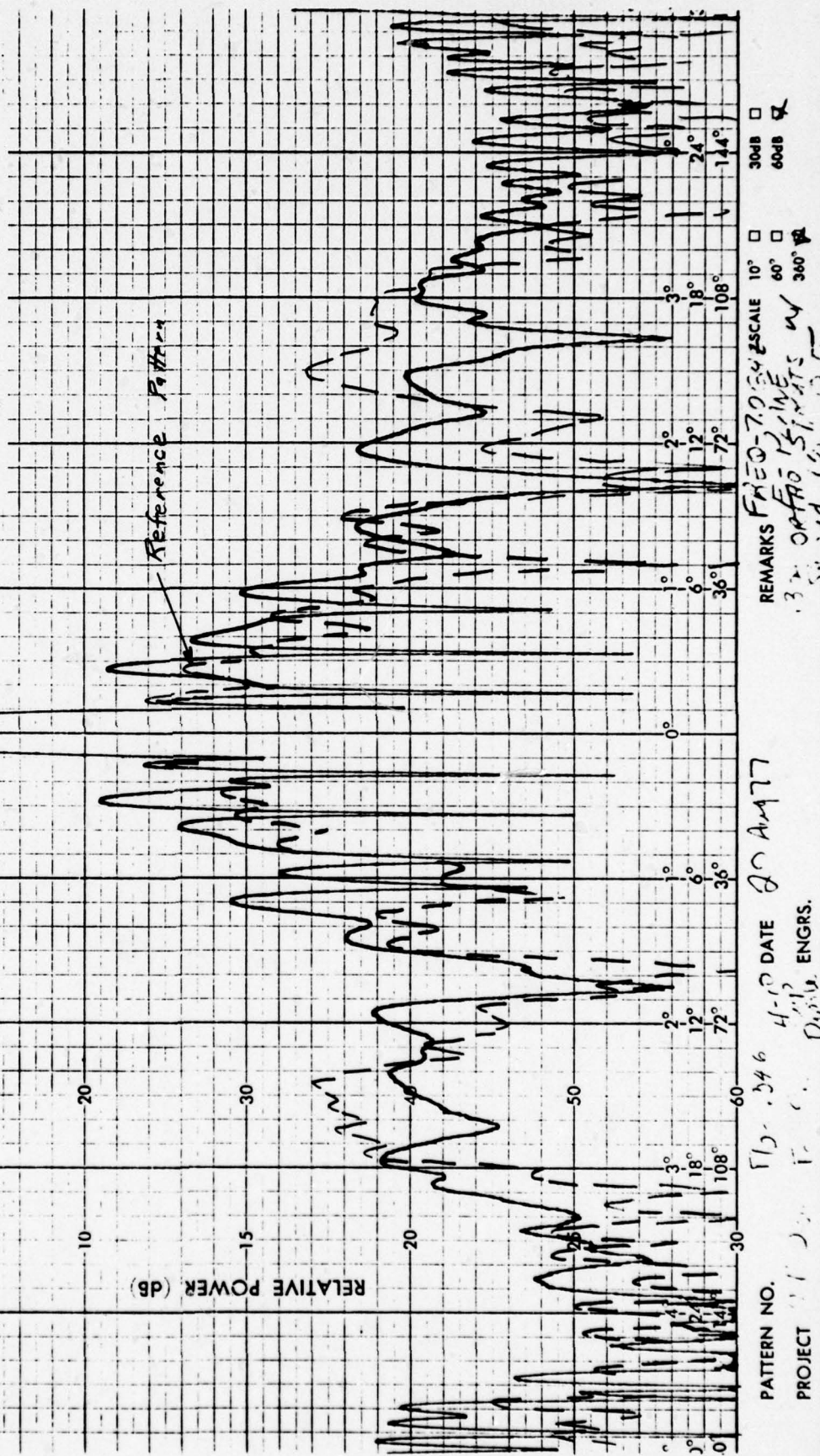
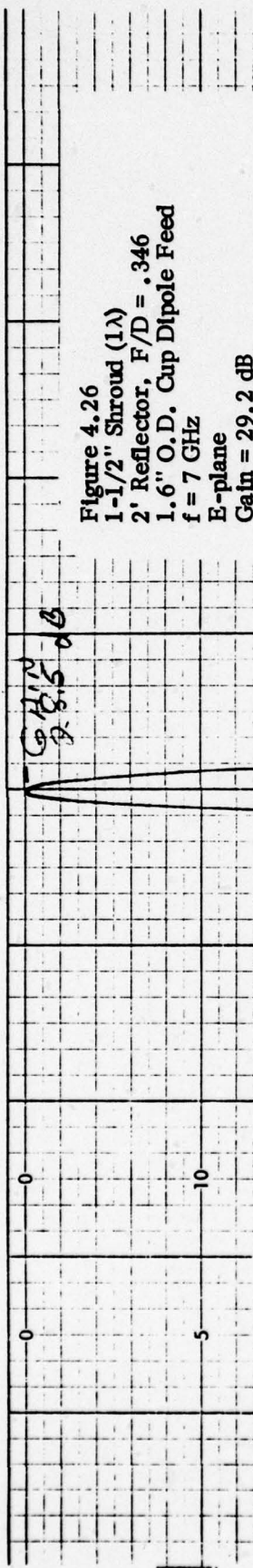
Since the use of a shroud to reduce the wide angle radiation has an effect which cannot easily be computed, a set of experimental measurements were made to determine the feasibility and advantages gained by such an approach on the system under consideration. Figures 4-26 and 4-27 show the effect of adding a 1-1/2" deep cylindrical shroud (about one wavelength) around the two-foot test dish, still configured with the four 0.18λ wide strut assembly. The pattern shape changes significantly, with the wide angle radiation dropping to about 37 dB, or about -7 dBi. Little change occurs near in, however the intermediate region sidelobes around 36° from boresight begin to increase. This is due to scattered energy from the shroud being redirected into this region.

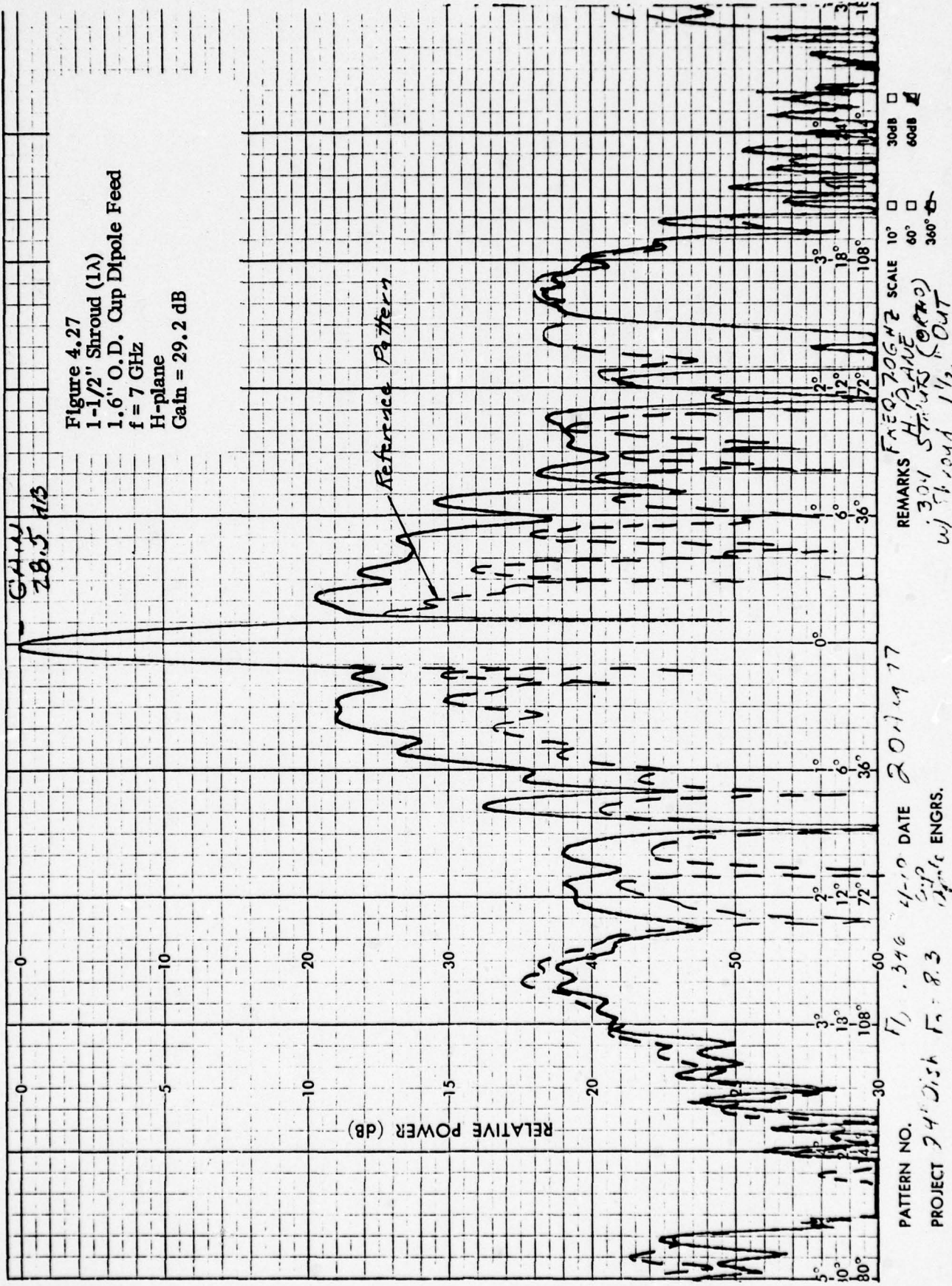
This shroud was further extended to 2-1/2" or about 1.5 wavelengths. Little significant change was noted for this case, although the radiation near 90° increased to its original level of -34 dB in the E plane. Some asymmetry was noticed in the wide angle radiation which may be due to the measurement setup. The detector and cable used on the back of the feed is asymmetrical and may be causing some measurement difficulty in these lower sidelobe regions.

THIS PAGE IS BEST QUALITY PRACTICABLE
FROM COPY FURNISHED TO DDC

SCIENTIFIC ATLANTA, INC., ATLANTA, GEORGIA, U.S.A.

CHAP. NO. 179





Use of the shroud did affect the gain. The reference case measured gain was about 29.7 dBi. With the one wavelength shroud the gain reduced to 29.2 dB, or 0.5 dB loss. The 1.5 wavelength shroud further reduced the gain to 29 dB, or a total of 0.7 dB loss.

Low Angle Multipath

One additional factor considered in response to the original requirement of low angle tracking was the effect of multipath interference for very low elevation angles. Figure 4-28 illustrates the unperturbed pattern calculated for the 10-foot reflector at an elevation angle of 5 degrees. Figures 4.29 and 4.30 illustrate the effects of multipath over sea water ($\epsilon_r = 81$ and $\sigma = 4.0$) for both the horizontal and vertical polarized component for an antenna elevation of 12 feet above a ground plane. Little main beam degradation occurs. The sidelobe level, however, has been chopped up and in general has increased several dB. If the antenna were to scan lower than five degrees a significant portion of the main beam would illuminate the ground. This could cause severe pattern degradation in the main beam region. Above five degrees elevation multipath should have little effect on system performance.

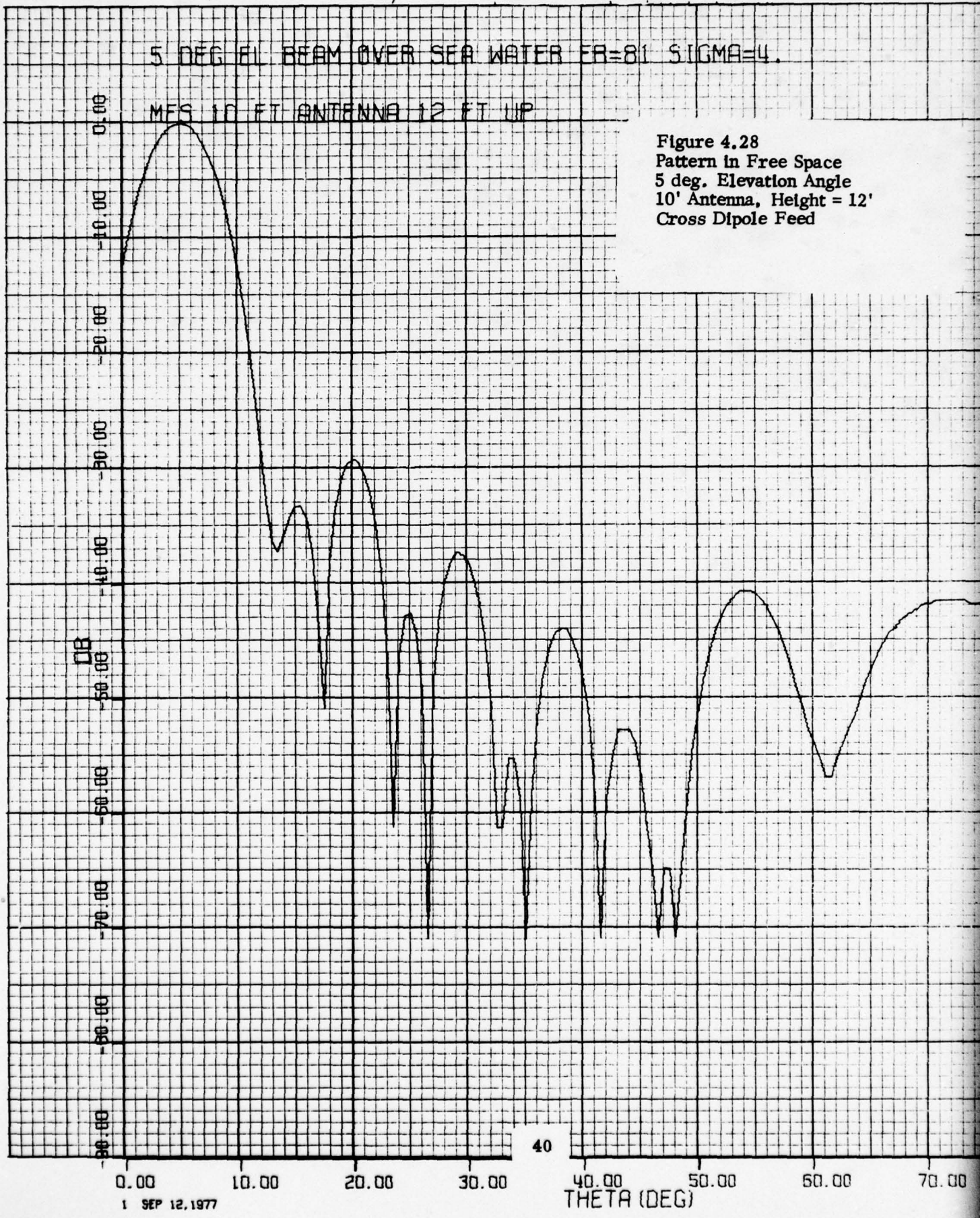
4.6 Tradeoff Summary

Table 4.2 summarizes the results of the experimental measurements made during the tradeoff studies. These measurements were made using a 2-foot diameter paraboloid at a scaled frequency of 7 GHz. The feed used was a cup dipole providing an edge taper of about 12 dB, rather than the recommended 14 to 17 dB for optimum G/T performance. The feed was supported by a 0.125" wide strut oriented orthogonal to the E-plane to minimize the blockage effect of the strut. Use of a feed with a higher taper would reduce both the near-in sidelobe level as well as the far-out spillover lobes directly by the amount of the additional taper.

For this size reflector, it appears the use of a one wavelength shroud would reduce the wide angle radiation (near 90°) by about 3 dB, however, this is at a cost of 0.5 dB in gain. This does not appear to be a desirable tradeoff for the small decrease in jamming susceptibility.

The use of a seven-element feed to achieve beamwidth control results in about 1.1 dB gain loss due to blockage and an increase in near-in sidelobe level which again appears to be a rather high price to pay for the added pattern control obtained. From the measured results, it seems that best compromise is the use of a single cup dipole feed optimized for overall performance.

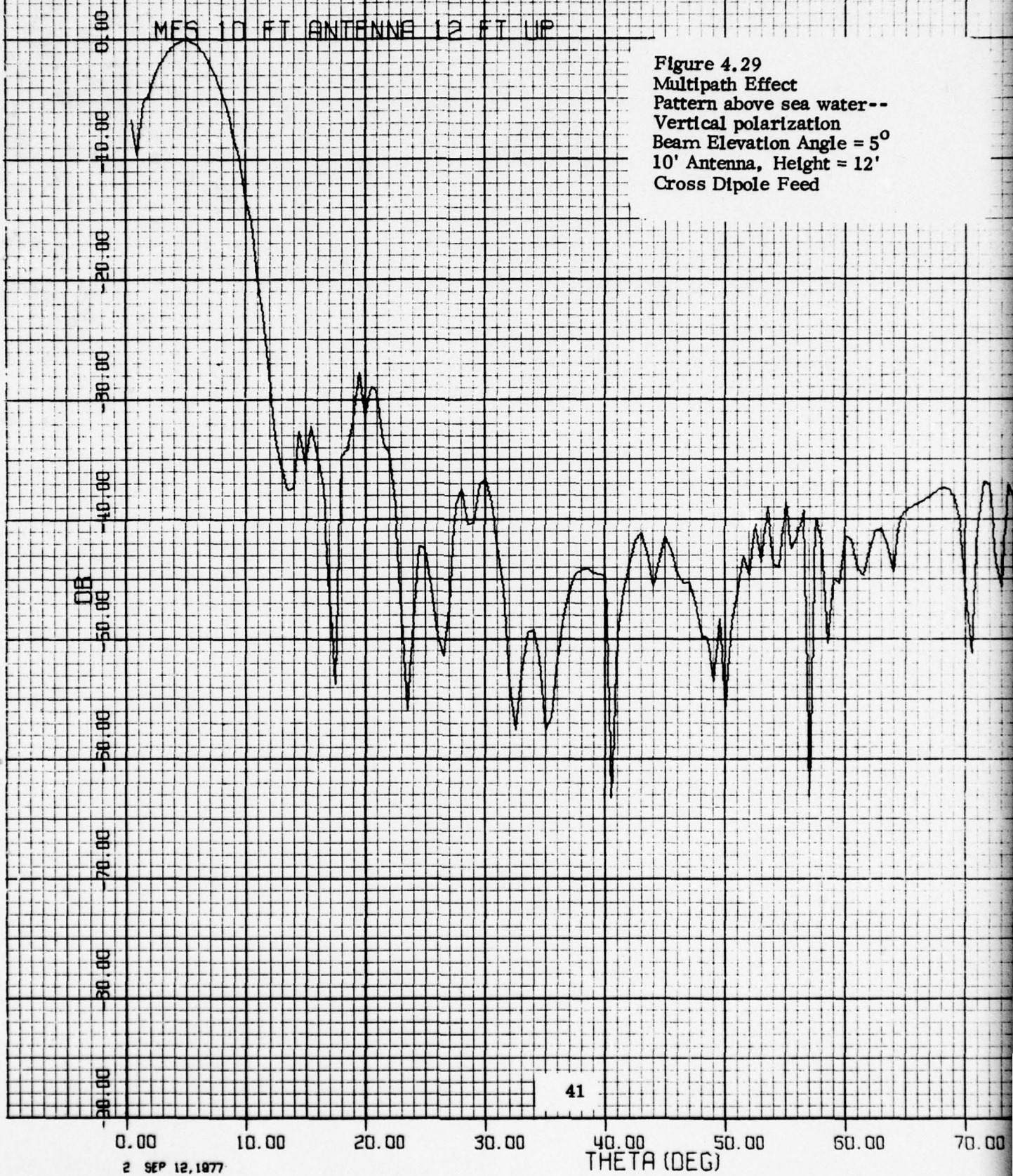
Based on the parameters considered, it appears that the best choice for the antenna design would be a 10-foot diameter, 0.35 F/D paraboloid fed with a single cross dipole feed designed to provide an edge illumination taper of about 15 dB. This design meets the G/T requirements at all elevation angles when used with a 36° K preamp, and has good far-out sidelobe performance. The simplicity of this approach would seem to outweigh any advantage of the seven-element feed, and the blockage effects are smaller. However, if excessive filter losses were encountered due to system filter requirements, the G/T would become marginal for



PATTERN ABOVE GROUND PLANE, VERT POL

5 DEG ELEV BEAM OVER SEA WATER FR=81 SIGMA=4.

MFS 10 FT ANTENNA 12 FT UP



PATTERN ABOVE GROUND PLANE, HORIZ. POL.

5 DEG ELEVATION ANGLE OVER SEA WATER FR=81 SIGMA=4.

MFS 10 FT ANTENNA 12 FT UP

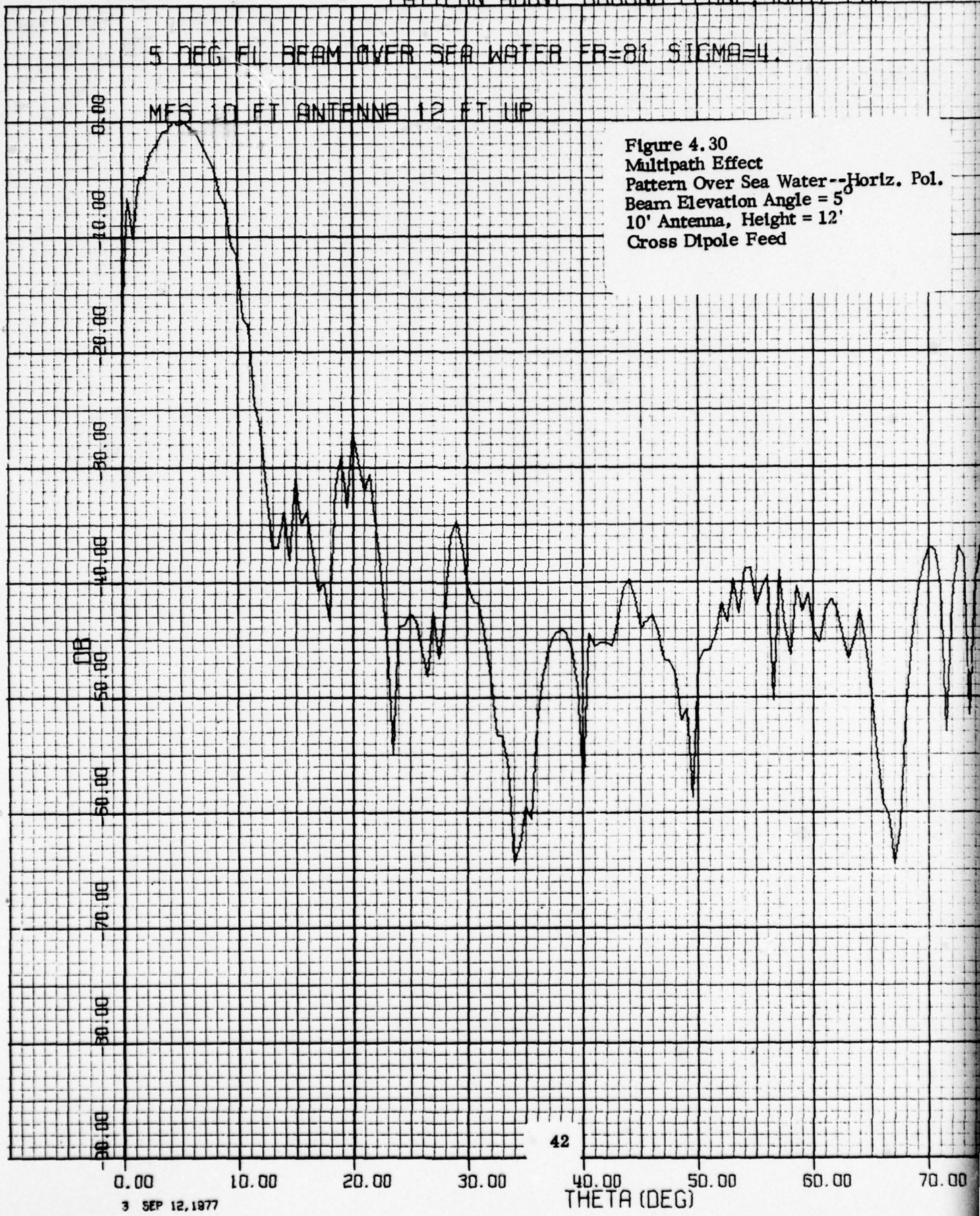


Figure 4.30
Multipath Effect
Pattern Over Sea Water--HORIZ. POL.
Beam Elevation Angle = 5°
10' Antenna, Height = 12'
Cross Dipole Feed

Table 4.2. Summary of Scale Model Measurements.

A. Strut Supported Cup Dipole

Case	Plane	Max SLL (0-20°) (dB)	Max SLL (60-90°) (dB)	Gain (dBi)
Ref. (single .125" strut)	E	24	34	29.7
.304" Struts	E	21	35	--
	H	20	32	
Struts and Shroud 1-1/2"	E	21	37	29.2
	H	20	37	
2-1/2"	E	22	34	29
	H	22	34	
Struts + 3" Disc	E	18	34	28.6
	H	18	36	

Frequency = 7 GHz
D = 24" Reflector
F = 8.3"
F/D = .346
Feed = 1.6" O.D. cup dipole
Edge Taper = 12 dB

B. Center Supported Cup Dipole

Case	Plane	Max SLL (0-20°) (dB)	Max SLL (60-90°) (dB)	Gain (dBi)
Reference	E	24.	32	Not Measured
	H	22.5	32	
0.304" Struts	E	20.5	35	Not Measured
	H	21	30.5	

24" Reflector
F = 8.3"
F/D = .346
Feed = 1.14" O.D. center supported cup dipole
Frequency = 7 GHz
Edge Taper \approx 8 dB

this design, and this factor should be considered in the final system definition.

An additional improvement in performance can be achieved by eliminating the feed support struts and using a center supported cup dipole. This reduces the forward region sidelobes by eliminating the strut blockage and scatter effects. The model of this type feed utilized in the experimental tests provided about an 8 dB edge taper resulting in fairly high spillover sidelobes. This design can be optimized to provide the desired 15 dB taper which would directly reduce the spillover lobes by the amount of the additional taper. Also, the forward sidelobes would be reduced due to the increased illumination taper. The overall performance would thus be improved by this technique.

5.0 System Tradeoffs, Mechanical

5.0 System Tradeoffs, Mechanical

5.1 Van Mounted Antenna

During the early part of this study, the antenna was to be mounted on a 40-foot long van with the antenna stowed in the top part of the van. It was to occupy a stowed volume of no more than 7-1/2' wide, 1-1/2' deep and 20' long. The deployment time was to be several tens of minutes. Figure 5-1 shows one concept that meets the above constraints. Step 1 shows the transportation mode on a 40' trailer. Step 2 shows where the upper rear part of the van is used for storage space. The cover is pulled back on top of the front portion of the van. Leveling is also done at this stage using the leveling jacks located on the outriggers and at the front of the van. The basic elevation and azimuth assemblies are preinstalled on the telescoping tower. The basic 7' diameter reflector is assembled to the elevation axis and drive crank shaft. The remainder of the reflector panels and feed support struts are attached to the antenna in Steps 4 and 5. In Step 6 final adjustment of the feed is done at the focal point and cables are attached to the stabilizers and towers. After elevating the antenna to an operation mode, the cables are preloaded.

Figure 5.2 shows the three views of the antenna in the operation mode. For normal operation, the antenna is elevated to 24 feet. Six feet additional extension is possible, but will require removal of the azimuth assembly. Figure 5.3 shows the reflector stowage concept of a 12-foot reflector. It has sufficient room to even store shrouds, if necessary. Obviously, a 10-foot reflector can be more readily stowed. Figure 5.4 shows the reflector assembly consisting of 7-foot diameter center section plus four extension pieces. Again shroud can be added if required.

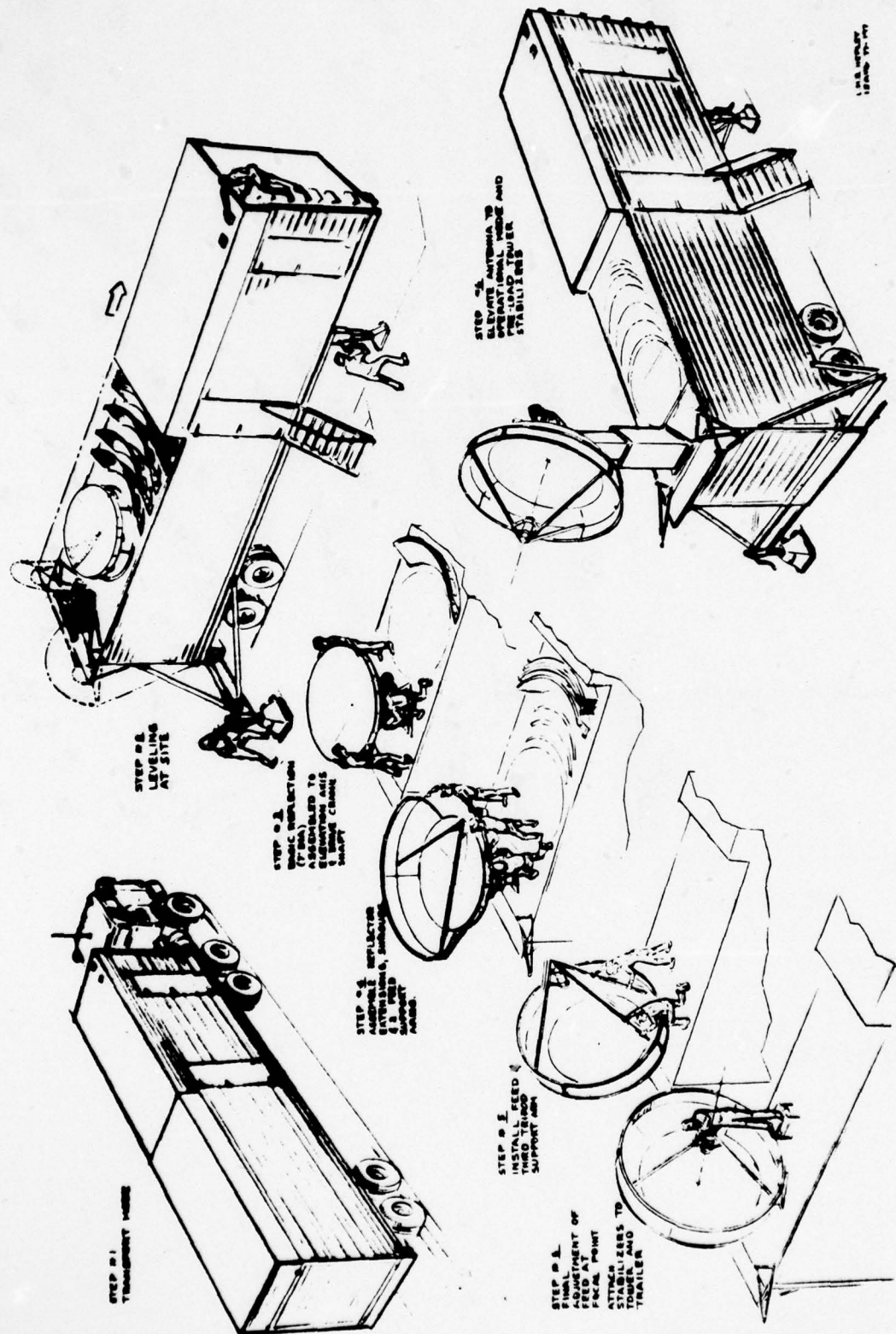
Figure 5.5 shows the detail of subassemblies, how they are stowed, and the method of assembly. Figure 5.6 shows the lift tower structure and azimuth pedestal.

The above concept is viable for the mechanical constraint imposed at the beginning of the program. However, this configuration does not meet the C130 transportability requirement added later.

5.2 Tower Mounted Antenna

The height that the antenna can be elevated with a mechanical erection method is somewhat limited due to the length of the stowing vehicle. Figure 5.7 shows a tower concept that can easily be assembled without a special crane to a height of over 60 feet. This scaffold-type structure is built from ground up one section at a time until the desired height is obtained. At appropriate intervals, guy wires are attached and anchored to the ground. To lift the parts, a small boom with a pulley is used. The cable to hoist the parts is driven by a small motor located at the base of the tower. After the tower is assembled, the antenna parts (pedestal, reflector and parts) are lifted using the same hoist mechanism and assembled at the top. For a ten-foot diameter dish and pedestal weighing a little over 1000 pounds, it takes four people approximately eight hours to erect and assemble

THIS PAGE IS BEST QUALITY PRACTICABLE
FROM COPY FURNISHED TO DDC



THIS PAGE IS BEST QUALITY PRACTICABLE
FROM COPY FURNISHED TO DDC

Figure 5.1
Van Mounted Antenna - Transportation and Erection Sequence

THIS PAGE IS BEST QUALITY PRACTICABLE
FROM COPY FURNISHED TO DDC

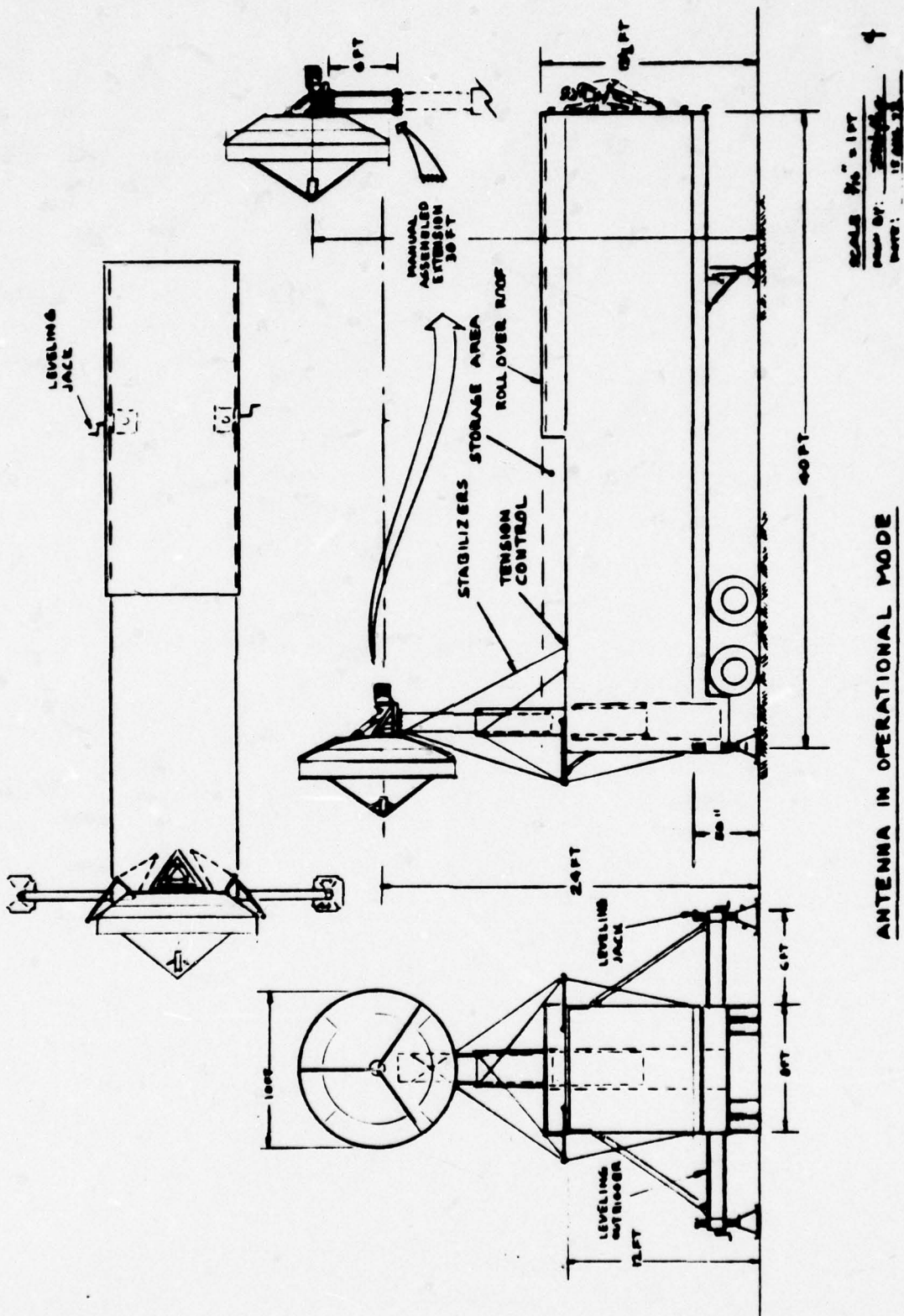
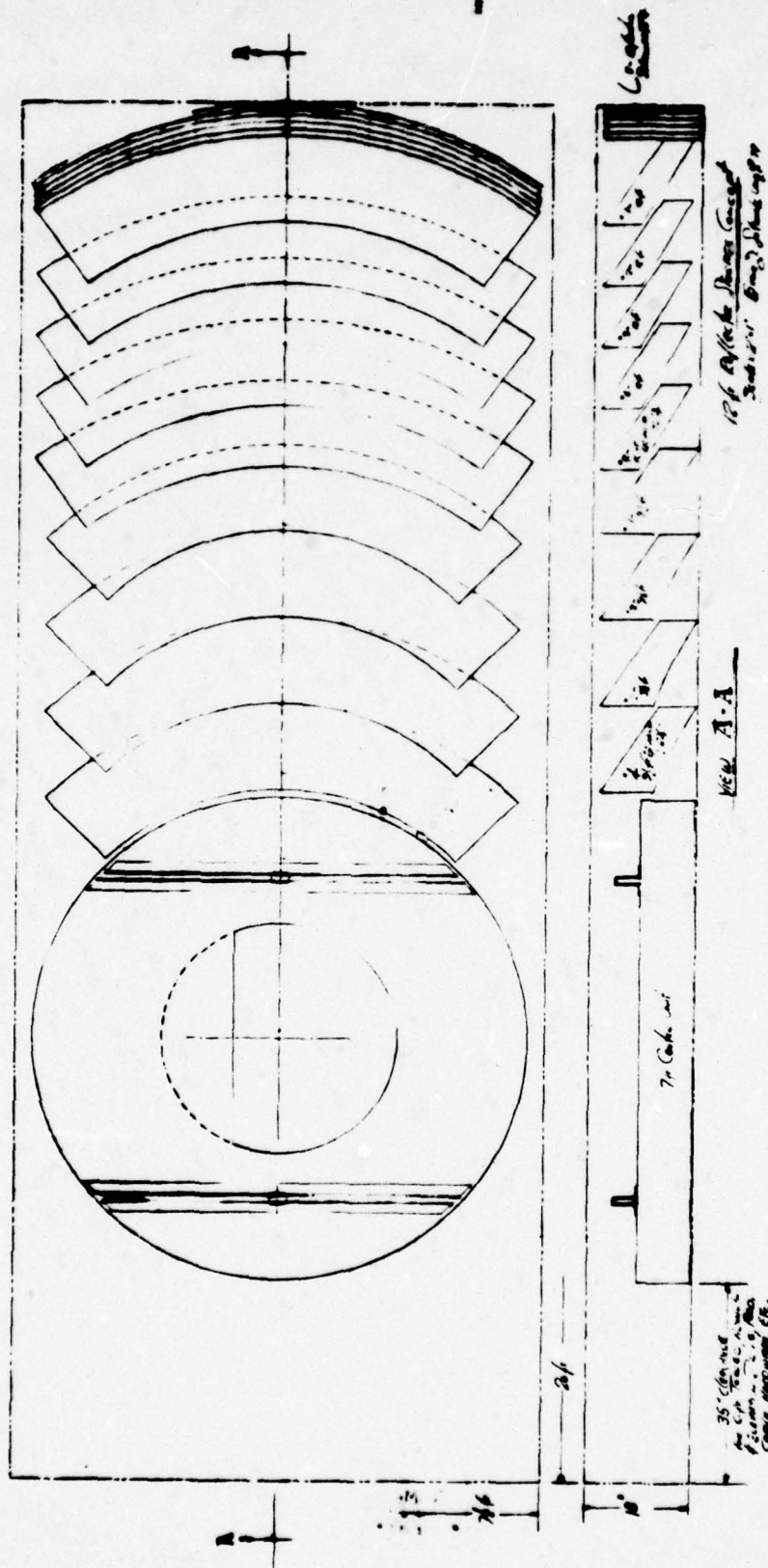


Figure 5.2

THIS PAGE IS BEST QUALITY PRACTICABLE
FROM COPY FURNISHED TO DDC

THIS PAGE IS BEST QUALITY PRACTICABLE
FROM COPY FURNISHED TO DDC



THIS PAGE IS BEST QUALITY PRACTICABLE
FROM COPY FURNISHED TO DDC

Figure 5.3

12' Reflector Storage Concept

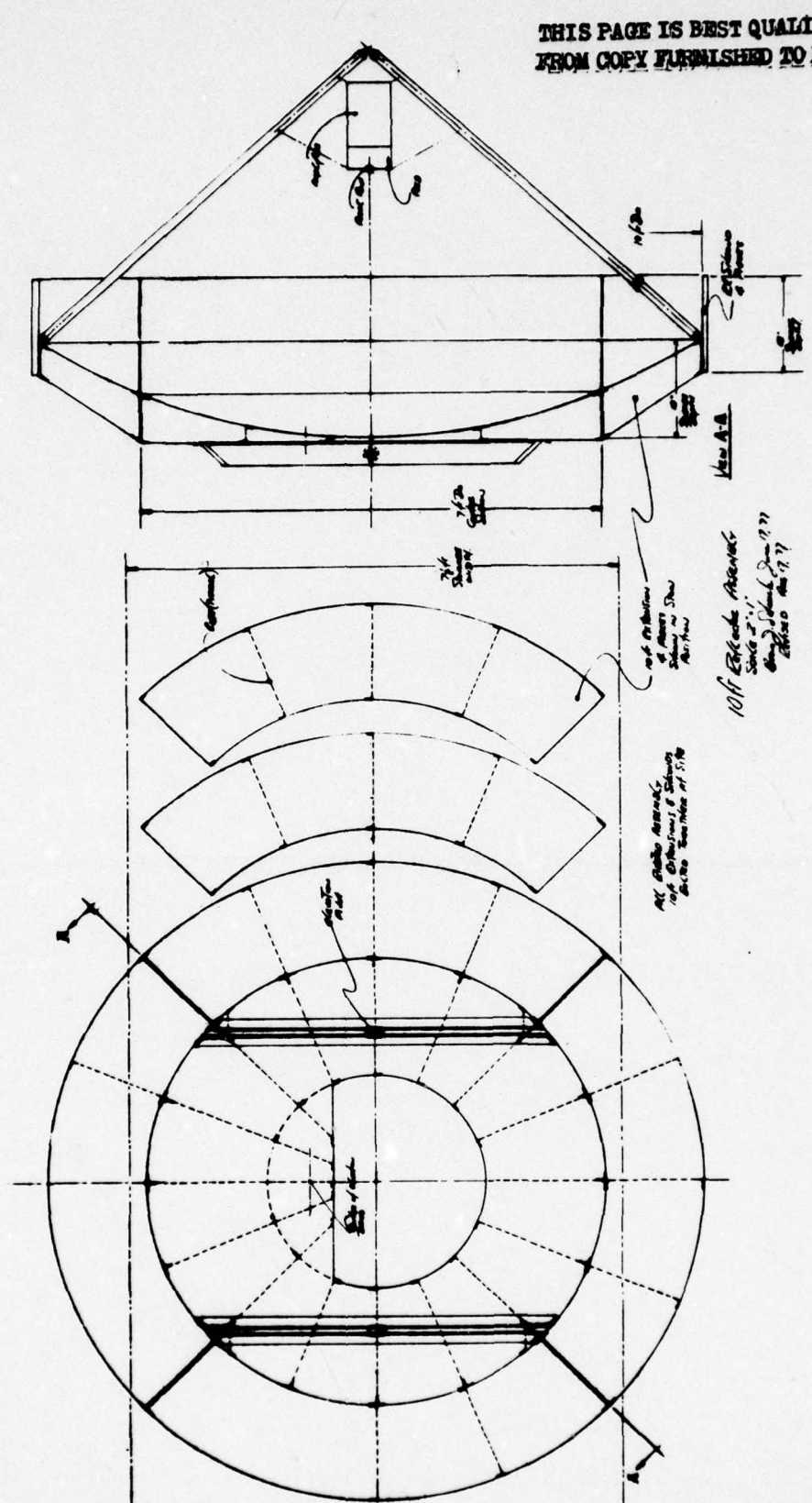


Figure 5.4
Reflector Assembly Concept

THIS PAGE IS BEST QUALITY PRACTICABLE
FROM COPY FURNISHED TO DDC

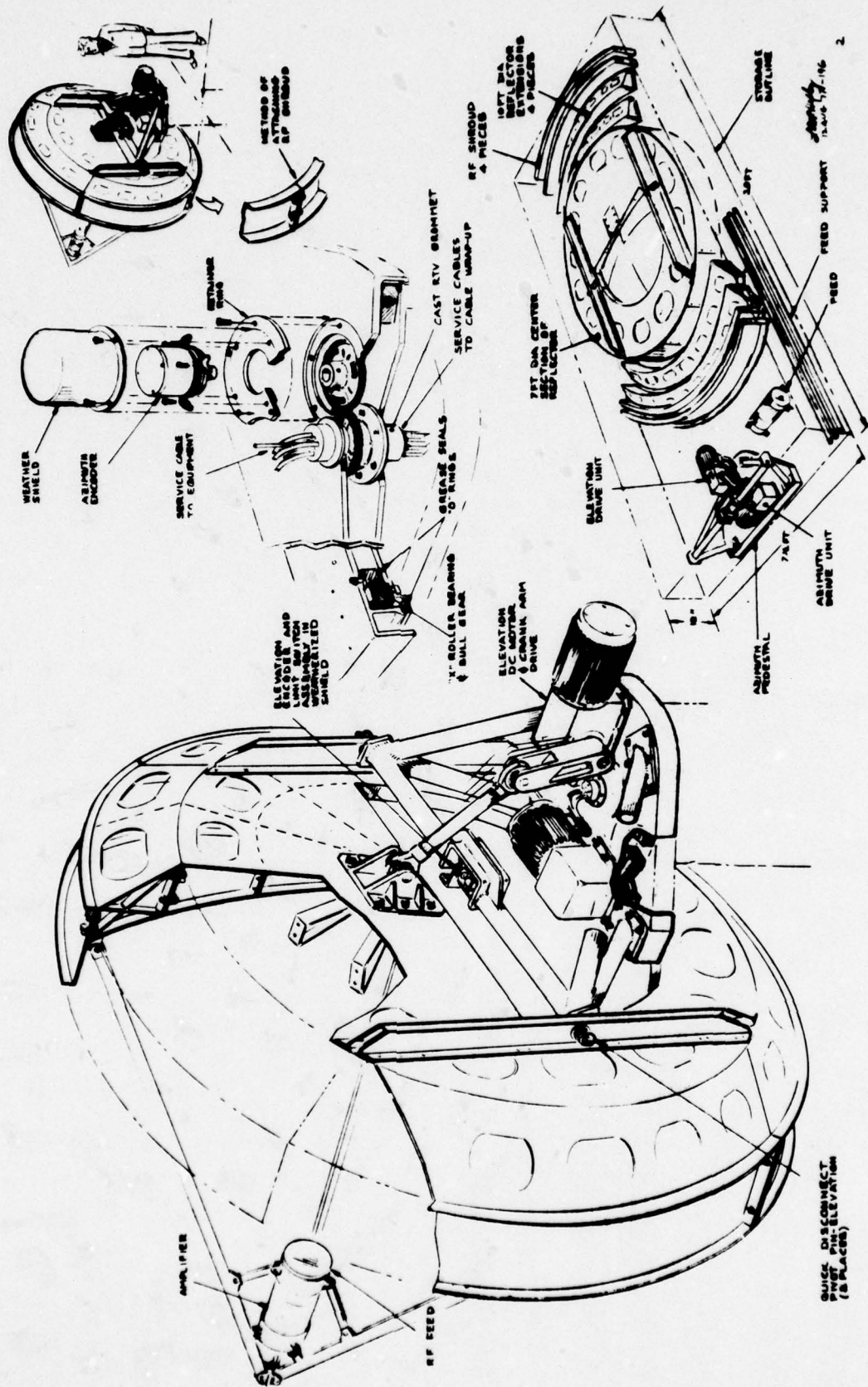
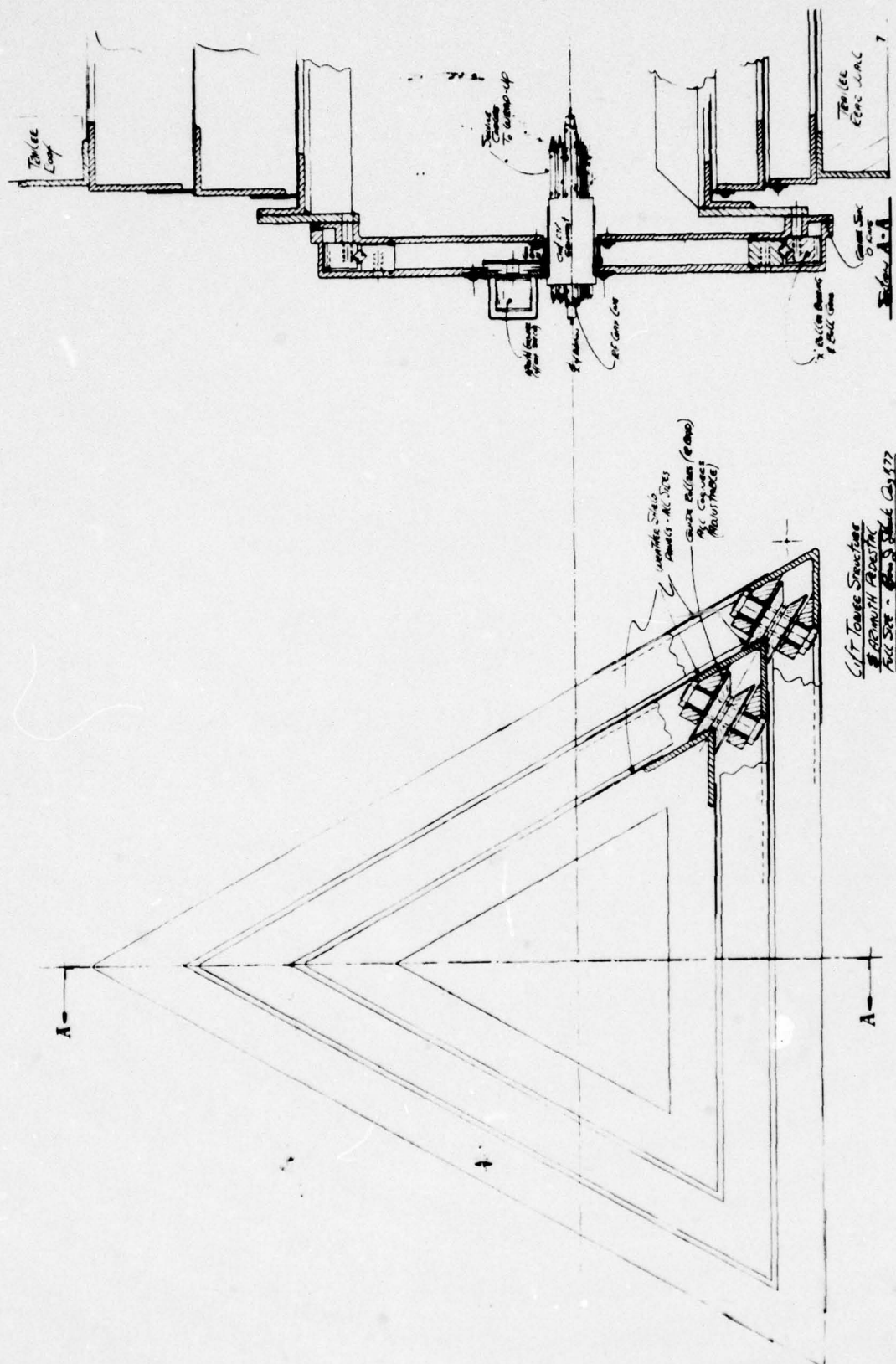


Figure 5.5
Antenna Subassembly Details

THIS PAGE IS BEST QUALITY PRACTICABLE
FROM COPY FURNISHED TO DDC

THIS PAGE IS BEST QUALITY PRACTICABLE
FROM COPY FURNISHED TO DDC



THIS PAGE IS BEST QUALITY PRACTICABLE
FROM COPY FURNISHED TO DDC



Figure 5.7 - Tower Mounted
Antenna Concept

the antenna. Two such antenna assemblies have been produced and are being used by the USAF. One drawback of this configuration is the requirement of a large number of guy wires and associated anchoring pegs that are specially designed. The pegs are generally not reusable and left in the ground when disassembling the tower.

5.3 Flat Bed Mounted Antenna

During the latter part of the program, it became necessary to add a C130 transportability requirement. The requirement to stow the antenna on the upper portion of a van was deleted. Under these conditions, it appears that a flat-bed mounted antenna is more cost effective and simple. Figure 5.8 shows the antenna and pedestal stowed on a 26-foot long flat-bed. The reflector panels can be further disassembled if transportation conditions are poor or extensive. Two hydraulic cylinders extend the base by pushing the inner member via a cable arrangement between the inner and outer member running over a sheave at the end of the piston rods. Figure 5.9 shows the antenna fully elevated in which case the distance from the ground to the elevation axis is 25 feet. It should be noted that the extensible base assembly pivots about the rear end of the trailer for erection and retraction. The trailer is fitted with jacks for leveling the trailer on the sides and outriggers are attached to stabilize the mount. No guy wires are required for operation in winds up to 50 mph, but it is recommended that guy wires be used. It is estimated that it will take two men three hours to erect the antenna system.

The antenna is attached to an elevation-over-azimuth pedestal (such as a Datron Model 8250 or Scientific Atlanta Model 3100). These pedestals provide 0-90° elevation and full $\pm 270^\circ$ azimuth pointing of the RF beam at rates up to 10°/sec.

The antenna trailer subsystem is 26 feet long overall and weighs approximately 12000 pounds. In the transport configuration (Figure 5.8) the assembly is 8 feet wide, 8'-8" high (104"), fits directly in the (smallest) standard configuration of C130 aircraft, and is trailerable without "wide load" permits.

THIS PAGE IS BEST QUALITY PRACTICABLE
FROM COPY FURNISHED TO DDC

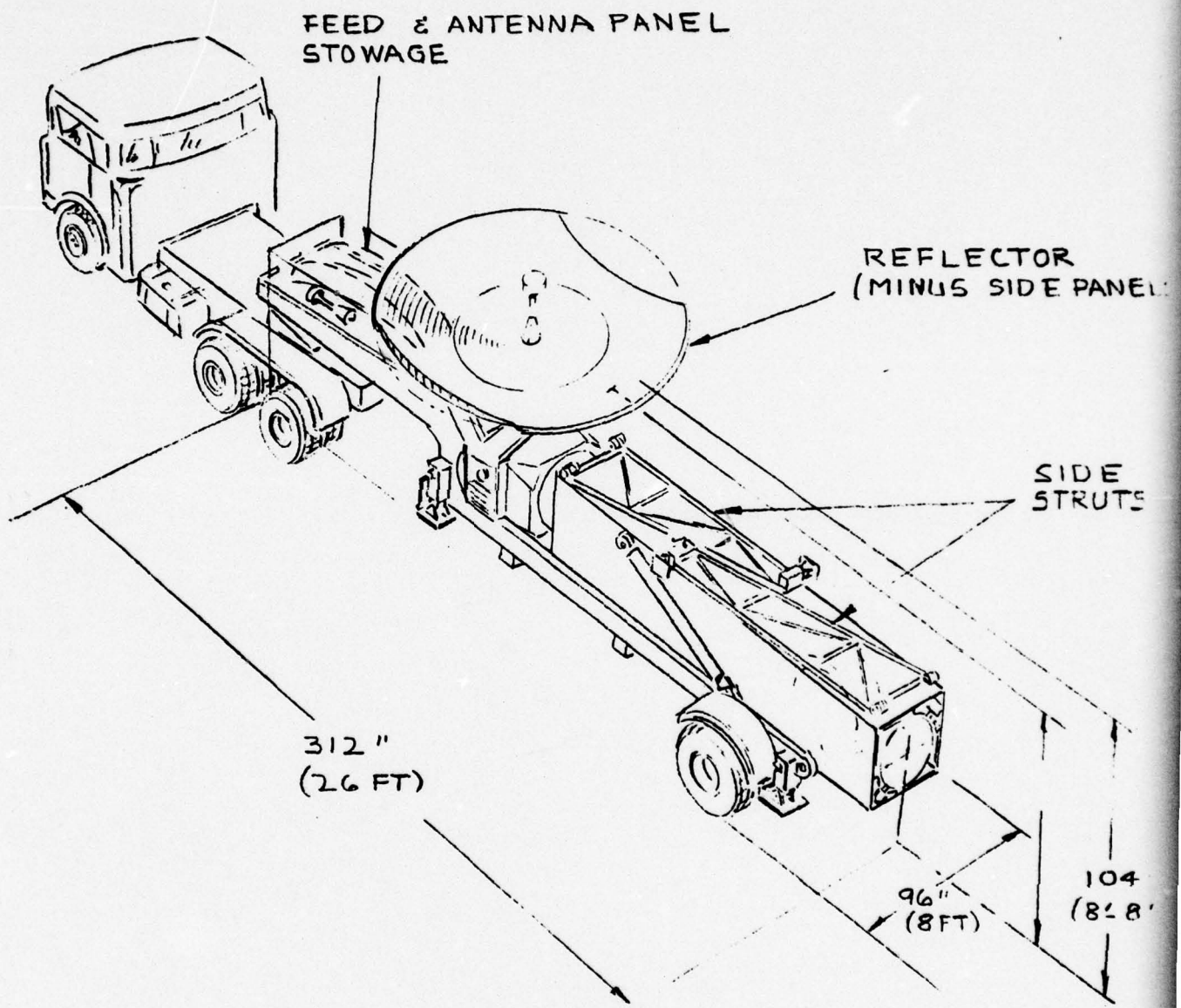


Figure 5.8 FLAT BED TRAILER, MOUNTED ANTENNA
TRANSPORT MODE.

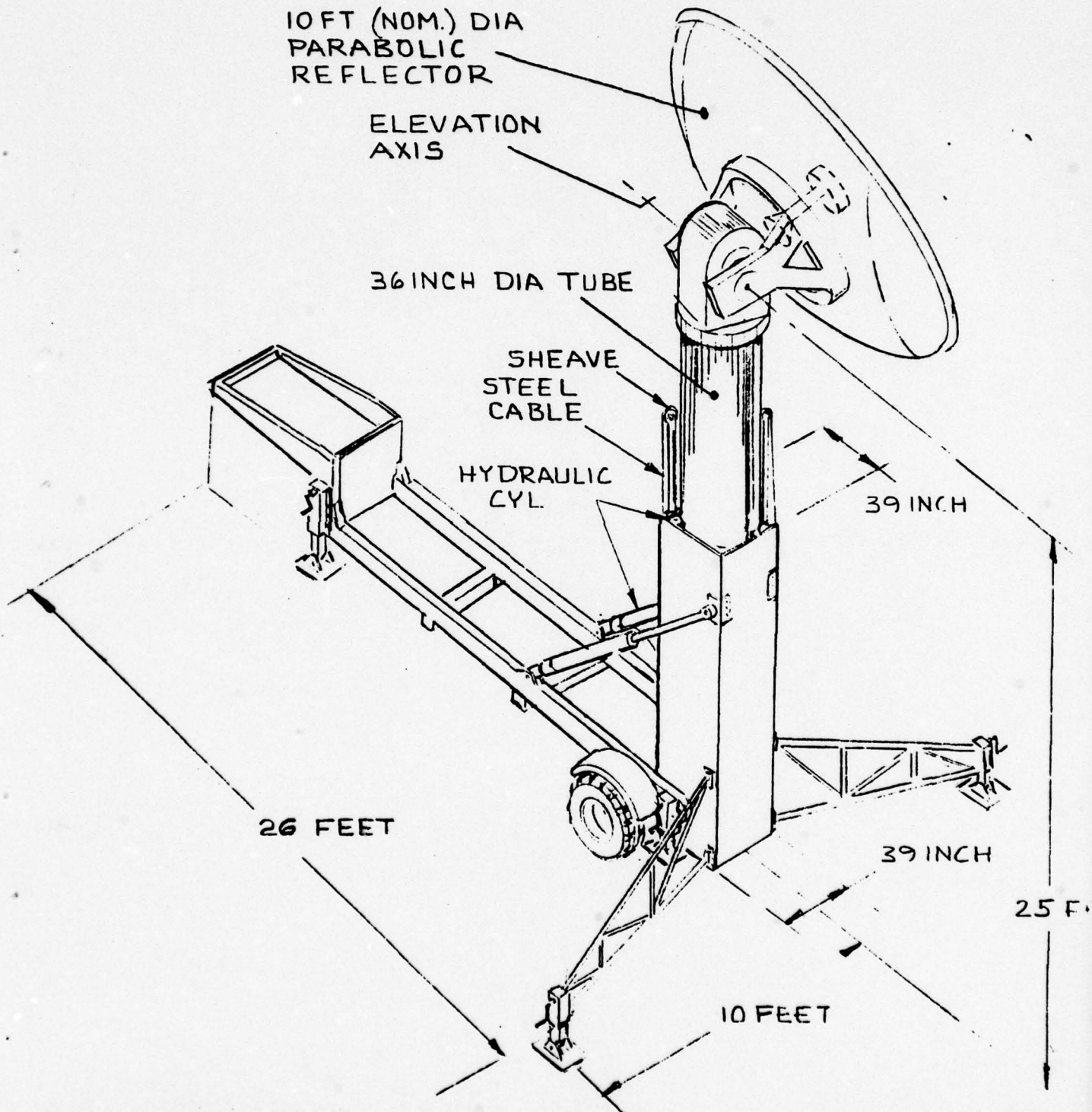


Figure 5.9 FLAT BED TRAILER, MOUNTED ANTENNA, OPERATION MODE

6.0 Baseline System

6.0 Baseline System

6.1 System Description

A block diagram of the proposed antenna system is shown in Figure 6.1. The system consists of three subsystems. These are the RF subsystem, positioning and control subsystem, and support subsystem. Estimates for the weight and costs of the major subsystems and for some lesser components are shown in Table 6.1. Also shown are proposed suppliers and the part number of similar items when such numbers exist. The total cost will be on the order of \$300 - \$400,000. The total weight will be about 12,000 pounds.

The RF subsystem is a 10-foot diameter parabolic reflector fed by a center supported, cavity backed, crossed dipole feed. This feed allows simultaneous use of both senses of circular polarization with high efficiency and low blockage. Duplexing of the signals is accomplished by a 90-degree hybrid located within the center support. The transmit and receive coax lines also run through this center support to the rear of the dish. Located immediately behind the reflector in the transmit line is a receive bandstop filter to stop noise generated by the transmitter in the receive frequency band. Also a solid state transmitter is mounted at this location.

In the receive line is a transmit bandstop filter to reject any transmit power coupled into the receive port to protect the low noise receiver from transmitter signals. If the environment of system operation is poor (i.e., has interfering signals) it may be necessary to use a band-pass filter in the receive line at the expense of additional loss and lower G/T. Also mounted on the rear of the reflector is a low noise preamp. Initially, it was expected that a Peltier cooled paramp would be used, however, this now appears to be rather cost ineffective. Present technology can achieve about 40° K without Peltier cooling with significant cost savings and higher reliability than the 36° K paramp.

The positioning and control subsystem points the antenna in the desired direction and consists of an elevation over azimuth pedestal similar to a Scientific Atlanta Model 3100. The specifications for this pedestal are shown in Table 6.2. The antenna controls will operate in three modes: manual position, manual slew and programmed track. A digital az-el readout will be provided to the operators. For programmed track a microprocessor based unit will provide azimuth and elevation predicts to follow an overhead pass.

The support subsystem is a 26-foot long flat-bed trailer with telescoping support that folds down on the back of the trailer for transport. As previously shown in Figures 5.8 and 5.10, the support mast is erected from horizontal to vertical by hydraulic lift and then extended vertically by means of cable assemblies. It is only necessary to extend the support when the local terrain or the operation van presents obstructions to line of sight signals. The erection mechanism and the antenna servo are run entirely by an external electrical power source which is not part of the antenna system. The prime power requirement is 120 V, 50/60 Hz 400 VA single phase source.

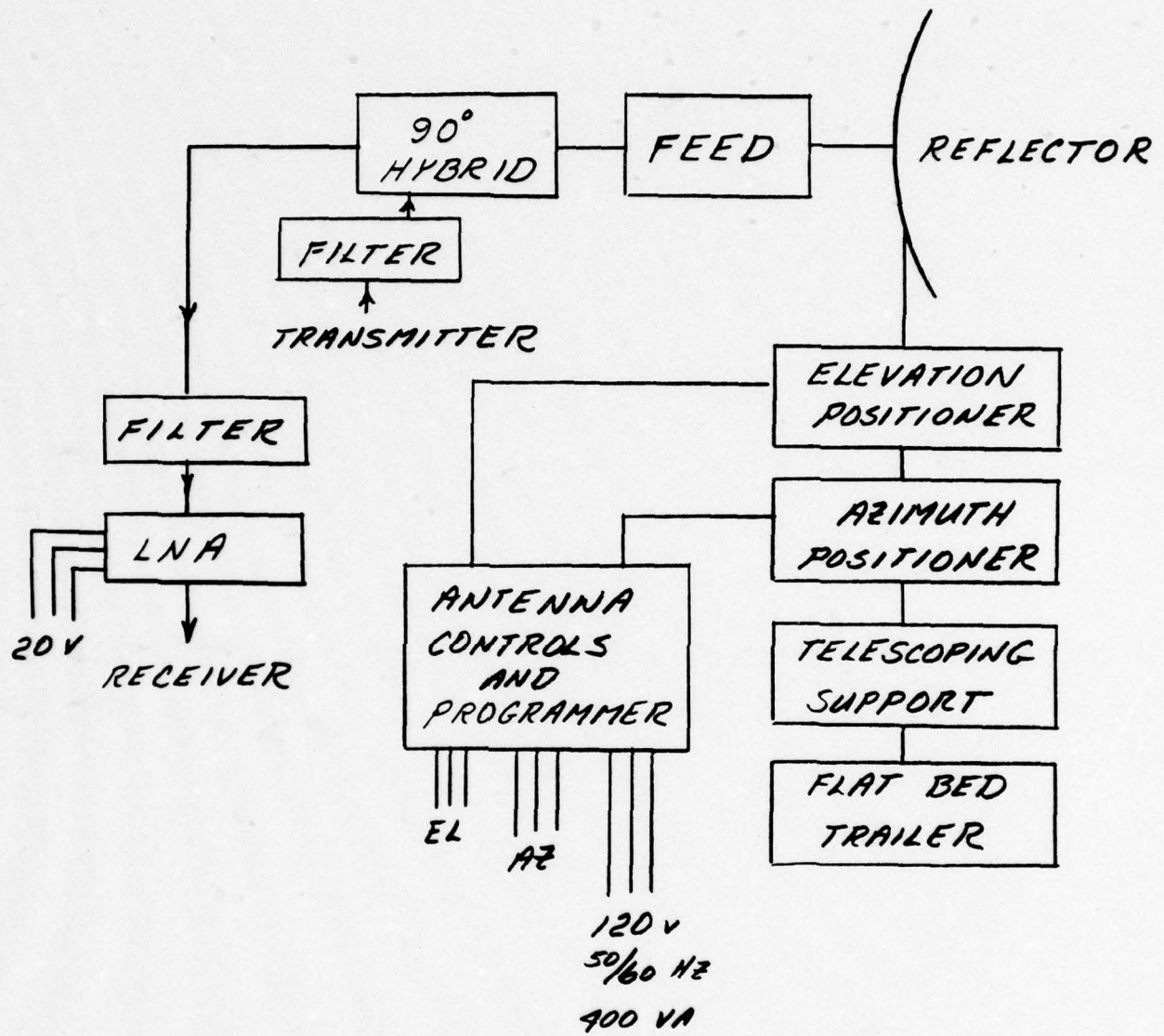


Figure 6.1 - Proposed Antenna System Block Diagram

TABLE 6.1
Cost and Weight Estimates of Recommended System

<u>Item</u>	<u>Proposed Supplier</u>	<u>Similar to Part Number</u>	<u>Approximate Cost</u>	<u>Weight</u>
Overall Design	(non recurring)	Hughes	100,000	
Flat Bed Trailer			22,000	3,500
Telescoping Support	Hughes Design	(non recurring)	33,300	6,750
AZ Positioner				
EL Positioner	Scientific Atlanta	3,100 Modified	74,000	800
Programmer	Hughes		10,000	50
Reflector	Prodelin	44-740 (modified)	4,000	
Feed	Hughes		15,000	
Diplexer	Hughes		2,000	
Filters	Hughes		4,000	
Low Noise Amplifier	Scientific Comm.		35,000	
System Integration	Hughes		100,000	
			399,400	

TABLE 6.2
SERVO-DRIVER PEDESTAL SPECIFICATIONS

Maximum velocity	15 deg/sec.
Maximum Acceleration	15 deg/sec/sec
Gearing Backlash	0.05 deg.
Internal inertia reflected to output	465 sl-ft-ft
Maximum delivered torque	1,400 ft-lbs.
Compliance	1×10^{-6} rad/ft-lb
Overspeed moment	30,000 ft-lbs
Maximum allowable dead weight load	3,000 lbs
Height	25 ft.
Weight	800 lbs

A summary of the antenna system parameters is shown in Table 6.3. The RF performance factors will be further discussed below.

6.2 Antenna Controls

Operational Modes Description

A block diagram of the antenna control system is shown in Figure 6.2. Three modes of antenna control are provided: manual position, manual slew and programmed track. Dual DC electric motors with individual silicon-controlled rectifier (SCR) power amplifiers and tachometer loops are used on each axis.

The manual rate slew is controlled by commanding a DC voltage directly into each tachometer loop. This DC voltage is set by manually controlled potentiometers located on the antenna control panel in the electronics van. The manual position loop is closed through synchros mounted on the antenna axis and hand-wheel driven synchros on the antenna control panel. The synchro outputs are demodulated and routed through servo compensation amplifiers to the tachometer loop.

Type I or Type II servo operation is selectable on the antenna control panel as well as a bandwidth selection of 0.5 and 1.0 Hz. The dual electric motors are driven by a power amplifier to provide an anti-backlash opposed drive. The velocity loop is closed with a tachometer integrally mounted on the motor. A loop gain of approximately 20 dB is provided. The position loops can be operated either as Type I or Type II.

Position information from synchros in the pedestal is converted to binary coded decimal (BCD) data and displayed on the digital position display unit. The BCD information is coupled to the digital comparator for program track operation.

The programmed track loop is a position loop which accepts BCD commands from the antenna programmer. The programmed track loop is closed as follows: 1 to 1 and 36 to 1 synchros on each antenna axis provide inputs to the synchro's analog to digital angular position indicator. The analog to digital converter also provides a BCD read-out that is used as a feedback signal for the programmed track loop. This digital feedback signal is then compared with the programmer command to develop a digital error signal. This digital error signal is, in turn, digital to analog converted to develop an analog error for antenna positioning.

The digital comparator is used to drive an analog servo system through the use of digital inputs. The unit accepts BCD angular information and sign from two selected input sources - a command input and a data input - computes their relative differences, and produces a DC output signal whose magnitude and polarity is directly proportional to the difference between the two BCD input words. This DC output signal is used to drive the analog servo system.

Programmer

For each of the passes, an nth order polynomial equation is used as the curve fit for the pass. N coefficients, generated from data supplied by

TABLE 6.3
ANTENNA DESCRIPTION

Type	Center Fed Paraboloid
Feed Type	Center supported, cavity backed, crossed dipoles
Frequency	1.4 GC
Gain	30.3 dB
Peak Sidelobe Level	-25 dB
Backlobe Level	-4 dBi
Beamwidth	5 degrees
F/D	0.35
Diameter	10 feet
Height above ground	up to 25 feet
Weight (reflector and feed)	500 pounds
Weight (entire system)	12,000 pounds

THIS PAGE IS BEST QUALITY PRACTICABLE
FROM COPY FURNISHED TO DDC

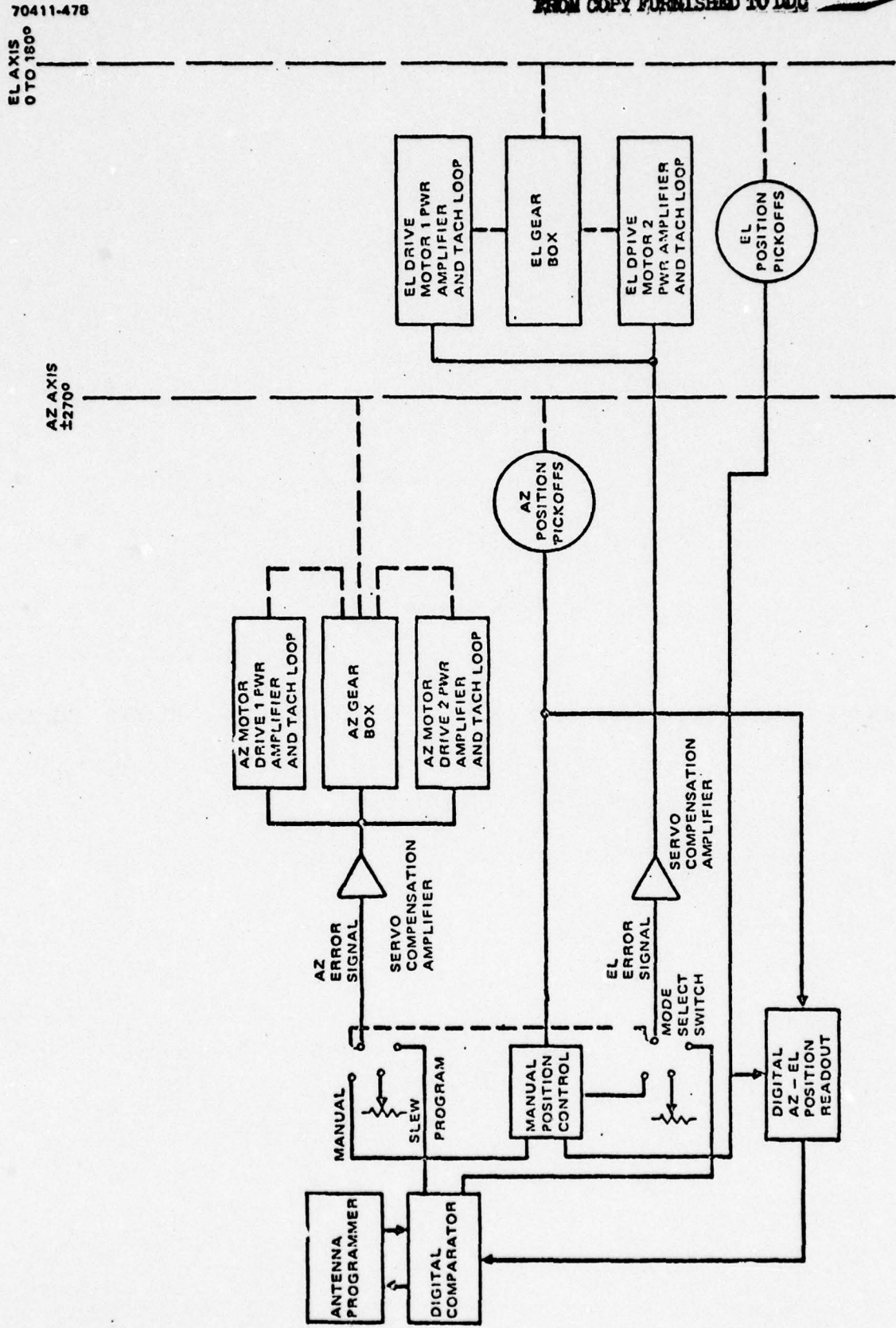


Figure 6.2-2 ANTENNA CONTROL SYSTEM FUNCTIONAL BLOCK DIAGRAM

the user, uniquely define each pass. These coefficients and initial antenna azimuth and elevation information are punched onto a paper tape. The paper tape now becomes the means by which to enter the required data into the antenna programmer unit for solving.

The antenna programmer is designed around a microprocessor, Figure 6.3. The program that solves the nth order polynomial equation is resident in ROM memory of the microprocessor. The paper tape reader interface furnishes an input to program the antenna track information found on the data tape. As a backup mode of operation, the TTY could be used to read in the data tape. Time of day (GMT) is provided in parallel form with second updates from the time code generator. Azimuth and elevation predicts are output in BCD form to a digital comparator which compares predicted position with actual position of the antenna and provides error signals to the antenna control subsystem.

The antenna programmer uses the Intel 8080A microprocessor for program control, Figure 6.4. The equation solving program is stored in ROM and the results stored in RAM. Interface with the various external devices is made by way of either serial or parallel I/O ports. Azimuth and elevation predicts for an entire set of passes may be generated once by the antenna programmer and stored in RAM memory along with a designated pass number. Prior to the occurrence of one of the passes, the predicted GMT orbit start time and pass number is programmed into the unit via a keyboard located on the front panel. When a comparison is reached between GMT time from the time code generator and predicted orbit start time the program will begin sequencing through the calculated azimuth and elevation angles stored in RAM memory.

6.3 System Performance

The proposed antenna system will meet the desired G/T values over the required beam areas using the same circularly symmetric beam at all elevation angles if a Peltier cooled 36° K paramp is used. However, as discussed previously this is probably not cost effective as a 40° K paramp is now available without cooling for about half the cost of a cooled paramp. Using this paramp, the expected system losses as illustrated in Figure 4.9, and the predicted antenna temperature shown in Figure 4.12 results in a system G/T as illustrated in Table 6.4.

The expected antenna gain is based on the efficiency analysis illustrated in Table 6.5. This analysis assumes that the center supported dipole has essentially the same primary patterns illustrated for the cup dipole feed in Figure 4.10. It is expected that this characteristic is attainable by optimization of the center supported design. For the loss budget, illustrated in Figure 4.9, the predicted peak gain is 30.3 dB.

The expected secondary patterns will be similar to those measured on the two-foot model with the single narrow strut, Figures 4.13 and 4.14. The off axis gains at the angles specified for the required G/T are shown in Table 6.4. Figure 6.5 shows the predicted G/T performance versus elevation.

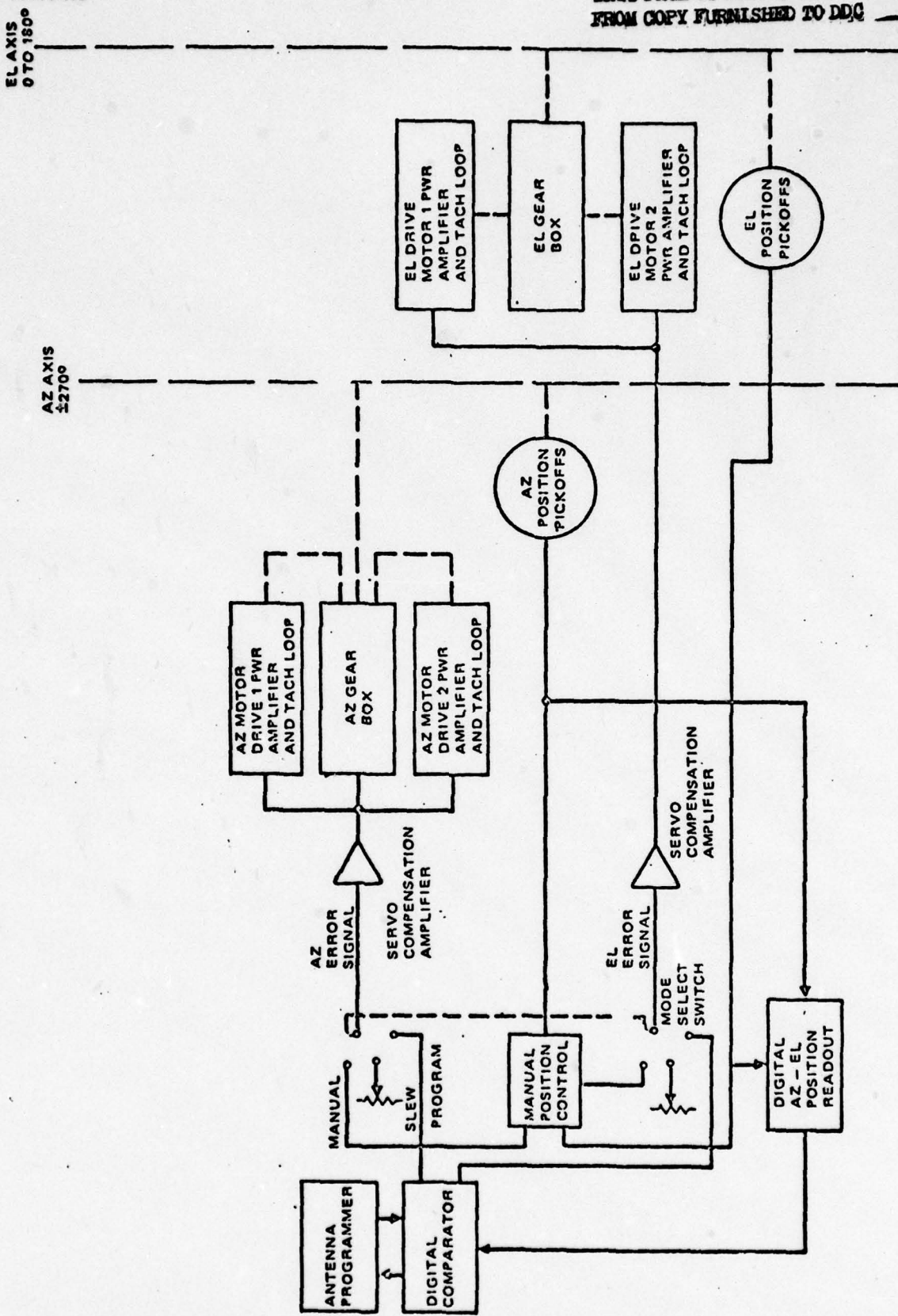


Figure 6.3 ANTENNA CONTROL SYSTEM FUNCTIONAL BLOCK DIAGRAM

THIS PAGE IS BEST QUALITY PRACTICABLE
FROM COPY FURNISHED TO DDC

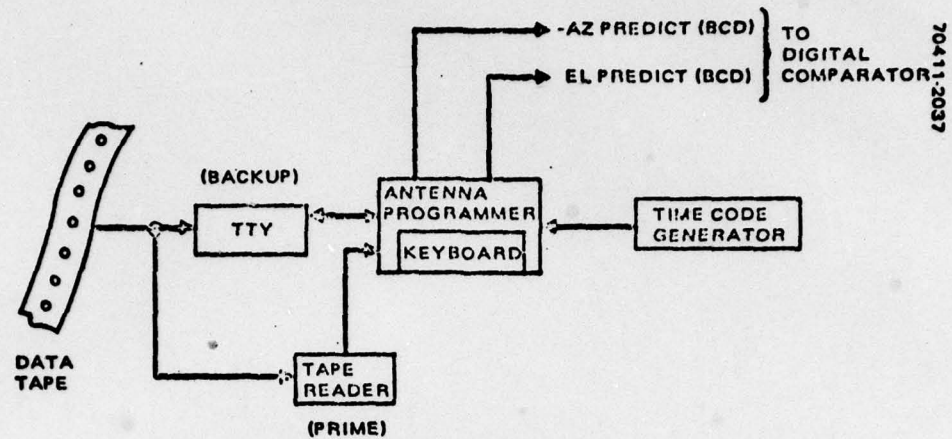


Figure 6.3 ANTENNA PROGRAMMER INTERFACE BLOCK DIAGRAM

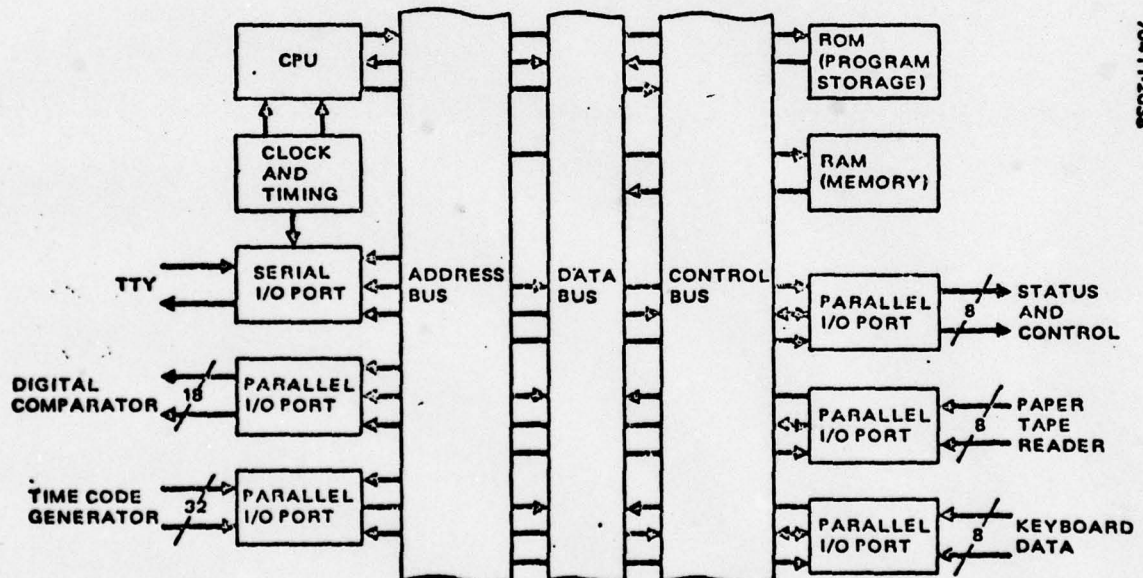


Figure 6.4 ANTENNA PROGRAMMER BLOCK DIAGRAM

Table 6.4 - Gain and G/T Performance

<u>Beam Peak Angle (Deg)</u>	<u>Angle from Beam Peak (Deg)</u>	<u>Gain (dB)</u>	<u>Antenna G/T (dB)</u>	<u>Required G/T (dB)</u>
5	<u>+0.8 vertical</u>	30.1	9.4	+8.5
5	<u>+1.25 horizontal</u>	29.7	9.0	+8.5
5	0	30.3	9.6	N/A
90	<u>+2.7 vertical</u>	26.7	7.3	-1.5
90	<u>+4.25</u>	20.9	1.5	-1.5
90	0	30.3	10.9	N/A

Table 6.5
ANTENNA EFFICIENCY ANALYSIS

TITLE Center Supported Cup Dipole Feed, 10' Reflector, F/D = 0.35
Freq. 1.4 GHz

Efficiency Factor		Value	Comments
A. PRIMARY FEED			
Spillover	η_s	0.962	
Illumination	η_i	0.689	From Primary Pattern Integration
Cross Polarization	η_x	0.999	
Feed Insertion Loss	η_1	0.891	$\eta_1 = 10^{-L/10}$ $L = \underline{0.5}$ dB
VSWR	η_v	0.960	$\eta_v = 4V/(1+V)^2$ $V = \underline{1.5}$
Phase Error Loss			
1. Quadratic	η_p	1	$\beta_2 = \underline{0}$
2. Astigmatism	η_{fa}	1	$\eta_{fa} = 1/(1 + .25 \eta_i \beta_a^2)$ $\beta_a = \underline{0}$
Feed Efficiency	η_f	0.566	
B. REFLECTOR			
Blockage			
1. Feed/Subreflector	η_b	0.984	$\eta_b = (1 - B^2/\eta_i)^2$ $B^2 = \underline{0.56}$ %
2. Strut	η_{sb}	1	$\eta_{sb} = (1 - A_s)^2$ $A_s = \underline{0}$ %
Surface Tolerance	η_r	0.994	$\eta_r = \exp[-16\pi^2(\sigma_m^2 + \sigma_s^2)/\lambda^2]$
			Paraboloid $\sigma_m = \underline{0.050}$
			Subreflector $\sigma_s = \underline{N/A}$
Astigmatism	η_{ra}	0.978	$\eta_{ra} = 1/(1 + .25 \eta_i \beta_{ra}^2)$ $\beta_{ra} = \underline{0.364}$
Edge Diffraction	η_d	N/A	Cassegrain Only
Reflector Efficiency	η_R	0.957	
C. RADOME LOSS	η_r	1	
Expected Efficiency	η_e	0.542	$\eta_e = \eta_F \times \eta_R \times \eta_r$
Measured Efficiency	η_m		

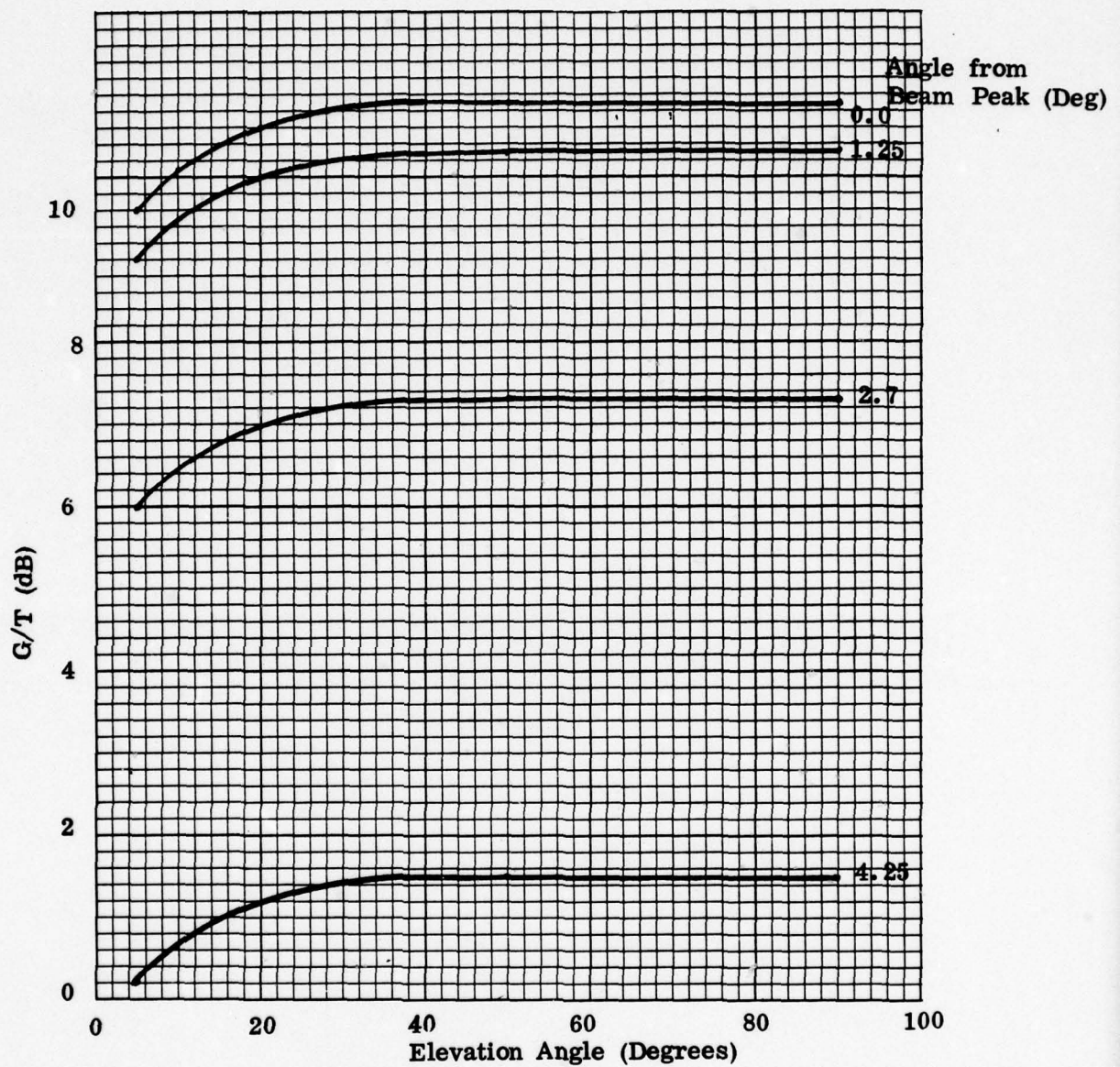


Figure 6.5 - G/T as a function of beam elevation angle with location on the beam as a parameter.

7.0 Conclusions

7.0 Conclusions

The proposed baseline system is recommended as the most cost effective method for obtaining the desired system performance. This recommendation is based on a series of tradeoffs made during the study. The recommended system is adequate in G/T performance even for low angles, and the cost of lowering G/T by 0.2 dB at 5° elevation would essentially double the paramp cost and lower the reliability as cooling would be required. The system proposed meets the desired performance utilizing state-of-the-art hardware.

A simple approach utilizing a single element feed eliminates the need for feed switching to accomplish beam control which increases reliability, reduces blockage and minimizes insertion loss. The use of a center supported feed also eliminates strut blockage.

The proposed flat bed transportation system provides a simple to erect drive mechanism and provides for an antenna height of 25 feet above the ground. The total assembly is easily transported by a C130 cargo plane.

APPENDIX I
ANTENNA EFFICIENCY ANALYSIS
CANDIDATE ANTENNA CONFIGURATIONS

ANTENNA EFFICIENCY ANALYSIS
 10-foot reflector
 F/D = 0.35
 1.6" O.D. Cup Dipole Feed

Efficiency Factor		Value	Comments
A. PRIMARY FEED			
Spillover	η_s	0.962	
Illumination	η_i	0.689	From Primary Pattern Integration
Cross Polarization	η_x	0.999	
Feed Insertion Loss	η_f	0.891	$\eta_f = 10^{-L/10}$ $L = \underline{0.5}$ dB
VSWR	η_v	0.960	$\eta_v = 4V/(1+V)^2$ $V = \underline{1.5}$
Phase Error Loss			
1. Quadratic	η_p	1	$\beta_2 = \underline{0}$
2. Astigmatism	η_{fa}	1	$\eta_{fa} = 1/(1 + 2.5 \eta_i \beta_a^2)$ $\beta_a = \underline{0}$
Feed Efficiency	η_f	0.566	
B. REFLECTOR			
Blockage			
1. Feed/Subreflector	η_b	0.984	$\eta_b = (1 - B^2 / \eta_i)^2$ $B^2 = \underline{0.56}$ %
2. Strut	η_{sb}	0.937	$\eta_{sb} = (1 - A_s)^2$ $A_s = \underline{3.18}$ %
Surface Tolerance	η_r	0.994	$\eta_r = \exp[-16\pi^2(\sigma_m^2 + \sigma_s^2)/\lambda^2]$ Paraboloid $\sigma_m = \underline{0.050}$ Subreflector $\sigma_s = \underline{N/A}$
Astigmatism	η_{ra}	0.978	$\eta_{ra} = 1/(1 + 2.5 \eta_i \beta_{ra}^2)$ $\beta_{ra} = \underline{0.364}$
Edge Diffraction	η_d	N/A	Cassegrain Only
Reflector Efficiency	η_R	0.896	
C. RADOME LOSS	η_r	1	
Expected Efficiency	η_e	0.507	$\eta_e = \eta_F \times \eta_R \times \eta_r$
Measured Efficiency	η_m		

ANTENNA EFFICIENCY ANALYSIS

10-foot Reflector

F/D = 0.30

1.6" O.D. Cup Dipole Feed

Efficiency Factor		Value	Comments
A. PRIMARY FEED			
Spillover	η_s	0.977	
Illumination	η_i	0.584	From Primary Pattern Integration
Cross Polarization	η_x	0.998	
Feed Insertion Loss	η_1	0.891	$\eta_1 = 10^{-L/10}$ $L = \underline{0.5}$ dB
VSWR	η_v	0.960	$\eta_v = 4V/(1+V)^2$ $V = \underline{1.5}$
Phase Error Loss			
1. Quadratic	η_p	1	$\beta_2 = \underline{0}$
2. Astigmatism	η_{fa}	1	$\eta_{fa} = 1/(1 + 25\eta_i \beta_a^2)$ $\beta_a = \underline{0}$
Feed Efficiency	η_f	0.437	
B. REFLECTOR			
Blockage			
1. Feed/Subreflector	η_b	0.981	$\eta_b = (1 - B^2/\eta_i)^2$ $B^2 = \underline{0.56}$ %
2. Strut	η_{sb}	0.937	$\eta_{sb} = (1 - A_s)^2$ $A_s = \underline{3.16}$ %
Surface Tolerance	η_r	0.994	$\eta_r = \exp[-16\pi^2(\sigma_m^2 + \sigma_s^2)/\lambda^2]$
			Paraboloid $\sigma_m = \underline{0.05}$
			Subreflector $\sigma_s = \underline{N}$
Astigmatism	η_{ra}	0.983	$\eta_{ra} = 1/(1 + 25\eta_i \beta_{ra}^2)$ $\beta_{ra} = \underline{0.34}$
Edge Diffraction	η_d	N/A	Cassegrain Only
Reflector Efficiency	η_R	0.499	
Antenna Loss	η_A	1.000	
Antenna Gain	η_G	1.000	

ANTENNA EFFICIENCY ANALYSIS
 12-foot Reflector
 F/D = 0.292
 1.6" O.D. Cup Dipole Feed

Efficiency Factor		Value	Comments
A. PRIMARY FEED			
Spillover	η_s	0.980	
Illumination	η_i	0.560	From Primary Pattern Integration
Cross Polarization	η_x	0.998	
Feed Insertion Loss	η_l	0.891	$\eta_l = 10^{-L/10}$ $L = \underline{0.5}$ dB
VSWR	η_v	0.960	$\eta_v = 4V/(1+V)^2$ $V = \underline{1.5}$
Phase Error Loss			
1. Quadratic	η_p	1	$\beta_2 = \underline{0}$
2. Astigmatism	η_{fa}	1	$\eta_{fa} = 1/(1 + .25 \eta_i \beta_a^2)$ $\beta_a = \underline{0}$
Feed Efficiency	η_f	0.468	
B. REFLECTOR			
Blockage			
1. Feed/Subreflector	η_b	0.986	$\eta_b = (1 - B^2 / \eta_i)^2$ $B^2 = \underline{0.39}$ %
2. Strut	η_{sb}	0.948	$\eta_{sb} = (1 - A_s)^2$ $A_s = \underline{2.65}$ %
Surface Tolerance	η_r	0.994	$\eta_r = \exp[-16\pi^2(\sigma_m^2 + \sigma_s^2)/\lambda^2]$ Paraboloid $\sigma_m = \underline{0.050}$ Subreflector $\sigma_s = \underline{0}$
Astigmatism	η_{ra}	0.984	$\eta_{ra} = 1/(1 + .25 \eta_i \beta_{ra}^2)$ $\beta_{ra} = \underline{0.340}$
Edge Diffraction	η_d	N/A	Cassegrain Only
Reflector Efficiency	η_R	0.914	
C. RADOME LOSS	η_r	1	
Expected Efficiency	η_e	0.428	$\eta_e = \eta_f \times \eta_R \times \eta_r$
Measured Efficiency	η_m		

ANTENNA EFFICIENCY ANALYSIS
 10-foot Reflector
 F/D = 0.35
 7-element Feed--High Gain

Efficiency Factor		Value	Comments
A. PRIMARY FEED			
Spillover	η_s	0.889	
Illumination	η_i	0.866	
Cross Polarization	η_x	0.998	
Feed Insertion Loss	η_l	0.851	$\eta_l = 10^{-L/10}$ $L = \underline{\hspace{2cm}} \text{ dB}$
VSWR	η_v	0.960	$\eta_v = 4V/(1+V)^2$ $V = \underline{\hspace{2cm}}$
Phase Error Loss			
1. Quadratic	η_p	1	$\beta_2 = \underline{\hspace{2cm}}$
2. Astigmatism	η_{fa}	1	$\eta_{fa} = 1/(1 + .25 \eta_i \beta_a^2)$ $\beta_a = \underline{\hspace{2cm}}$
Feed Efficiency	η_f	0.657	
B. REFLECTOR			
Blockage			
1. Feed/Subreflector	η_b	0.959	$\eta_b = (1 - B^2 / \eta_i)^2$ $B^2 = \underline{\hspace{2cm}} \%$
2. Strut	η_{sb}	0.938	$\eta_{sb} = (1 - A_s)^2$ $A_s = \underline{\hspace{2cm}} \%$
Surface Tolerance	η_r	0.994	$\eta_r = \exp [-16 \pi^2 (\sigma_m^2 + \sigma_s^2) / \lambda^2]$
			Paraboloid $\sigma_m = \underline{\hspace{2cm}}$
			Subreflector $\sigma_s = \underline{\hspace{2cm}}$
Astigmatism	η_{ra}	0.972	$\eta_{ra} = 1/(1 + .25 \eta_i \beta_{ra}^2)$ $\beta_{ra} = \underline{\hspace{2cm}}$
Edge Diffraction	η_d	N/A	Cassegrain Only
Reflector Efficiency	η_R	0.869	
C. RADOME LOSS	η_r	1	
Expected Efficiency	η_e	0.571	$\eta_e = \eta_F \times \eta_R \times \eta_r$
Measured Efficiency	η_m		

ANTENNA EFFICIENCY ANALYSIS
 10-foot Reflector
 F/D = 0.35
 7-element Feed--Low Gain

Efficiency Factor		Value	Comments
A. PRIMARY FEED			
Spillover	η_s	0.991	
Illumination	η_i	0.440	From Primary Pattern Integration
Cross Polarization	η_x	0.999	
Feed Insertion Loss	η_f	0.767	
VSWR	η_v	0.960	
Phase Error Loss			
1. Quadratic	η_p	1	$\beta_2 = \underline{\hspace{2cm}}$
2. Astigmatism	η_{fa}	1	$\beta_a = \underline{\hspace{2cm}}$
Feed Efficiency	η_f	0.321	
B. REFLECTOR			
Blockage			
1. Feed/Subreflector	η_b	0.921	$\eta_b = (1 - B^2 / \eta_i)^2$ $B^2 = \underline{\hspace{2cm}} \%$
2. Strut	η_{sb}	0.938	$\eta_{sb} = (1 - A_s)^2$ $A_s = \underline{\hspace{2cm}} \%$
Surface Tolerance	η_r	0.994	$\eta_r = \exp [-16 \pi^2 (\sigma_m^2 + \sigma_s^2) / \lambda^2]$
			Paraboloid $\sigma_m = \underline{\hspace{2cm}}$
Astigmatism	η_{ra}	0.986	Subreflector $\sigma_s = \underline{\hspace{2cm}}$
Edge Diffraction	η_d	N/A	$\eta_{ra} = 1 / (1 + .25 \eta_i \beta_{ra}^2)$ $\beta_{ra} = \underline{\hspace{2cm}}$
			Cassegrain Only
Reflector Efficiency	η_R	0.847	
C. RADOME LOSS	η_r	1	
Expected Efficiency	η_e	0.271	$\eta_e = \eta_F \times \eta_R \times \eta_r$
Measured Efficiency	η_m		

APPENDIX II
COMPUTED SECONDARY PATTERNS
CANDIDATE ANTENNA SYSTEMS

CHART NO. 179

SCIENTIFIC ATLANTA, INC., ATLANTA, GEORGIA, U.S.A.

10-foot Reflector
F/D = 0.35
1.6" O.D. Cup Dipole Feed
Feed Blockage = 9 in. square
Four Struts 1.5 in. dia. in
diagonal planes

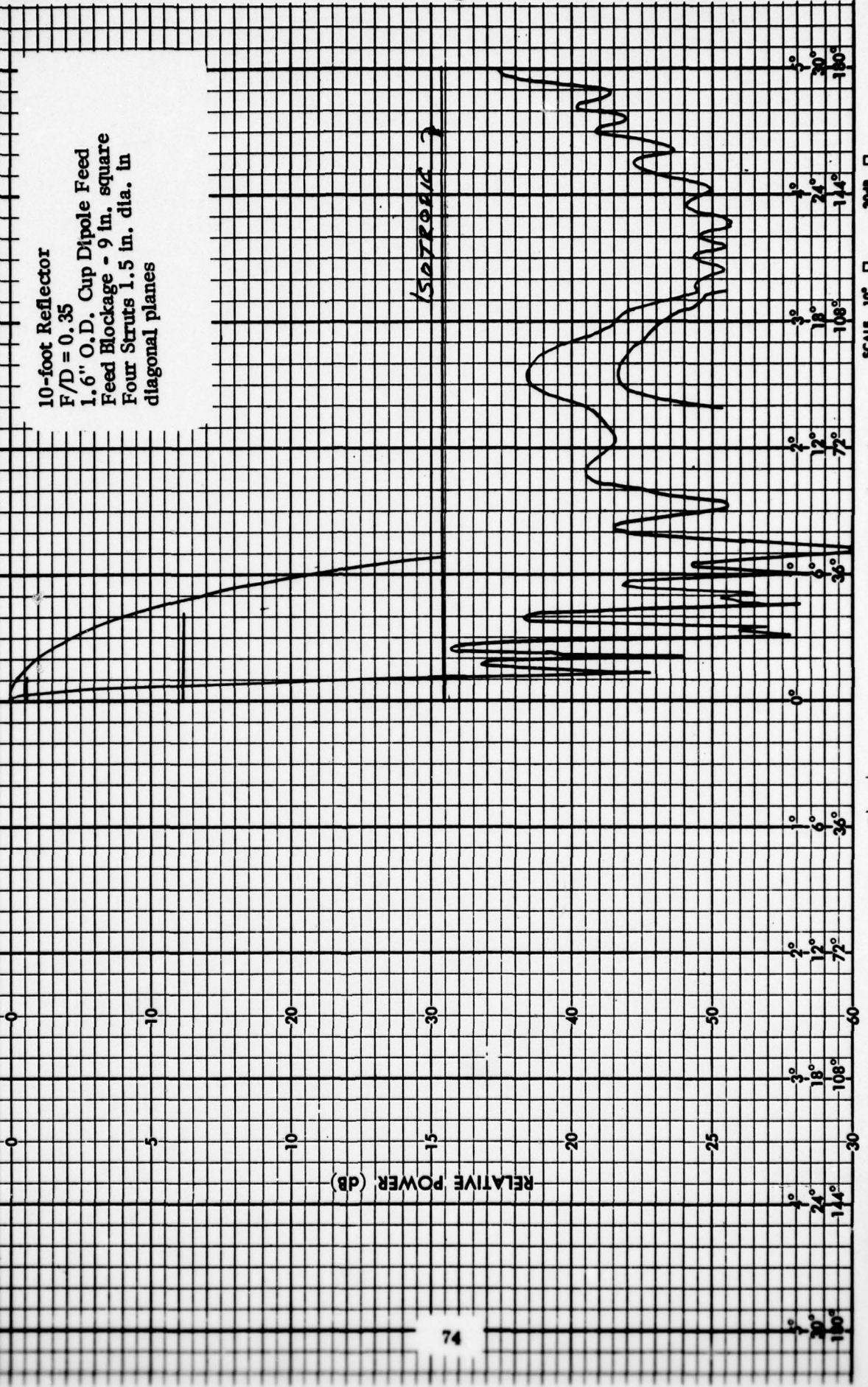


CHART NO. 17

SCIENTIFIC ATLANTA, INC., ATLANTA, GEORGIA, U.S.A.

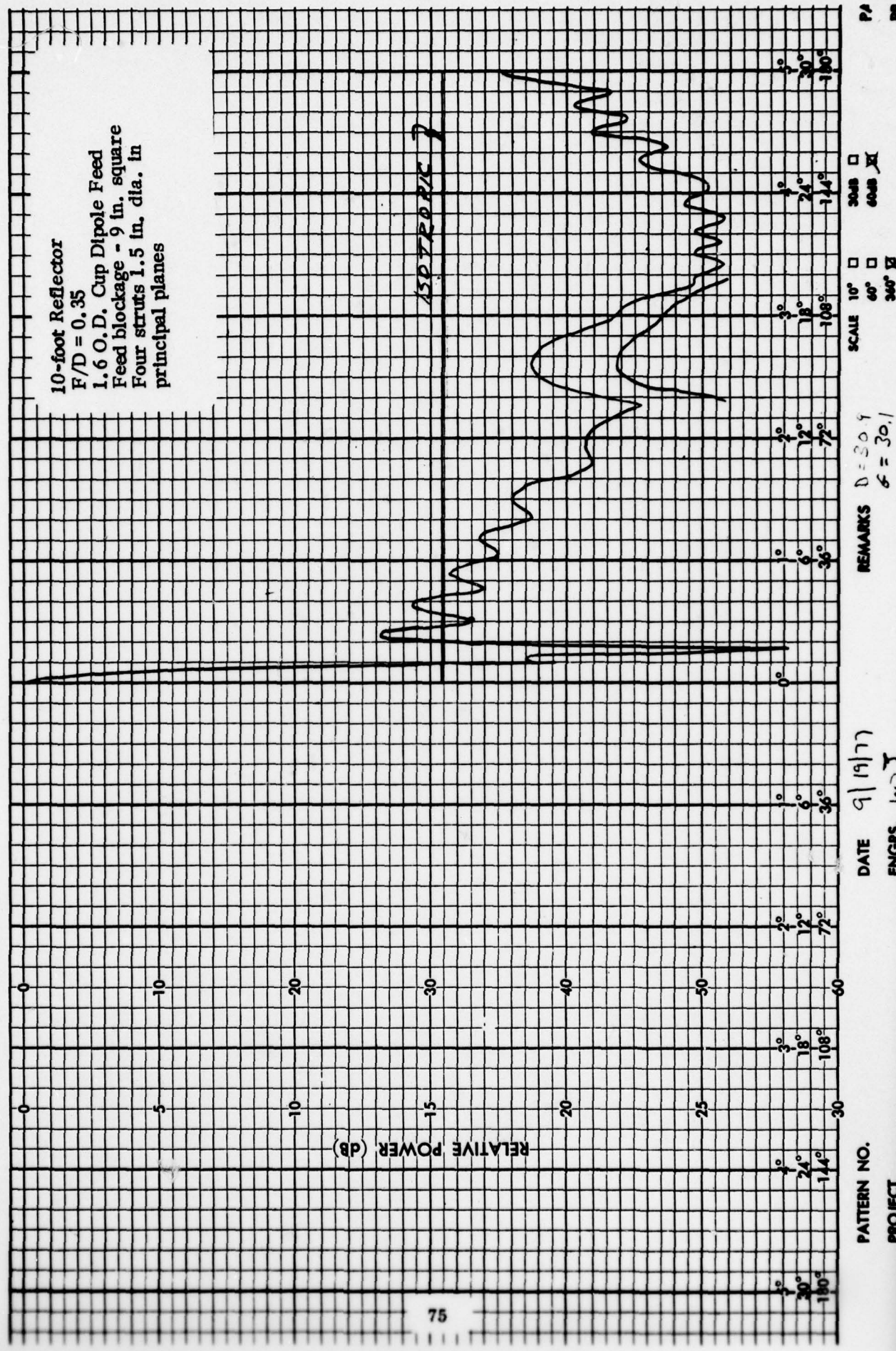


CHART NO. 177

SCIENTIFIC-ATLANTA, INC., ATLANTA, GEORGIA, U.S.A.

10-foot Reflector
F/D = 0.30
1.6" O.D. cup dipole feed
feed blockage - 9 in. square
four struts 1.5 in. dia. in
principal planes

RELATIVE POWER (dB)

76

PATTERN NO.
PROJECT

DATE 9/19/71
ENGRS. J.L.

REMARKS $D = 32.7$
 $G = 27.4$

SCALE 10° 40° 20dB 40dB 300°

10° 20° 30° 40° 50° 60° 70° 80° 90° 100° 110° 120° 130° 140° 150° 160° 170° 180° 190° 200° 210° 220° 230° 240° 250° 260° 270° 280° 290° 300°

ISOPHASE 2

CHART NO. 177

SCIENTIFIC ATLANTA, INC., ATLANTA, GEORGIA, U.S.A.

10-foot reflector
F/D = 0.30
1.6" O.D. cup dipole feed
Feed blockage = 9 in. square
Four struts 1.5 in. dia. in
diagonal planes

RELATIVE POWER (dB)

77

PATTERN NO.
PROJECT

DATE 9/16/77
ENGRS. W.W.J.

REMARKS D = 50.1
G = 29.4
SCALE 10° □ 30° □ 60° □ 300° □ 600° □ 360° □

CHART NO. 177

SCIENTIFIC-ATLANTA, INC., ATLANTA, GEORGIA, U.S.A.

12-foot reflector
F/D = 0.292
1.6" O.D. cup dipole feed
feed blockage - 9 in. square
four struts 1.5 in. dia. in
principal planes

RELATIVE POWER (dB)

78

PATTERN NO.
PROJECT

DATE 9/19/77
ENGRS. 142

REMARKS D-31-8
G = 30.9

SCALE 10° □ 60° □ 300° □ 600° □

P

CHART NO. 177

SCIENTIFIC-ATLANTA, INC., ATLANTA, GEORGIA, U.S.A.

12-foot Reflector
F/D = 0.292
1.6" O.D. Cup Dipole Feed
Feed blockage - 9 in. square
Four struts 1.5 in. dia. in
diagonal planes

RELATIVE POWER (dB)

79

PATTERN NO.
PROJECT

DATE 9/19/77
ENGRS. W/71

REMARKS D = 31.3
G = 30.9
SCALE 10° □ 30° □
60° □ 60dB -20dB
360° □ 360dB -20dB

P
n

CHART NO. 177

SCIENTIFIC-ATLANTA, INC., ATLANTA, GEORGIA, U.S.A.

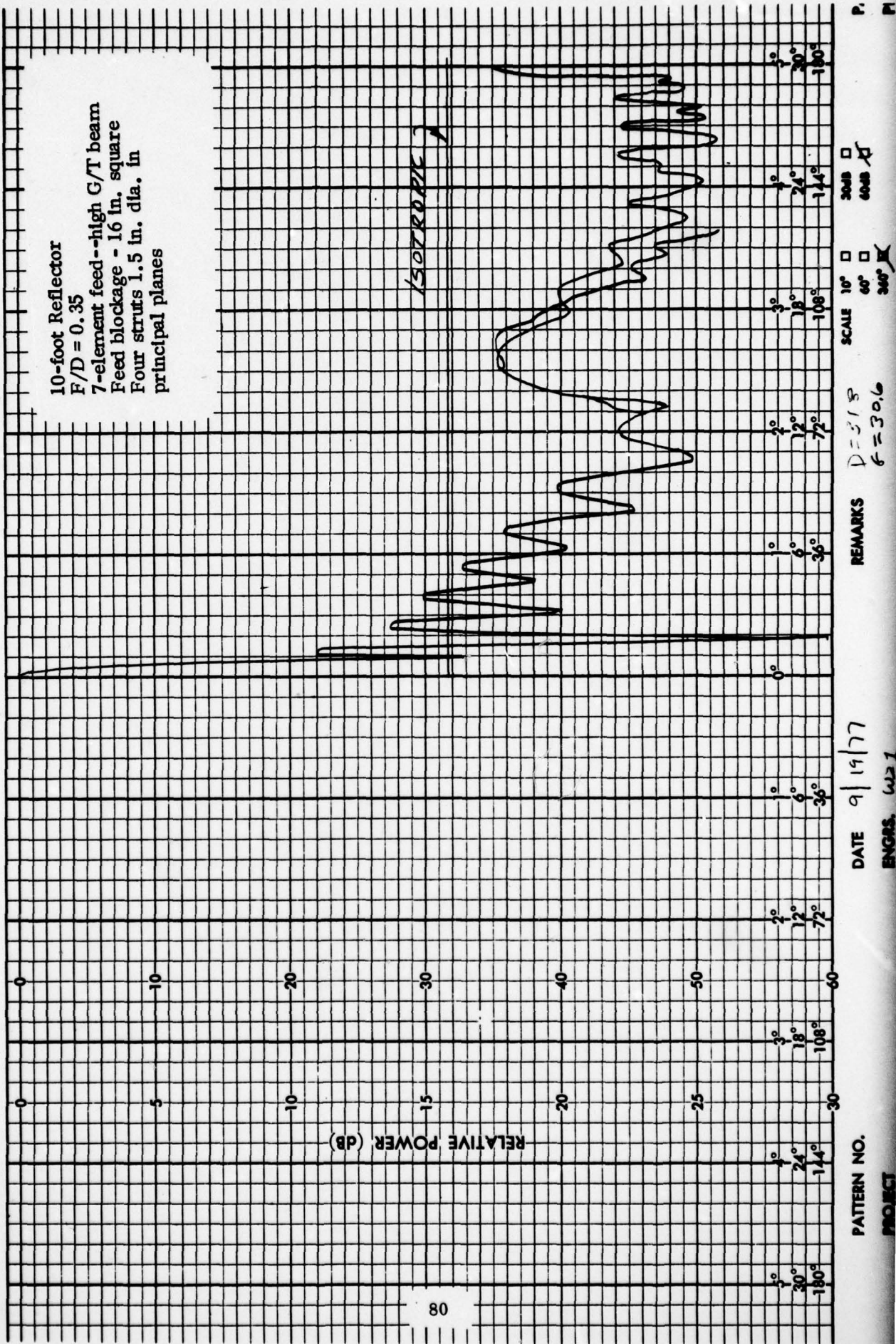
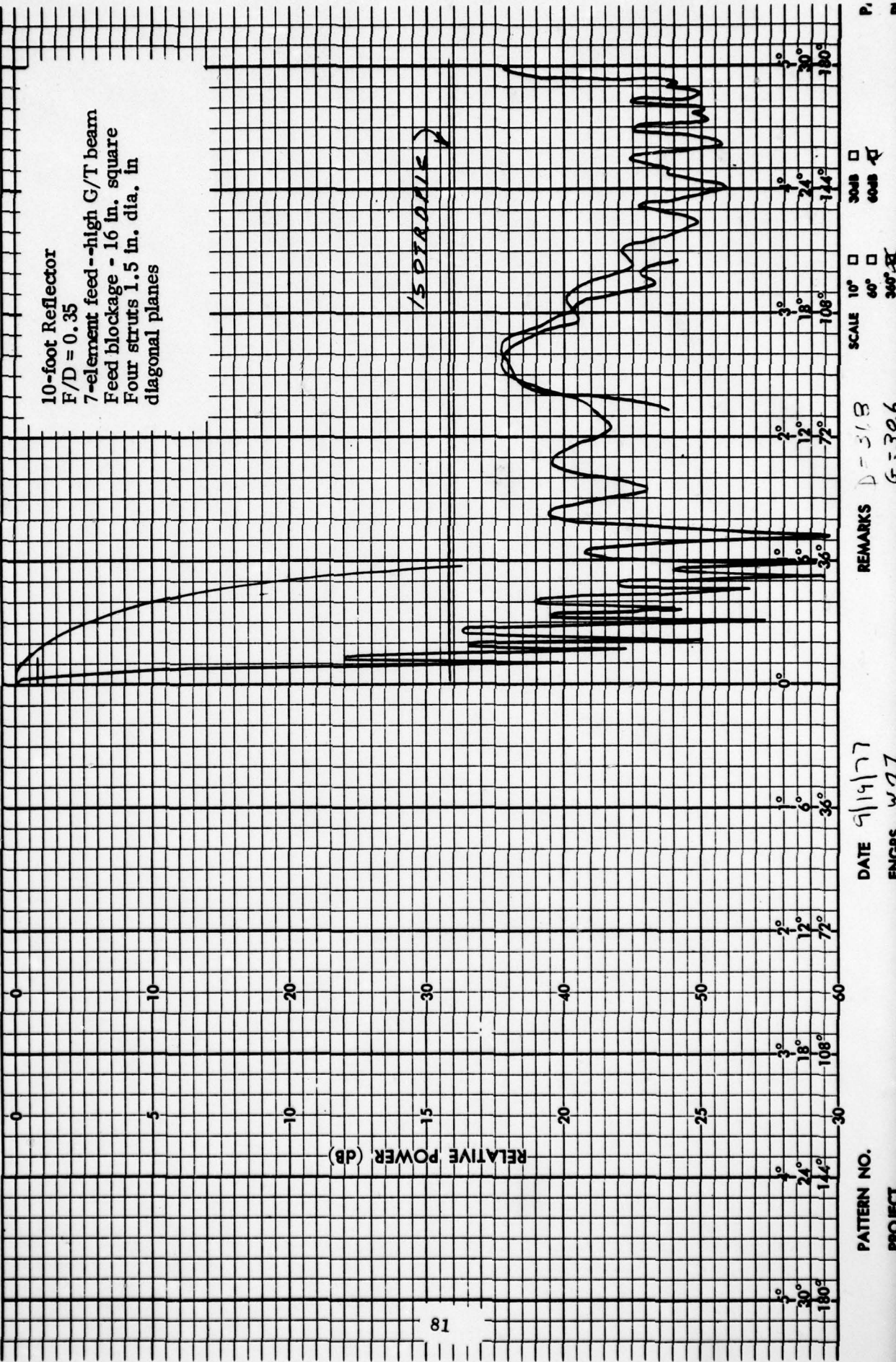


CHART NO. 179

SCIENTIFIC-ATLANTA, INC., ATLANTA, GEORGIA, U.S.A.

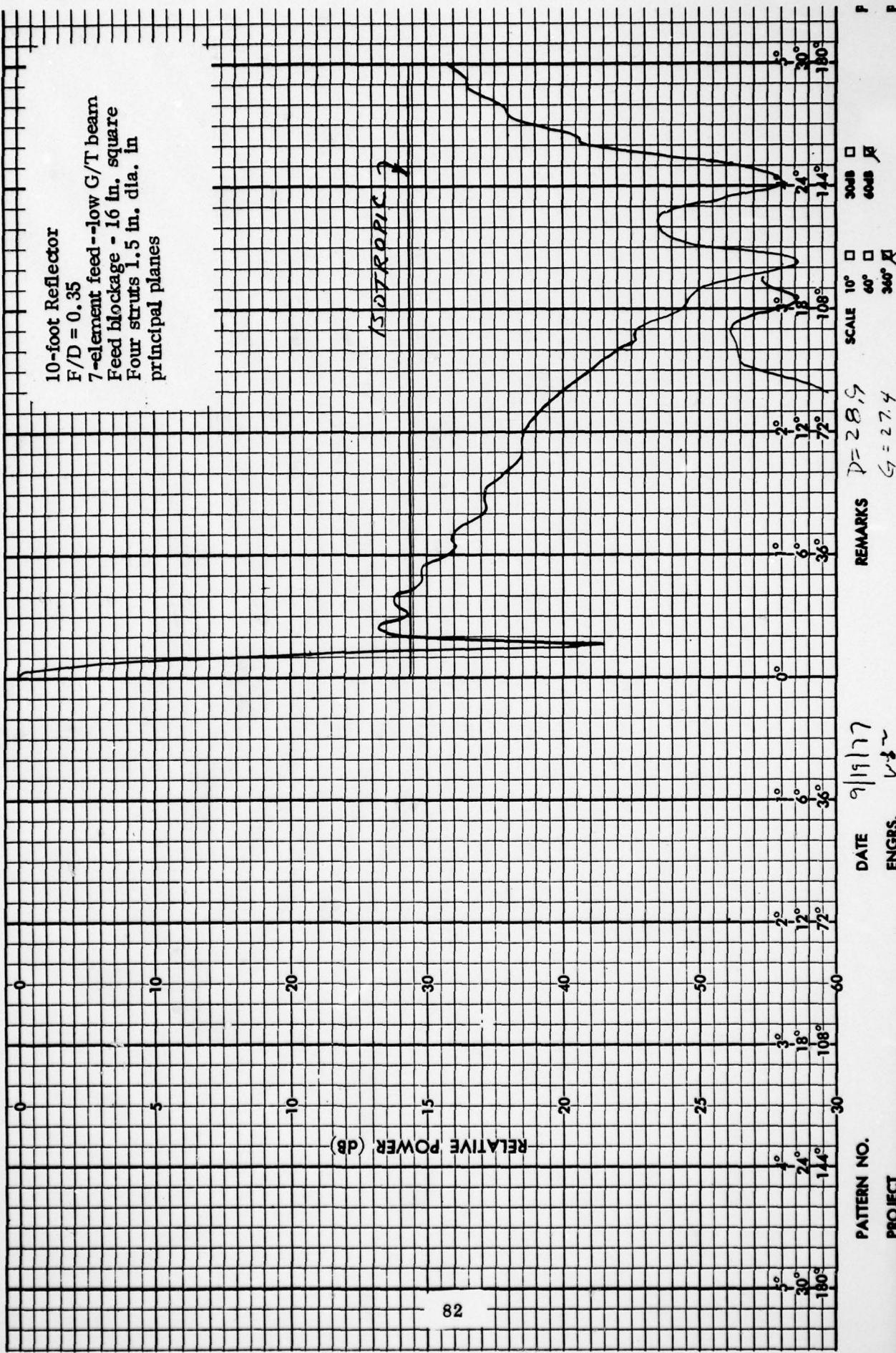
10-foot Reflector
F/D = 0.35
7-element feed--high G/T beam
Feed blockage = 16 in. square
Four struts 1.5 in. dia. in
diagonal planes



SCIENTIFIC ATLANTA, INC., ATLANTA, GEORGIA, U.S.A.

CHART NO. 17

10-foot Reflector
 F/D = 0.35
 7-element feed--low G/T beam
 Feed blockage - 16 in. square
 Four struts 1.5 in. dia. in
 principal planes



AD-A054 791

HUGHES AIRCRAFT CO FULLERTON CALIF
PORTABLE EARTH STATION ANTENNA STUDY SYSTEM. (U)
MAR 78

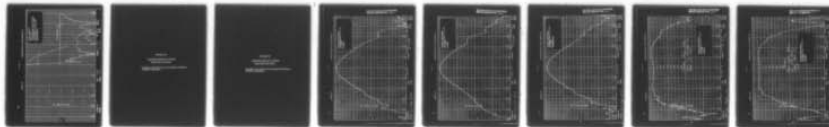
F/G 17/2.1

UNCLASSIFIED

FR-78-14-287

NL

2 OF 2
AD
A054 791

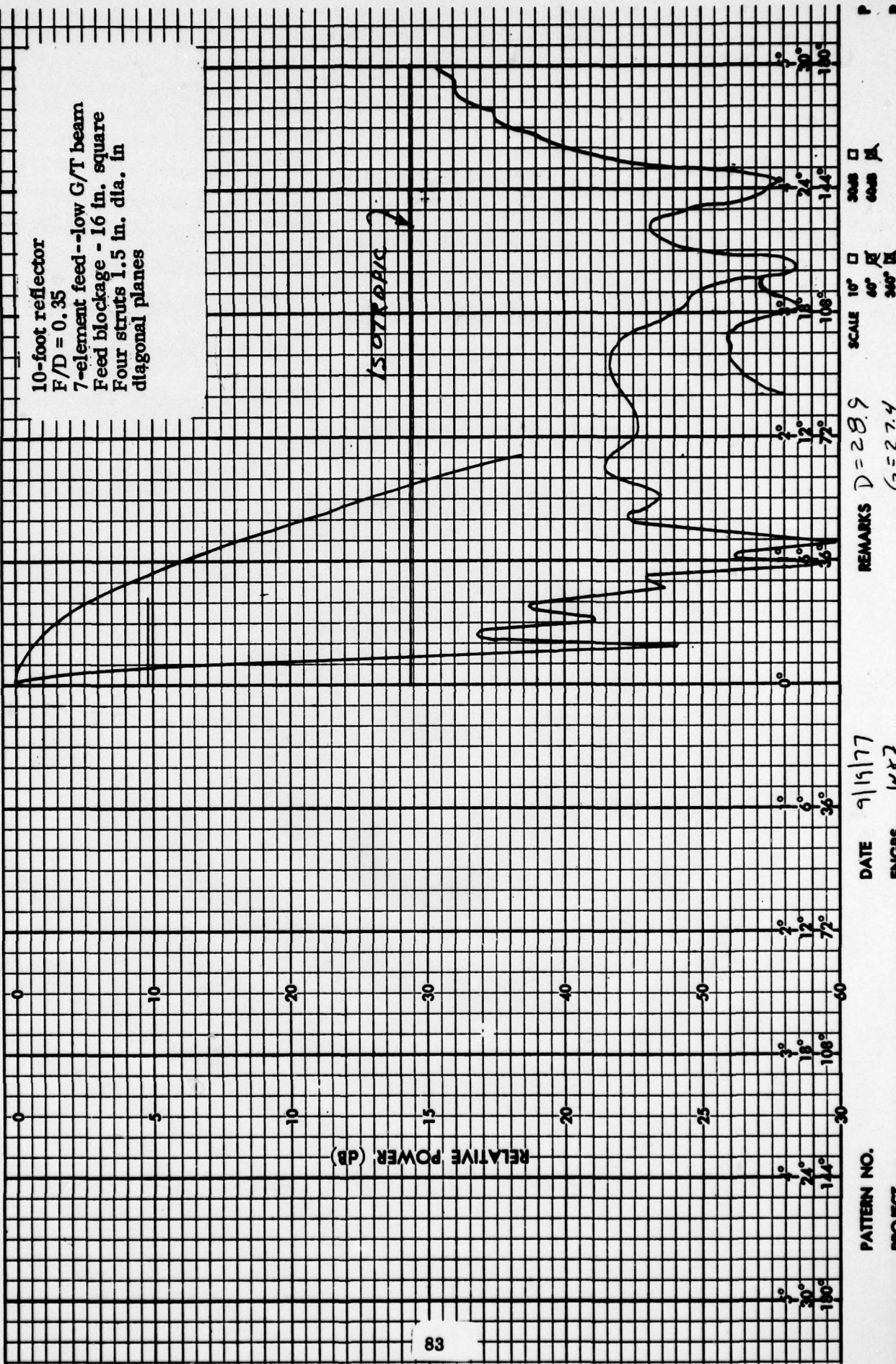


END
DATE
FILMED
7-78
DDC

SCIENTIFIC ATLANTA, INC., ATLANTA, GEORGIA, U.S.A.

CHART NO. 17

10-foot reflector
 $F/D = 0.35$
 7-element feed--low G/T beam
 Feed blockage - 16 in. square
 Four struts 1.5 in. dia. in
 diagonal planes



APPENDIX III

MEASURED PRIMARY PATTERNS AMPLITUDE AND PHASE

**Cup Dipole Feed Utilized for Experimental Verification
of Pattern Computation.**

APPENDIX III

MEASURED PRIMARY PATTERNS AMPLITUDE AND PHASE

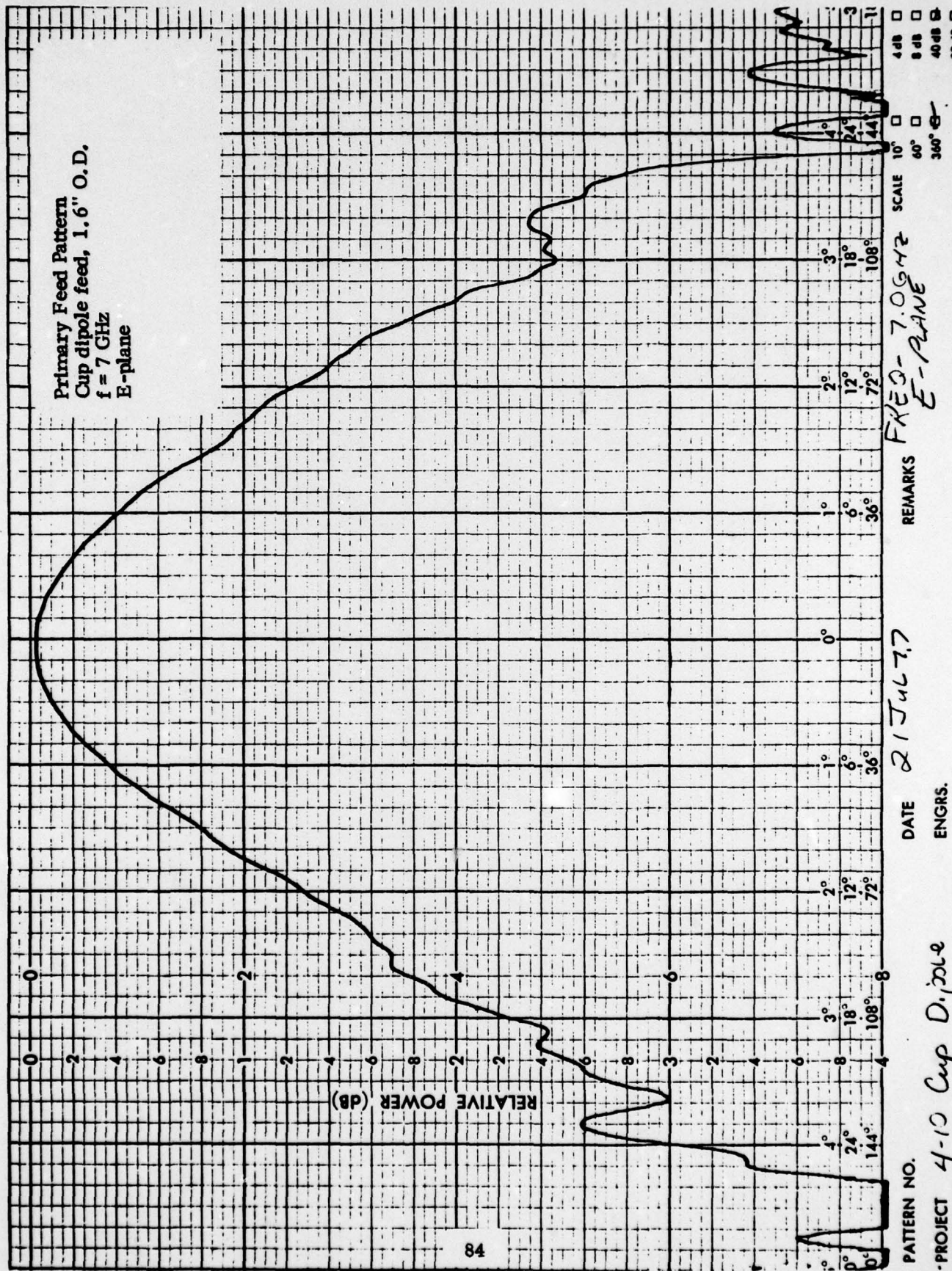
**Cup Dipole Feed Utilized for Experimental Verification
of Pattern Computation.**

THIS PAGE IS BEST QUALITY PRACTICABLE
FROM COPY FURNISHED TO DDC

SCIENTIFIC ATLANTA, INC. ATLANTA, GEORGIA, U.S.A.

CHART NO. 177

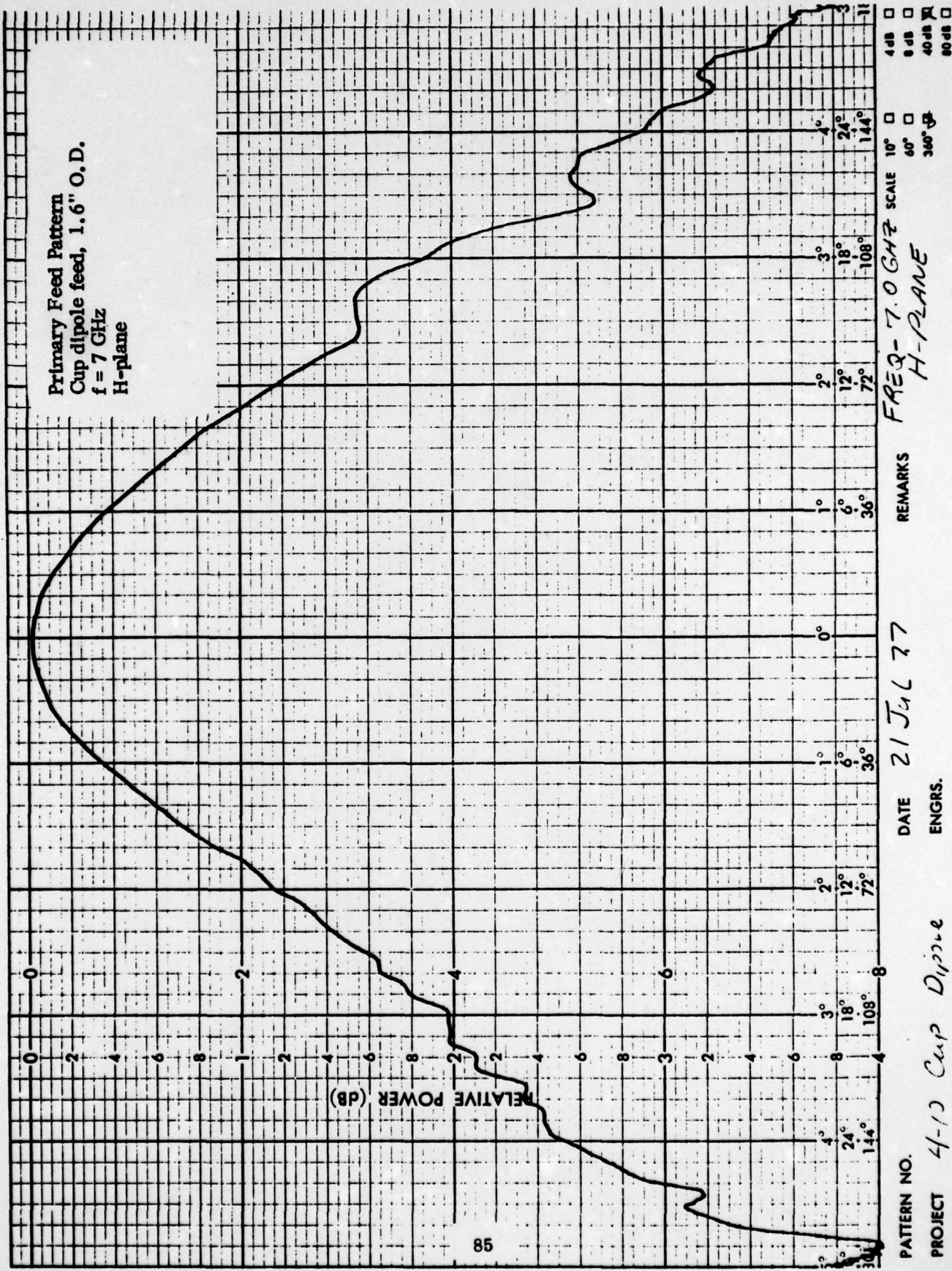
Primary Feed Pattern
Cup dipole feed, 1.6" O.D.
f = 7 GHz
E-plane



THIS PAGE IS BEST QUALITY PRACTICABLE
FROM COPY FURNISHED TO DDC

SCIENTIFIC-ATLANTA, INC. ATLANTA, GEORGIA, U.S.A.

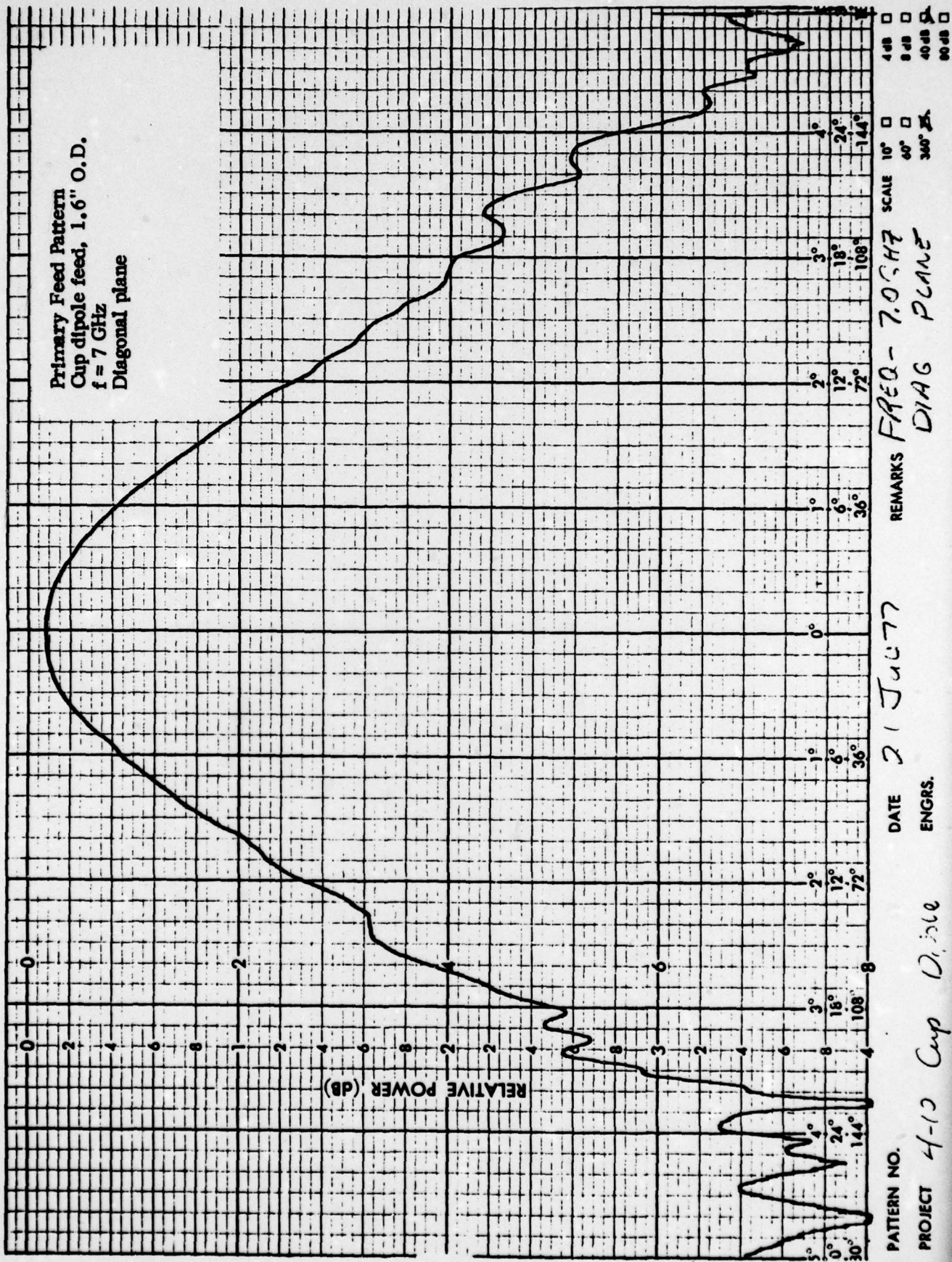
CHART NO. 177



THIS PAGE IS BEST QUALITY PRACTICABLE
FROM COPY FURNISHED TO DDC

SCIENTIFIC-ATLANTA, INC., ATLANTA, GEORGIA, U.S.A.

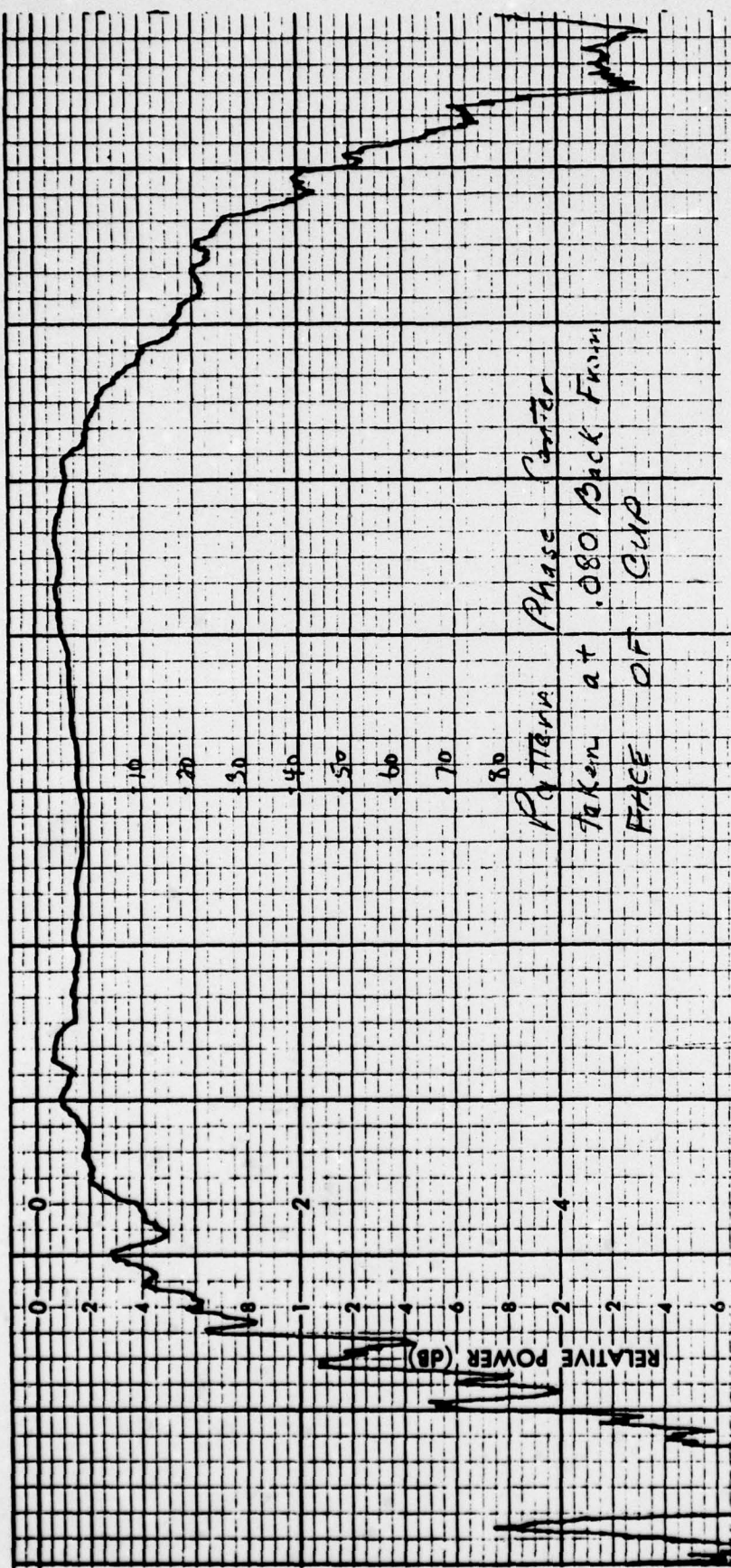
CHART NO. 177



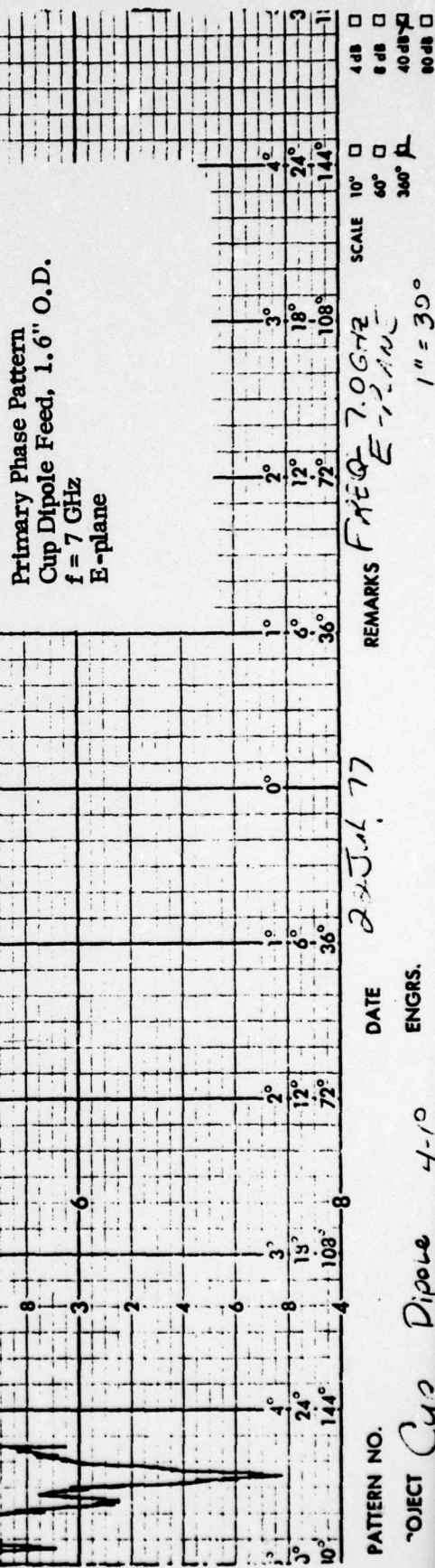
THIS PAGE IS BEST QUALITY PRACTICABLE
FROM COPY FURNISHED TO DDC

SCIENTIFIC ATLANTA, INC., ATLANTA, GEORGIA, U.S.A.

CHART NO. 177



Primary Phase Pattern
Cup Dipole Feed, 1.6" O.D.
 $f = 7$ GHz
E-plane



PATTERN NO.

PROJECT C-13 Diorite 4-10 ENGRS.

Dipole - 4/10

١١٠

$$1'' = 30^\circ$$

$$1'' = 39^{\circ}$$

THIS PAGE IS BEST QUALITY PRACTICABLE
FROM COPY FURNISHED TO DDC

SCIENTIFIC ATLANTA, INC. ATLANTA, GEORGIA, U.S.A.

CHART NO. 177

